5-2017

Management of Islanded Operation of Microgirds

Md Riyasat Azim
University of Tennessee, Knoxville, mazim@vols.utk.edu

To the Graduate Council:

I am submitting herewith a dissertation written by Md Riyasat Azim entitled "Management of Islanded Operation of Microgirds." I have examined the final electronic copy of this dissertation for form and content and recommend that it be accepted in partial fulfillment of the requirements for the degree of Doctor of Philosophy, with a major in Electrical Engineering.

Fangxing Li, Major Professor

We have read this dissertation and recommend its acceptance:

Kai Sun, Hector A. Pulgar, James Ostrowski

Accepted for the Council:
Dixie L. Thompson

Vice Provost and Dean of the Graduate School

(Original signatures are on file with official student records.)

Management of Islanded Operation of Microgirds

A Dissertation Presented for the

Doctor of Philosophy

Degree

The University of Tennessee, Knoxville

Md Riyasat Azim

May 2017

I dedicate my work to my beloved parents, my loving wife, my dearest sister, and my wonderful friends.

Acknowledgements

I would like to express my gratitude to everyone who helped me with various aspects of this research and preparing this dissertation.

First and foremost, I would like to express my deepest gratitude to my major advisor, Dr. Fangxing 'Fran' Li for his continuous guidance and persistent help for this dissertation and all other research works during my Ph.D. study at the University of Tennessee at Knoxville (UTK). I am also grateful to Dr. Fangxing Li for funding my Ph.D. study.

I would like to thank Dr. Kai Sun, Dr. Hector A. Pulgar-Painemal, and Dr. James Ostrowski for their time and efforts in serving as the members of my dissertation committee.

In addition, I would like to express my special thanks to Dr. Hao Huang, Dr. Yao Xu, Dr. Qinran Hu, Dr. Xue Li, Dr. Kumaraguru Prabakar, Dr. Haoyu Yuan, Dr. Can Huang, Dr. Xin Fang, Dr. Linquan Bai, and Mr. Hantao Cui for being supportive to my works as well as their kind advice in my course study and research. Also, I would like to thank all my friends and professors at the Center for Ultra-Wide-Area Resilient Electric Energy Transmission (CURENT) who created a warm and friendly atmosphere for education and research.

Last but not the least, I want to thank the entire UTK family for such a wonderful experience over the last four and half years.

Abstract

Distributed generations with continuously growing penetration levels offer potential solutions to energy security and reliability with minimum environmental impacts. Distributed Generations when connected to the area electric power systems provide numerous advantages. However, grid integration of distributed generations presents several technical challenges which has forced the systems planners and operators to account for the repercussions on the distribution feeders which are no longer passive in the presence of distributed generations.

Grid integration of distributed generations requires accurate and reliable islanding detection methodology for secure system operation. Two distributed generation islanding detection methodologies are proposed in this dissertation. First, a passive islanding detection technique for grid-connected distributed generations based on parallel decision trees is proposed. The proposed approach relies on capturing the underlying signature of a wide variety of system events on a set of critical system parameters and utilizes multiple optimal decision tress in a parallel network for classification of system events. Second, a hybrid islanding detection method for grid-connected inverter based distributed generations combining decision trees and Sandia frequency shift method is also proposed. The proposed method combines passive and active islanding detection techniques to aggregate their individual advantages and reduce or eliminate their drawbacks.

In smart grid paradigm, microgrids are the enabling engine for systematic integration of distributed generations with the utility grid. A systematic approach for

controlled islanding of grid-connected microgrids is also proposed in this dissertation. The objective of the proposed approach is to develop an adaptive controlled islanding methodology to be implemented as a preventive control component in emergency control strategy for microgrid operations.

An emergency power management strategy for microgrid autonomous operation subsequent to inadvertent islanding events is also proposed in this dissertation. The proposed approach integrates microgrid resources such as energy storage systems, demand response resources, and controllable micro-sources to layout a comprehensive power management strategy for ensuring secure and stable microgrid operation following an unplanned islanding event.

In this dissertation, various case studies are presented to validate the proposed methods. The simulation results demonstrate the effectiveness of the proposed methodologies.

Table of Contents

List of Tables

List of Figures

Chapter 1

Introduction

The classic electricity generation and distribution is based on centralized power generation units (typically based on coal, natural gas, oil, and nuclear) providing power to distribution areas and load centers through transmission and sub-transmission infrastructures for power transfer. This traditional electricity generation and distribution paradigm suffers from major technical and environmental disadvantages such as- power loss of long transmission lines, reduced efficiency, expensive and difficult nature of system monitoring, infrastructure security, and environmental impacts through greenhouse gas emissions leading to global warming etc.

In contrast, distributed generation (DG) or on-site generation utilize small scale generating units located close to distribution area or load centers. Distributed generation technologies typically utilize small scale modular electricity generation technologies which is capable of providing low-cost electricity with high reliability and security with minimal environmental impacts compared to traditional generation technologies. Distributed energy resources (DERs) are small-scale power generation technologies with typical power capacities ranging from fraction of a kilowatt (kW) to about 10 megawatt (MW)[1]. However, utility-scale distributed energy resources have capacities more than 10 megawatt (MW)[1]. Prominent DER technologies include- combined heat and power (CHP), fuel Cells, micro-combined heat and power

(MicroCHP), Micro-turbines, photovoltaic (PV) systems, small-scale wind power systems, and small-scale hydro power generation units etc.

The smart grid paradigm envisions an electric power system (EPS) that offers energy security, resiliency, reliability, and efficiency through a more decentralized, consumer-interactive and responsive system operation. Smart grids utilize advanced metering infrastructure (AMI) and communication networks to allow distributed generations (DG), energy storage system (ESS), electric vehicles (EV) or plug-in hybrid electric vehicles (PHEV), and demand side management (DSM) techniques to function in a more cooperative and responsive manner [2, 3]. In essence, the smart grid concept intelligently integrates and manages different power system components (such as- generation and storage units, transmission and distribution networks, communication and control infrastructure, and consumer loads) to enable sustainable, secure, and economic operations of electric power systems.

Traditional fossil-fueled large power plants operate as base load generation units enabling steady supply of base load demands in the power system. In addition to the base load units, generation units based on diesel and natural gas generators are utilized as peak load generating units to account for the peak electricity demands. Thus the balance between generation and demand of electricity can be ensured in the electric power system. Distributed generations based on renewable energy resources such as- solar and wind are dependent on continuously variable resources. To account for these variability associated with these distributed energy resources (DERs) based on intermittent renewable energy sources, smart grid technologies can integrate appropriate management strategies based on utilization of energy storage resources, demand response, and demand side management techniques. Thus an interactive management framework integrating various power system resources can be enabled by the smart grid technologies to help mitigate the effects of variability and intermittency associated with the DERs based on renewable energy resources.

Moreover, smart grid platform with continuous monitoring can provide real-time data to enable reliable and efficient operation of the distributed energy resources

(DERs). Further, smart meters which allow two-way communication enabling real-time pricing linking electricity price signals to responsive consumer loads, thereby optimization of the consumers' consumption patterns can be achieved. Hence, demand side management and demand response can be enabled through responsive system loads in smart grid framework.

The US Department of Energy (DOE) office of electricity delivery and energy reliability (OE) visions a grid modernization effort with objectives such as integration of 80% clean electricity by 2035, access to reliable and affordable electricity, incorporate new technologies, and energy security and resiliency [1]. The grid of the future should offer modularity and agility with both centralized and distributed generations along with the incorporation of demand side management, energy storage and communication features.

Microgrids provide a platform to integrate distributed energy resources (DERs) with the existing power system in a systematic manner using monitoring, control, and management strategies.Microgrids are defined by US Department of Energy (DOE) as A group of interconnected loads and distributed energy resources (DER) with clearly defined electrical boundaries that acts as a single controllable entity with respect to the grid [and can] connect and disconnect from the grid to enable it to operate in both grid-connected or island mode [1]-[4].

This chapter provides a brief overview of prominent distributed generation technologies, and also discusses microgrid structure, components and management strategies. Objectives, contributions, and organization of this dissertation is discussed at the end of this chapter.

1.1 Distributed Generation Technologies

A brief overview of different types of distributed generation (DG) technologies is presented in this section. DG technologies can be classified in several ways. Based on the type of the energy resource utilized, DG technologies can be classified as- 1)

renewable energy based DGs and 2) non-renewable energy based DGs. Based on the type of interface with the utility grid, DG technology can be divided into two groups- 1) electronically interfaced (inverter based) DGs, and 2) DGs connected to the grid directly using interconnection transformers. The rest of this section discusses a few of the prominent DG technologies.

1.1.1 Microturbines

Microturbines are small sized electricity generators consisting of compressor, combustor, turbine, alternator, recuperator to capture the waste heat to improve the compressor efficiency, and generator. Typical capacity of microturbines range from 1 kW to 500 kW [5, 6]. Based on the microturbine configuration, efficiency figures range from 15 percent for unrecuperated microturbines, 20-30 percent for recuperated turbines, and up to 85 percent for microturbines with heat recovery. Microturbines generally operate over 40 kHz frequency range with the operating frequency for single shaft microturbines ranges from 90 kHz to 120 kHz, and hence, the generator output frequency ranges from 1500-4000 Hz. Thus, a power conversion stage consisting of AC-DC-AC power conversion is required to connect the microturbines/generator to the utility grid [5, 6].

Primary applications of microturbines include distributed generation applications, peak shaving, stand-by power, combined heat and power (CHP) etc. Microturbines are compact in size, lightweight, have low emissions, and also have less number of moving parts. On the other hand, disadvantages are low fuel to electricity efficiencies, and loss of power output and efficiency with higher ambient temperature and elevation.

1.1.2 Gas Turbines

Gas turbines utilize compressor, combustor, turbine, and generator to generate electrical power by compressing air and igniting it using a gaseous fuel. The fuel

can be natural gas, hydrogen, and bio-gas etc. In gas turbines, the compressor and turbine have multiple stages and axial blading as compared to microturbines which are single-stage and consist of radial blades. Typical gas turbine systems have capacities in the range from 1 to 400 MW in combined cycle applications [5, 6, 7], with typical capacity in distributed generation applications being 100 MW or less [6]. Typical efficiencies for gas turbines range from 35 to 40 percent. Gas turbines are widely employed for combined heat and power (CHP) applications in the United States, with the installed capacity representing 64 percent of the installed CHP capacity [7].

1.1.3 Reciprocating Engines

Reciprocating engines are combustion engines using reciprocating pistons to convert pressure into rotating motion [5, 6]. Reciprocating engines are widely employed for CHP applications with typical capacities ranging from 10 kW to 10 MW [5, 6]. Reciprocating engines fueled by natural gas allows rapid start-up and load-following capabilities. Reciprocating engines accounts for around 54 percent of the entire population of the installed CHP systems in the US, amounting to nearly 2.4 GW in total capacity. Popular applications of reciprocating engine CHP systems include industrial, commercial buildings, university campuses, and hospitals [7].

1.1.4 Fuel Cells

Fuel cells utilize an electro-chemical process for converting chemical energy into electrical energy. Typical structure of fuel cells involves a negative side, a positive side, and electrolyte that allows charges to move between two sides. Generally, a chemical reaction with oxygen or other oxidizing are utilized in the process and the byproducts of the chemical reaction are water, heat, and carbon dioxide. Fuel cell capacities typically range from 5 kW to 5 MW with efficiency ranging from 35 to 60 percent [6]. A total of 126 fuel cells utilized for CHP are installed in the United States totaling to a generation capacity of 67 MW [7]. Main applications of these installed fuel cells are

in commercial and institutional infrastructures such as universities, hospitals, and office buildings, where the coincidental demand for electricity and thermal energy is relatively high [7]. Fuel cells are well suited for distributed generation applications, but their expensive nature makes them uneconomical compared to other types of distributed generation technologies.

1.1.5 Combined Heat and Power

Combined heat and power (CHP) which is also known as cogeneration, is the concurrent production of electricity and thermal energy (used for heating and cooling). Various generation technologies (such as- steam turbines, microturbines, fuel cells, reciprocating engines etc.) can be employed in CHP for electricity production, and subsequently, the heat produced from the electricity generation process is recovered and utilized to provide the necessary heating and/or cooling. A wide variety of fuel sources can be utilized in CHP including both fossil-fuel based sources and renewable energy based sources. CHP technology enables cost-effective and efficient operations with efficiency ranging from 65 to 75 percent [5, 6, 7].

1.1.6 Solar Photovoltaic

Solar photovoltaic (PV) is by far the most important distributed generation technology. Solar PV is the quintessential DG technology capable of delivering power to consumer location anywhere in the world utilizing the energy available in sunlight. Solar PV technology uses solar panels consisting of solar cells to convert energy available in the sunlight into electrical power. The most popular solar cell technology is based on crystalline silicon. The improvements in energy conversion efficiency, reduction in installation cost per watt, energy pay-back time (EPBT), and levelized cost of electricity (LCOE) enabling solar PV technology to achieve grid parity and to be employed in broad range of applications such as residential, commercial as well as utility scale applications [5, 6]. Solar PV offer numerous benefits such as-

zero emissions, zero fuel costs, and minimal operating and maintenance costs. The disadvantages include the variable and non-dispatchable nature. However, with the improving energy storage technologies, limited amount of control on the variability and dispatch capability can be achieved.

1.1.7 Wind Power

Wind turbines transforms available kinetic energy in the wind into electrical power through the utilization of turbine-generator sets. Wind energy conversion systems include wind turbine which is connected to a rotating shaft through a gear-box. The rotating shaft and gear box assembly allows transformation of the slow rotational speed from the wind turbines to high rotational speeds to drive the generator. Although, wind power can be employed in small scale suitable for distributed generation applications as well as utility scale applications, the cost factors associated with small scale wind power applications often make them uneconomical from DG standpoint [5, 6]. Wind power has the advantages of being clean and cost-effective. But the disadvantages are its variable and non-dispatchable nature similar to solar PV.

1.1.8 Energy Storage

Distributed energy resources (DERs) also include energy storage technologies in addition to generation technologies. Energy storage systems for DER applications include several types of energy storage technologies such as- different types for battery energy storage systems (BESS), pumped hydro energy storage, compressed air, and thermal energy storage systems. DER applications may include different energy storage systems including lead-acid batteries, lithium-ion batteries, flow batteries, and flywheels. Energy storage technologies provide grid support in renewable generation integration by minimizing the variability and accommodating their non-dispatchable characteristics by gaining limited control over the dispatch of power.

Fig. 1.1 presents the distributed generation technology continuum comparing technical maturity and commercial maturity for each of the DG technologies as presented in [6].

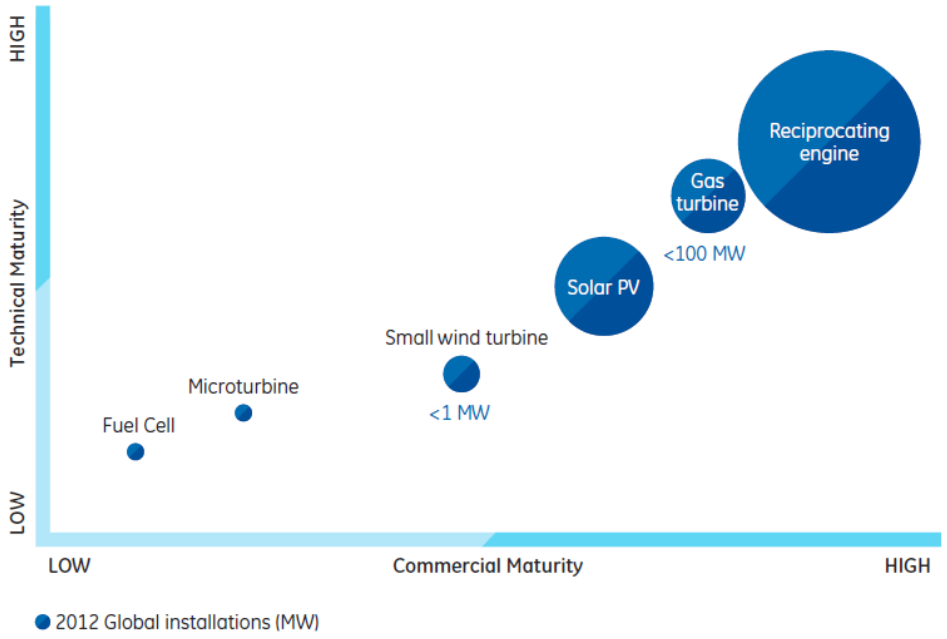

Figure 1.1: Distributed generation technology continuum [source- General Electric].

1.1.9 Small-Scale Hydroelectric Power

Small-scale hydro electric power are essentially hydroelectric power with smaller capacities in the range of 1-20 MW. Small-scale hydroelectric power generations can be further divided into mini hydro (100-1000 kW) and micro hydro (5-100 kW). Small scale hydroelectric projects are efficient and reliable energy sources, and can function as 'Run-of-River' system without requiring a reservoir, thus eliminating the adverse effects on surrounding ecology. However, requirements for suitable sites, low seasonal generations, environmental impacts, and difficulties in capacity expansion are major concerns.

Table 1.1: Overview of distributed generation technologies [source: General Electric and U.S. Environmental Protection Agency Combined Heat and Power Partnership.]

Characteristics	Reciprocating Engines	Gas Turbines	Microturbines	Fuel Cells	Solar PV	Small Wind
Typical Capacity range	20 kW - 20 MW	10-100 MW	30-250 kW	5kW-5MW	1 kW+	200 W+
Representative efficiency range (%)	28-49%	21-45%	18-20%	35-60%	-	-
Fuel options	Diesel Natural gas Alternatives	Natural gas Alternatives	Natural gas Alternatives	Hydrogen Natural gas	Renewable resources	Renewable resources
Thermal outputs	Heat Hot water Low pressure steam	Heat Hot water Low/high pressure steam	Heat Hot water Low/high pressure steam	Hot water Low/high pressure steam	None	None
Power density (kW/MW)	35-50	20-500	5-70	5-20	-	-
Min start time	10 sec	10 min	60 sec	3 hours	Immediate	Immediate
Required fuel pressure (psig)	1-45	100-500 (compressor)	50-80 (compressor)	0.5-45	-	-
Noise level	Moderate	Moderate	Moderate	Low	None	Low
Typical Applications	Power CHP	Power CHP	Power	Power	Power	Power

1.2 Microgrids: Structure, Components, Operation and Management

Conventional power distribution networks are going through radical transformations with the ever-increasing penetration levels of distributed energy resources (DERs). The integration of DERs and incorporation of ancillary service capabilities through active and reactive power controls of distributed generations (DGs) allow the distribution system to operate as active power networks which necessitates high reliability requirements.

Microgrids have emerged as the enabling engine for the smart grid technologies. Microgrids are defined as active distribution networks consisting of distributed generations, energy storage systems, and local loads which can operate in grid-connected mode (normal operation), islanded mode (emergency operation) and ride through between two modes [8]. Microgrids function as grid resources by supplying local loads when supply from area EPS is unavailable, thereby enabling faster system response and recovery for enhanced grid resilience and flexibility. The advantages of grid-interconnectivity allow microgrids to improve system energy efficiency and reliability, and avail the power of grid-independence to the end-user sites. A map of operational microgrid deployments is presented in Fig. 1.2 [1].

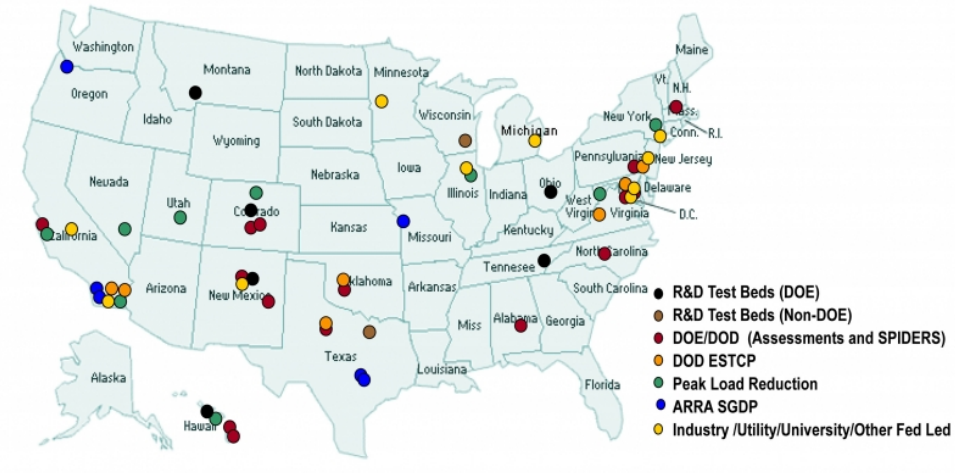

Figure 1.2: Map of operational microgrid deployments in the US.

The U.S. DOE has set goals to develop commercial-scale microgrid systems (capacity $<$ 10 MW) capable of reducing outage time of required loads by $>$ 98 percent at a cost comparable to non-integrated baseline solutions (uninterrupted power supply [UPS] plus diesel gen-set), while reducing emissions by 20 percent and improving system energy efficiencies by $>$ 20 percent, by 2020 [1].

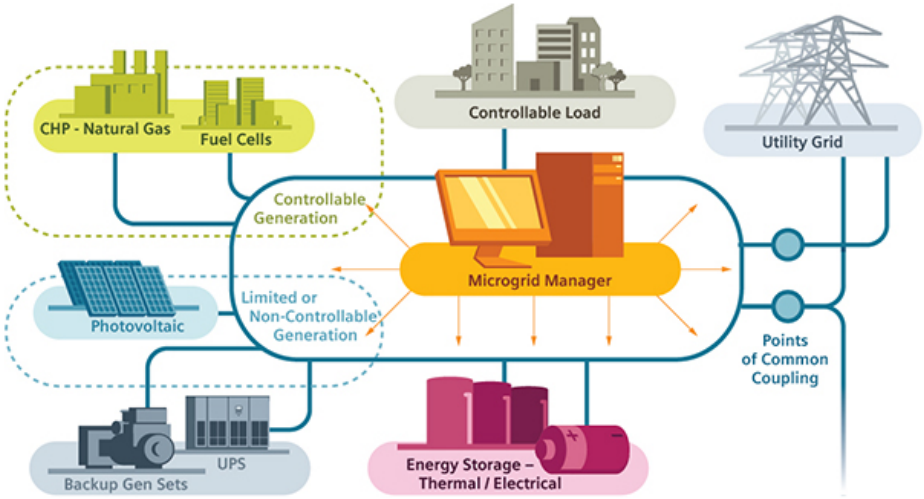

Figure 1.3: Microgrid architecture [source- Siemens microgrid].

1.2.1 Microgrid Structure and Components

A microgrid is essentially a distribution network consisting of a cluster of distributed energy resources (DERs) and loads with advanced controls, protections and energy management system to operate in grid-connected (normal operation) mode, islanded (autonomous or emergency operation) mode and ride through between the two modes. Distributed energy resources (DERs) in microgrid are mainly composed of distributed generations (DGs) and energy storage systems (ESS). DERs and local loads along with the necessary controls for management and operation are the main building blocks of microgrids.

The distributed generations (DGs) in microgrids mainly consists of generations based on renewable energy sources (such as- photovoltaic and wind), low carbon

technologies (such as micro-turbines and fuel cells), and back-up diesel gen-sets. Distributed generations in microgrid can be broadly classified into two main categories: 1) direct-coupled conventional rotating machine based generations (such as synchronous diesel generator), and 2) electronically interfaced generators (such as photovoltaics, fuel cells, micro-turbines etc.). Distributed generations (DGs) can be grouped based on their controllability as well. Dispatchable DG units (such as diesel generators) can be controlled to achieve desired power outputs; whereas non-dispatchable DG units (such as wind generators and PV farms) are variable in nature and their outputs are usually dependent on the natural resources (i.e. wind and sun respectively).

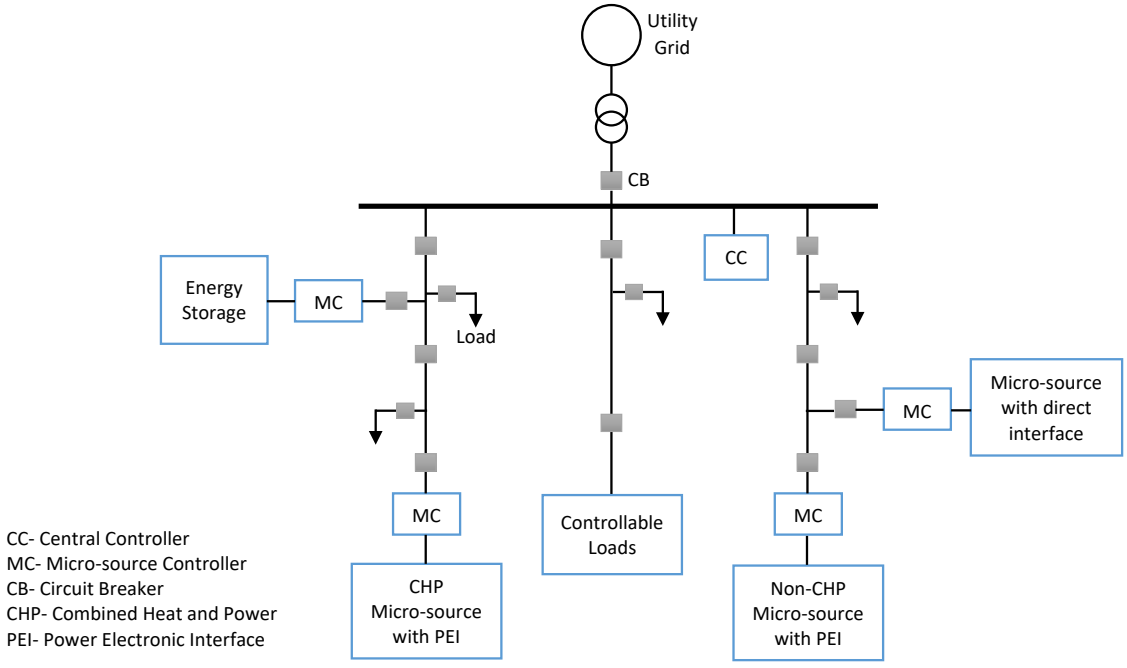

Figure 1.4: Microgrid structure and components.

Energy storage systems in microgrid include battery energy storage systems (BESS), flywheels, super-capacitors etc. Energy storage systems are deployed to compensate for the mismatch between microgrid demand and generations in islanded mode of operation for primary frequency regulation before generations

from controllable micro-sources (MS) can be adjusted to provide the secondary frequency regulation. Moreover, energy storage system can be utilized to minimize or compensate for the variable and non-dispatchable nature of the renewable generation based DERs.

Loads in microgrid systems mainly composed of residential and commercial loads. Loads can be grouped into two main categories: 1) critical loads and 2) non-critical loads. Critical loads are the group of loads requiring uninterrupted power supply meeting certain power quality standards. Non-critical loads may include responsive loads and curtailable loads, which can be deferred or interrupted during microgrid emergency operations.

The US Department of Energy (DOE) categorizes microgrids based on the capacity and applications as presented in Table 1.2 [1].

Table 1.2: The US DOE Microgrid Categorization Based on Capacity and Applications.

Applications	**Power Category**
Commercial	Greater than 50 kW, three phase, functionally expandable
Community/Campus	1-10 MW, may be modular or single rating
Utility Scale	>10 MW, possibly using multiple interconnected microgrids

1.2.2 DER Interface Types in Microgrids

The DER units present within a microgrid depends on factors such as- microgrid architecture, operation strategy (grid-connected or stand-alone), geographical location of the microgrid system, and overall purpose of the microgrid system. The DERs within a microgrid can be broadly classified as- 1) direct-coupled conventional rotating machine based generations (such as synchronous diesel generator), and 2) electronically interfaced generators (such as photovoltaics, fuel cells, micro-turbines etc.).

Conventional generation based DGs can be connected directly to the microgrid network through interconnection transformers. Whereas, variable-speed generators (i.e. wind turbines using synchronous generators, microturbines etc.) are connected to the microgrid network through AC-to-AC power conversion stages to meet the frequency and voltage requirements of the microgrid network. Distributed generation technologies such as solar PV and fuel cells require DC-to-AC power conversion stages to be connected with the microgrid networks. Wind turbines employing full-converter topologies are also connected via DC-to-AC power converter stages. On the other hand, wind turbines using induction generators or doubly fed induction generators are connected directly to the microgrid via interconnection transformers. Energy storage units are generally integrated through DC-to-AC power conversion stages. Fig.1.5 presents a generalized overview of the DER interfaces in microgrids as presented in [9].

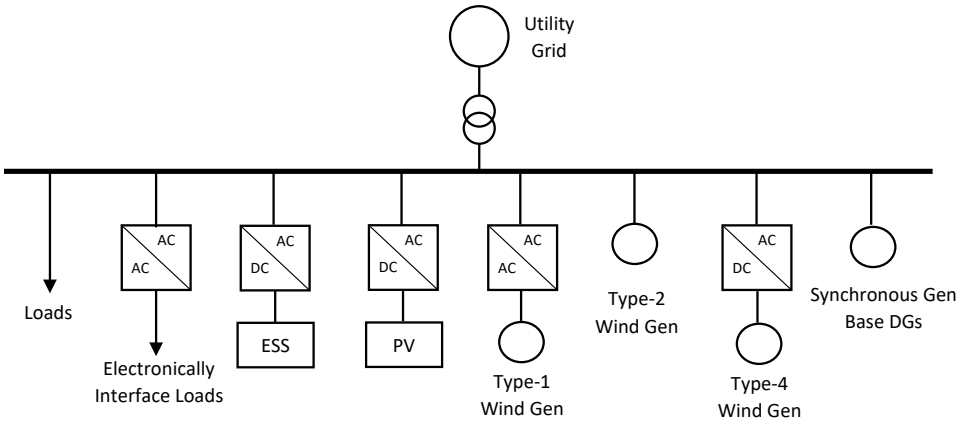

Figure 1.5: Microgrid component interface methodologies.

1.2.3 Control of Operation and Management Architecture

Primary control is the local control framework completely based on local measurements without requiring any communication with the central controller or other local controllers [9, 10]. Power output control of individual DERs and power sharing

between DG units are the main aspects of the primary control architecture. In synchronous generator based DGs, control of power outputs and power sharing between DGs are achieved using voltage regulators, governor units, and using the inertia of the machine itself. In inverter based DG units, the inverter controller is utilized to control the power output of individual DG units as well as to achieve power sharing between various DG units. Inverter controller regulates output of the DG unit by controlling the voltage and current of the inverter unit by utilizing two control loops (i.e. an outer loop for voltage regulation and an inner loop for current regulation). Power sharing in inverter based DGs is implemented using active power-frequency (P-f) and reactive power-voltage (Q-V) droop controllers [9, 10]. Primary control is also known as the primary frequency regulation in microgrids and is the first level of controls in the control hierarchy.

Secondary control architecture, which is based on energy management system (EMS); ensures secure, reliable, and economic operation of microgrids. The primary objectives of microgrid EMS include economic operation of microgrids by optimizing the operation of individual DER units in the microgrid and eliminate the voltage and frequency errors from the primary control actions to achieve secure and reliable system operation [9, 10]. Both centralized and decentralized EMS architectures can be utilized for microgrid secondary control. In contrast to primary control stage, secondary controls operate with a slower operational time-frame to decouple the secondary control actions from primary control actions, minimize the bandwidth requirements for communication channels and to perform complex optimization calculations required to achieve optimal system operations.

Tertiary control is utilized to coordinate the operation of microgrids to meet the performance requirements and goals of the host power system. Tertiary control operates in several minutes timeframe and actuate control signals to secondary controls of microgrids and to other control systems in the main grid. Tertiary control is generally considered as a part of the host power system, not part of the microgrid

control architecture itself [9, 10]. Fig. 1.6 presents a hierarchical microgrid control framework [10].

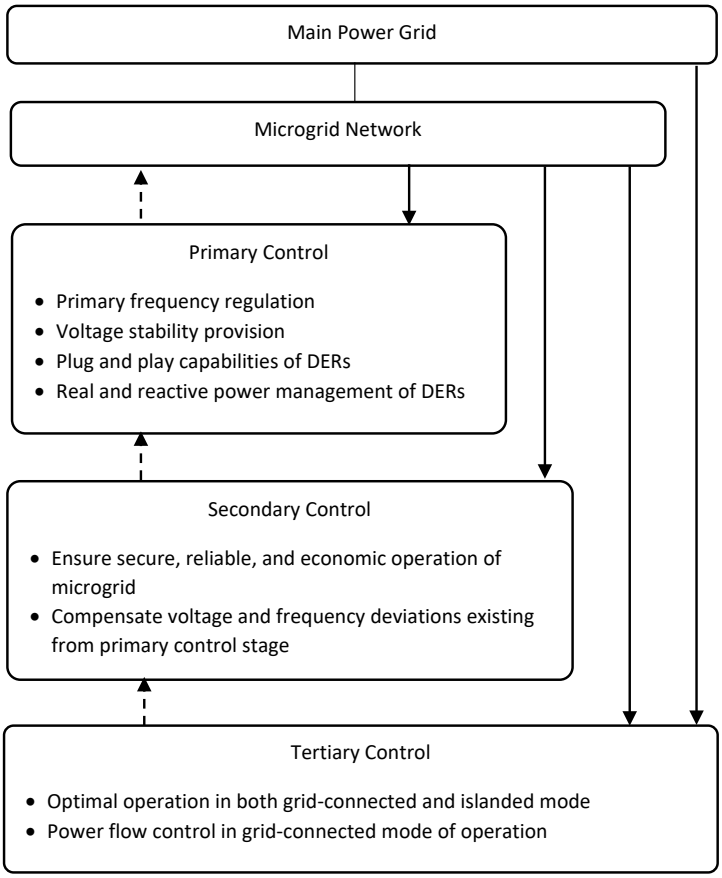

Figure 1.6: Microgrid hierarchical control framework.

1.2.4 Microgrid Applications and Benefits

Microgrid Applications

The main microgrid applications are as follows:

- Plug and play integration of distributed energy resources.
- Peak-shaving and provisions for other ancillary services to the utility grid.

- Enhance reliability and system security by intentional islanding operations.
- Energy surety and supply availability through islanding operation during main grid outages and emergency conditions.
- Arbitrage of energy price differentials to minimize total energy and operational costs.

Microgrid Benefits

The intended major benefits of microgrids include:

- Facilitate the integration of distributed and renewable energy resources to minimize carbon emission, reduction of peak load demand, and minimization of line congestions and losses by locating generations near the demand.
- Enabling resiliency in the grid-infrastructure, provide local compensations for variable renewable energy sources, and supplying ancillary services and voltage regulation to sections of the bulk power system.
- Ensuring supply availability to critical loads, controlling power quality and reliability at local level and utilize demand side management (DSM) techniques to promote customer participation in electricity supply.
- Support grid modernization and interoperability of multiple smart grid interconnections and technologies.

1.2.5 Microgrid Operational Challenges

Interconnected and Islanded Operation

Microgrids interconnected with utility grids must satisfy the operational and interconnection requirements adhered by that utility grid. Microgrid systems must ensure power quality, equipment protection, synchronization, voltage control, harmonic

distortion limits, surge capabilities and ancillary services. The IEEE Std. 1547 [11] recommended practice for interconnection and islanded operation is the most commonly accepted practice at present, which does not allow islanding operation of DERs. But a new interconnection standard under development (IEEE Std. 1547a) as well as the modified IEEE Std. 1547.4 have provisions for islanding operation of DERs. Islanded mode operation of DERs is essential towards extracting the highest benefit from DERs and Microgrids. Hence seamless transition from grid-connected mode to islanded mode satisfying the interconnection and islanding requirements is crucial for successful microgrid operation. Islanding detection is the primary step towards such autonomous operation.

Dispatched, Scheduled, and Automatic Microgrid Operation

The future advanced microgrids are envisioned to have capabilities such as automatic resource scheduling and dispatch based on the system operating scenario. However such advanced operation depends upon several factors such as- energy storage and peak power delivery capabilities of ,microgrids, speed of islanding detection and speed of response of all equipment, communications, codes and standards requirements etc. Hence, power or energy management strategies to schedule the available microgrid resources to compensate for the intermittency of the renewable generations as well as forecasting of system load demands is mandatory for secure and stable microgrid operation.

1.3 Statement of Problems and Objectives

Microgrids are envisioned to have advanced features such as ability to interact with, interconnect to, and disconnect from the main grid etc. along with the essential abilities such as the ability to balance electrical demand with generation, scheduling of resources, preserve reliability and security of operations etc.

A major goal for microgrid system research and development activities is to develop promising new solutions for integrating advanced microgrids capable of operating in parallel with the utility distribution system and transition seamlessly to an autonomous power system complete with independent controls, protection, and operating algorithms. Compatible on site power generation sources and/or energy storage systems (ESS) are essential towards microgrid operation in islanded mode. Thus, distributed energy resources (DERs) including the distributed generations (DGs) and energy storage systems (ESS) along with the compatible microgrid control mechanisms become the foundation of modern microgrid technology. Moreover, demand side management (DSM) techniques such as- demand response (DR) can be incorporated in advanced microgrid system operation. Innovative DR strategies can play a crucial role in ensuring microgrid energy balance in islanded operations, and help in reduction of peak loads allowing secure and efficient system operation.

Hence, seamless transition between grid-connected mode and islanded mode of operations is crucial towards microgrid operation. The transition between different operating modes involves switching of control modes (i.e., from grid-connected controls to islanded mode control) as well as management and scheduling of available microgrid resources following the transition for secure and stable system operation.

The main objectives of this thesis are two fold:

- Development fast and accurate islanding detection methodology (IDM) to facilitate seamless transition of microgrids from grid-connected mode to islanded mode.

- Development of efficient and effective power management strategies for microgrids to ensure secure and stable microgrid operation in islanded mode.

1.4 Thesis Contributions

The major contributions of this thesis are as follows:

- A passive islanding detection method for DG units in microgrids is proposed in this thesis. The proposed method uses a unique set of critical system features derived from voltage and current measurements at target DG location, and utilizes multiple optimal decision tree classifiers in parallel for detection and classification of event specific signatures associated with islanding events. The proposed approach is capable of detection of islanding events in the presence of multiple types of DG units, under different system operating and loading conditions.

- Further, a hybrid islanding detection technique for inverter based DGs in microgrids is proposed. The proposed method combines the principles of decision trees (DTs) for passive islanding detection and Sandia frequency shift (SFS) for active islanding detection in order to enhance detection accuracy and reliability by reducing NDZ and degradation in power quality.

- A decision tree (DT) assisted controlled islanding methodology for utility-interconnected microgrids is also proposed. The proposed approach aims at the implementation of the DT based controlled islanding methodology as a preventive control component within the emergency control framework for microgrids. In the proposed approach, a contingency-oriented DT classifier trained with learning set (LS) obtained from extensive offline simulations is employed for detection of system events that require controlled islanding of microgrids a preventive measure. The proposed controlled islanding strategy is initiated upon the detection of contingency events.

- An emergency power management strategy for microgrid autonomous operation subsequent to inadvertent islanding events is proposed in this thesis. The proposed approach integrates microgrid resources such as energy storage

systems (ESS), demand response (DR) resources and controllable micro-sources (MS) to layout a comprehensive power management strategy for ensuring secure and stable microgrid operation following an unplanned islanding event. The proposed strategy consists of two main modules: 1) look-ahead scheduling module and 2) real-time dispatch module. The look-ahead scheduling module periodically defines the most adequate power management scheme considering the forecasted and available microgrid resources for that period of operation. The real-time dispatch module integrates the real-time system operating conditions with the power management scheme from the look-ahead scheduling layer to formulate the power management scheme to be implemented in the operational period of the microgrid operation.

1.5 Thesis Organization

The thesis is organized in seven chapters. This chapter presents brief overviews of distributed generation technologies and the concept of microgrids, as well as describes the motivations and contributions of the thesis in general.

Chapter 2 presents the pertinent literature reviews on DG islanding detection methodologies, controlled islanding of microgrids, and power management methodologies for microgrids.

Chapter 3 presents the proposed passive islanding detection methodology based on parallel decision trees.

Chapter 4 presents the proposed hybrid islanding detection methodology based on decision trees and Sandia frequency shift method.

Chapter 5 introduces the proposed decision tree based controlled islanding methodology for preventive control in microgrids.

Chapter 6 presents a power management strategy combining distributed generations, demand response, and energy storage systems for emergency islanding operation of microgrids.

Chapter 7 presents the overall conclusions of the thesis and also overviews the future works.

Chapter 2

Literature Review

This chapter presents literature review of the past and on-going research findings in distributed generation islanding detection methodology, and power management strategies for grid-connected and autonomous islanded operation of microgrids. A brief overview of controlled islanding applications in power systems is also presented.

2.1 Literature Review on Distributed Generation Islanding Detection Methodologies

Integration of DERs with area electric power system (EPS) enables the benefits of on-site generations which include enhanced reliability, improved power quality, reduced system losses along with other economic and environmental benefits. However, integration of DERs into the area EPS introduces several operational and technical challenges. Inadvertent islanding of distributed generations (DGs) is one of the major technical concerns associated with integration of DERs. Islanding is defined in IEEE Std. 1547 [11] as "A condition in which a portion of an area electric power system (EPS) is energized solely by one or more local EPSs through the associated points of common couplings (PCC) while that portion of the area EPS is electrically separated from rest of the area EPS". IEEE Std. 1547 recommends isolation of DG units within

a maximum of 2 seconds in events of island formation in order to prevent customer/ utility equipment damage, power quality degradation, and safety hazards [11].

Islanded operations of DGs, although capable of improving reliability and supply security, requires meticulous considerations regarding several technical and operational aspects including voltage and frequency control, protection, power quality standards, and power management strategy etc. before such islanded operations can be implemented in practice. Hence, integration of DERs requires fast and accurate islanding detection scheme as the primary step for secured system operation.

Islanding detection techniques are broadly classified as remote and local techniques. Remote techniques are essentially communication-based-techniques such as-supervisory control and data acquisition (SCADA), power line signaling and signal produced by disconnect (SPD) based methods [12, 13, 14]. Local techniques rely upon measurements of voltages and currents at target DG location for detection of islanding events. Local techniques can be further sub-divided into active and passive islanding detection methods (IDMs).

SCADA based methods, as presented in [12], allows control and monitoring of grid-connected equipment through wide area communication networks consisting of sensors for measurement of system parameters and monitoring of equipment status. Hence, SCADA networks can be utilized as a highly effective means for islanding detection. However, the cost associated with this method is uneconomical from DG standpoint. Power line carrier communications based technique for DG islanding detection presented in [13], utilizes continuous transmission of a low-energy signal between utility grid and DG. Any disruption in the communication signal is the indication of DG being islanded from the main grid. The signal produced by disconnect (SPD) method, presented in [14], is based on communication between the DG and the utility grid to detect islanding conditions. SPD differs from power line signaling in the type of transmission method utilized (microwave link, data network, etc.). Although, these techniques are reliable, but the cost associated with

the communication infrastructure requirements often makes them uneconomical from DG standpoint.

Active IDMs utilize controlled injections of small perturbations in a continuous manner into the system and observe responses of the system to the injected perturbations for islanding detection. In grid-connected mode, injected perturbations produce insignificant variations in system parameters. However, significantly larger variations in system parameters are observed when the DG is islanded.

Active IDMs proposed in literature include- harmonic injection or impedance monitoring [15], reactive power export error [16], active frequency drift (AFD) [17, 18], Sandia frequency and voltage shift (SFS/SVS) [19, 20], slip-mode frequency shift (SMS) [21], automatic phase shift (APS) [22] for grid-connected inverter based DGs, and destabilization methods based on DG frequency control mechanism [23] for synchronous generator based distributed generations.

Harmonic injections or impedance monitoring method presented in [15], utilizes intentional injections of specific current harmonic at the PCC. In grid-connected mode, if the grid impedance is lower than the local load impedance, then the injected harmonics will flow into the grid. Whereas, in islanded mode, the injected harmonics will flow through the local DG loads, producing specific harmonic voltages. The generated harmonic voltages will be proportional to the load impedance at that particular harmonic frequency. Performance of this technique is unaffected in the presence of multiple inverters in the system. However, it is sensitive to grid perturbations, which makes the threshold establishment more difficult for islanding detection. For instance, with non-linear loads, the voltage distortion at the PCC can be so high that islanding scenario may be erroneously detected even if the grid is present. Additionally, with linear loads, variations in total harmonic distortion in voltage may be too low to be detected.

The active frequency drift (AFD) method presented in [17, 18], varies the frequency of the inverter output current through introduction of phase error between the inverter output current and voltage at the PCC. This method enables easy

implementation and can be applied to multiple inverters scenarios. However, the AFD method produces degradation in the power quality of the DG output and the inverter has an NDZ that depends on the value of the AFD parameters.

Sandia frequency shift (SFS) method presented in [19] is essentially a variation of AFD method with positive feedback. SFS method injects small perturbations in inverter output current and uses positive feedback to destabilize system frequency. In grid-connected mode, injected perturbations produce insignificant variations in system frequency; whereas, in islanded mode, system will observe significantly larger frequency variations are caused by the injected perturbations. Perturbations are injected in inverter output current as one zero time segment per line semi-cycle. The ratio of zero time to half of the period of voltage waveform, is called chopping fraction. Positive feedback formulated as linear function of deviation in frequency of PCC voltage is applied to chopping fraction which causes frequency to deviate from nominal value in absence of the grid. SFS method is implemented in conjunction with OFP/UFP protection schemes.

Sandia voltage shift (SVS) method presented in [19, 20], applies positive feedback to the magnitude of the PCC voltage of the DG unit. With any decrease in the voltage magnitude, the PV inverter reduces its current output and thus its power output. If the utility grid is connected, there is little or no effect when the power is reduced. However, in the absence of the utility grid (i.e. in islanded mode of operation), any reduction in voltage magnitude, will cause further reduction in the magnitude of voltage as dictated by the Ohm's law response of the RLC load impedance to the reduced current. This additional reduction in the amplitude of voltage leads to a further reduction in PV inverter output current, leading to an eventual reduction in voltage that can be detected by the under voltage protection (UVP). It is possible to either increase or decrease the power output of the inverter, leading to a corresponding OVP or UVP trip. It is however preferable to respond with a power reduction and a UVP trip as this is less likely to damage load equipment [20].

In order to prevent the degradation of performance of active frequency drifting IDM with positive feedback (i.e. Sandia Frequency Shift) and also of Sandia voltage shift (SVS) technique caused by averaging effects in multi-inverter systems, all the inverters in the system should have the same frequency/voltage drift directions (drift up/down). Although, performance degradation resulting from parameter settings and measurement errors can happen, but the overall effect on the islanding detection capability in the system is negligible as discussed in [17].

Slip-mode frequency shift (SMS) [21] method utilizes positive feedback to destabilize the PV inverter when the utility grid is not present, thereby preventing a steady state operation that would allow a long run-on in islanded mode. SMS applies positive feedback to the phase angle of the inverter voltage as a method to shift the phase, hence the short-term frequency. In grid-connected mode of operation, the frequency of the grid will not be impacted by this feedback. However, in islanded mode, the frequency of the grid will drift from nominal frequency value. SMS techniques has disadvantages similar to other active islanding detection techniques such as - periodic injections of small perturbations and degradation in power quality.

The automatic phase shift (APS) [22] method is based on the phase shift of the sinusoidal inverter output current. When the utility malfunctions, the phase-shift algorithm keeps the frequency of the inverter terminal voltage deviating until the protection circuit is triggered. The effectiveness of this technique relies on the initial phase difference between the inverter output current and inverter terminal voltage in islanded mode of operation, the technique still works for completely resistive loads or paralleled RLC loads with resonant frequency equal to line frequency [22].

Positive feedback based destabilization methods for synchronous generator based DGs are discussed in [23]. Positive feedback is applied to destabilize the frequency or voltage in the islanded system, which results in the activation of UFP/OFP or UVP/OVP protection schemes. In grid-connected mode of operation, the destabilization method has little effect on the system frequency or voltage, whereas, in islanded mode of operation, the destabilization method induces significant

variations in system frequency or voltage. As synchronous generator based DGs are characterized by higher inertia and longer time constants, two different positive feedback based techniques are introduced in [23]. Active power based islanding detection scheme utilizes the variations in system frequency to modify the active power reference of the DG unit, whereas, reactive power based islanding detection scheme utilizes system voltage variations to modify the reactive power reference of the DG unit.

Although active IDMs have smaller non-detection zones (NDZ), but power quality degradations caused by perturbation injections and longer detection times are major impediments. Moreover, as the perturbations are continuously injected at predefined intervals, any islanding events occurring between intervals may have to wait until next perturbation injection in order to be detected, which further prolongs the detection time.

Passive IDMs rely upon local measurements of critical system parameters (such as- voltage, current etc.) and detect islanding events by searching for abrupt variations in these system parameters induced by various system events (such as load/capacitor switching events, faults and islanding events etc.). Passive IDMs are simple and easy to implement, and inexpensive. However, passive IDMs suffer from detection inaccuracies for system operating scenarios when generation and load in the islanded system are approximately balanced (i.e. low generation and demand mismatch scenarios). Passive IDMs proposed in literature include methods based on over/under voltage (OVP/UVP) [24], over/under frequency (OFP/UFP) [24], rate-of-change of frequency (ROCOF) [25], rate-of-change of voltage (ROCOV) [26], vector surge relays (VSR) [25], rate-of-change of phase angle deviation (ROCPAD) [27], and voltage unbalance/total harmonic distortion (VU/THD) [28]. A passive islanding detection technique based on directional reactive power detection for synchronous generator based DGs is also proposed in [29].

The over/under voltage (OVP/UVP) [24] and over/under frequency (OFP/UFP) [24] methods for islanding detection are based on predefined voltage and frequency set

points of frequency based protection and voltage based protection respectively. These methods are simplest of the passive islanding detection methodologies. However, these methods suffer from larger non-detection zones in cases where generation and demand are approximately balanced in the islanded system. The ROCOF relay for islanding detection is presented in [25] utilizes the rate-of-change of frequency to detect the islanding events instead of relying on frequency magnitudes. Islanding detection methodology based on rate-of-change of voltage ROCOV [26] depends on the rate at which the magnitude of the system voltage at the point of common coupling is changing following a system event. An islanding detection methodology based on rate-of-change of phase angle deviations (ROCPAD) is proposed in [27]. The methodology proposed, utilizes the variations in changes in voltage phase angle to detect the islanding events. An islanding detection methodology utilizing voltage unbalance and total harmonic distortion in voltage (VU/THD) is presented in [28] which utilizes changes in voltage unbalance and voltage total harmonic distortion caused by system events to detect islanding scenarios. All of these islanding detection methodologies are based on measurement of specific system parameters and utilization of a predefined threshold setting for detection of islanding events.

The vector surge relay presented in [25] functions by monitoring the rate of change of the rotor displacement angle of the generator. During parallel operation there is an angular difference between the terminal phase voltage and the internal synchronous voltage of the generator. This is due to the fact that the generator rotor is magnetically coupled to the generator stator and is forced to rotate at the grid frequency. The angle between the vector of the mains voltage and synchronous electromotive force is known as the rotor displacement angle. This angle is constantly varying and is dependent on the torque produced by the generator rotor. In the case of the grid failure, there is sudden change in the rotor displacement angle. This causes a surge in the generator voltage. The relay works by monitoring the time taken between the zero-crossings in the waveform. Under normal operation, the time interval between two consecutive zero-crossings is almost constant. During the grid

failure, the vector surge which occurs causes a delay in the zero-crossing. This delay is detected by a highly sensitive timer inside the relay and the relay operates. The relays are usually set to operate for a change in the rotor displacement angle of 0 to 20 degrees.

Several passive IDMs based on intelligent approaches have also been proposed in literature. Intelligent based approach using decision trees to classify system events is proposed in [30, 31] which is mainly based on critical system attributes derived from voltage measurements. System voltages measured in real-time are utilized to extract a set of critical system attribute which is utilized in the classification of system events. The set of extracted crititcal system parameters are used in development of a classification tool based on decision tree classifiers.

A decision tree based threshold setting methodology is for islanding detection relays is proposed in [32]. The proposed approach utilizes decision tree based data mining algorithm to define the threshold values for detection of islanding events in islanding detection relays. The approach uses offline simulations of system events to generate training data for decision tree training and development of classification model for threshold setting in the proposed methodology.

An islanding detection method using wavelet transformation for feature extraction and decision trees to classify the events is presented in [33]. Wavelet transformation is utilized to allow a time-varying representation critical system attributes. The critical attributes are mainly derived from current measurements. Decision tree classifiers were used to extract the classification model and detection of islanding events. Ref. [34] presents a performance comparison of the islanding detection scheme presented in [33] with other conventional islanding detection schemes. It is demonstrated that building individual DT classifiers for each of the DGs provides more accurate results compared to developing a generalized DT classifier for all of the DGs in the system.

An islanding detection method based on Random Forest classifier is presented in [35], which utilizes techniques similar to the previous approaches for measurement of system parameters, but utilizes Random Forest classifiers for classification of system

events. A brief comparison of the several islanding detection methodologies based on data mining techniques is also provides. Comparison results indicate that RF classifiers offers more accurate performance over other data mining based passive islanding detection methodologies. Although, random forest (RF) classifiers are robust and accurate, however their black-box nature is makes their implementation in practical systems challenging.

Microgrid security assessment and islanding control using Support Vector Machine (SVM) is investigated in [36]. A comparative analysis of intelligent classifiers based on data mining techniques is presented in [37]. Five different classification techniques were investigated- decision tree (DT), Nave-Bayes classifier, Support Vector Machines (SVM), Multilayer Perceptron (MLP) neural networks, and Radial Basis Function (RBF) neural networks. Among the classification methods considered, multi-layer perceptron (MLP) and decision tree (DT) based classifiers offer best performances. Overall classification accuracy for MLP classifiers is slightly higher than the DT classifiers. However, DT classifiers offer higher dependability in islanding detection which is critical, since the cost of misclassifying an islanding case as non-islanding is often larger than misclassifying a non-islanding case.

Passive islanding detection techniques for synchronous generator based DGs are proposed in [29] and [38]. Anti-islanding scheme utilizing directional reactive power measurements for synchronous generator based DG is presented in [29]. In the proposed approach, generator automatic voltage regulator (AVR) setting is used to extract the pre-fault reactive power at the PCC, based on which a reactive power export level is determined, for which directional reactive power relay can be set to trip for islanding conditions. A decision tree based islanding detection methodology is proposed in [38] for protection of synchronous generator based DGs. The proposed method extracts system parameters from voltage and current measurements and utilizes decision tree based classifiers to detect islanding events.

An intelligent protection scheme combining wavelet transformation and data-mining technique is presented in [39]. The process retrieves current signals and

pre-processes the retrieved current signals using wavelet transformation to extract system attributes, which are then used in decision tree based classifiers to detect and classify system faults. Two classifiers were developed for fault detection and fault classification.

In general, Passive methods offer simpler implementation and faster detection time without any degradation in power quality. However, passive methods can be less accurate, especially when generation and demand are approximately balanced in the islanded system.

Hybrid islanding detection methods combining active and passive islanding detection methods are also proposed in literature [40, 41, 42]. Hybrid IDMs based on average rate-of-change of voltage/real power shift [40] and voltage unbalance/ frequency shift [41] are proposed in literature. Hybrid islanding detection methods combine passive techniques and active techniques to enhance the detection accuracy and minimize the power quality degradation. The methods presented in the literature, consider synchronous/asynchronous DGs only (e.g. diesel generators, wind turbine generators, etc.) and requires manual selection of the threshold values based on designer or operator experience for the passive detection scheme. Hybrid IDMs improve detection accuracy and reduce NDZ, hence the reliability of the detection process is improved.

2.2 Literature Review on Intentional Islanding Operation of Distributed Generations

Islanded operation of distributed generations (DGs) has been extensively investigated in literature [43, 44, 45, 46]. Ref.[43] discusses the microgrid concept and elaborates control methodologies for control of micro-sources withing the microgrid. Different control strategies for real and reactive power control of individual DG units as well as power sharing between DG units are discussed. Control methods such as

voltage/reactive power droop, flow/active power droop, frequency/active power droop etc. are investigated.

Control of grid-connected and intentional islanding operations of distributed generations is investigated in [44, 45]. Various aspects of both grid-connected and autonomous operations of distributed generations such as- loss of mains detection, load shedding in autonomous mode of operation, synchronization for grid re-connection etc. are discussed. Ref. [46] discusses the AEP/CERTS microgrid test system. Microsources used in the system, control methodologies for grid-connected and autonomous mode of operation are discussed, and results from field tests are presented.

Grid-connected and autonomous controls of inverter based DGs are investigated in [47]. A new control strategy for implementation of intentional islanding operation of inverter based DGs is proposed which utilizes two different control schemes for grid-connected and islanded operations. A hybrid islanding detection scheme is also proposed for islanding detection and switching the controls to appropriate method based on system operation status is also presented.

Power management and control methods for intentional islanding operations of inverter fed microgrids are proposed in [48, 49]. Ref. [48] presents a power management strategy for distributed energy resources in a distribution feeder. The proposed methodology categorizes the DGs into two groups- utility owned DGs and independent power producer (IPP) owned DGs. The utility owned DGs are allowed to operate in the islanded mode, whereas, DGs owned by IPPs are stopped to avoid any damage to the grid and/or the DGs. The power management strategy operates the controllable DGs in order to maximize the efficiency of the islanded system. A detailed case study investigating transition management in various modes of microgrid operation (i.e. islanding, reconnection, black start etc.) are presented in [49]. A microgrid test system based on IEEE 34 bus distribution test system with high penetration of renewables is utilized in the study.

Intentional islanding of DGs for improvement of service reliability are studied in [50, 51, 52]. Ref. [50] discusses an algorithm for optimal placement of automatic sectionalizing switching devices (ASSDs) to improve the reliability of active distribution networks consisting of distributed generations. The optimal number and position of ASSDs were determined by the availability of distributed generations capable of meeting the load demand in the islanded system and maintaining acceptable voltage and frequency in the islanded system. Control strategies for microgrid intentional islanding during network emergencies are discussed in [51]. Technical challenges associated with microgrid islanding operation such as - frequency, steady state voltage, and protection issues are discussed, and a control strategy for intentional islanding operations of microgrid is presented as well. In Ref. [52], regulation of distributed generations using intentional islanding operations in smart grid environment is investigated. Analysis of the microgrid with generator PQ control and PV control for islanding operation has been carried out using the Real Time Digital Simulator (RTDS) platform.

Impact of intentional islanding of distributed generations on electricity market prices is evaluated in [53]. The effects of intentional islanding operation of DGs on close-to-real-time electricity market prices is examined. Market clearing price is determined using optimal power flow problem with additional constraint accounting for the effects of intentional islanding. The cost associated with unsatisfied electricity demand because of the intentional islanding is also investigated.

Intentional islanding operation has the capability to enhance reliability and availability of microgrids comprising of distributed generations (DGs) and energy storage systems. Through safe intentional islanding operations, it is possible to contain the effects of disturbances and maintain availability of supply with required power quality to critical loads [54]. Pattern recognition techniques have been extensively applied in wide variety of power system related applications. Decision tree based pattern recognition techniques have found broad acceptance in power system applications due to its simplicity, ease of implementation and speed of

execution. DT based techniques have been applied to power system applications such as- online dynamic security assessment of power systems [55], high impedance fault detection in power systems [56], dynamic security assessment, and online preventive and corrective control [57], controlled islanding in power system [58], online voltage security assessment [59], and detection of impending loss of synchronism [60].

2.3 Literature Review on Power Management Methodologies for Microgrid Operation

Microgrid management strategies can be divided into energy and power management strategies [61, 62]. Energy management strategies optimize system operation with the objective of minimizing the operating costs in longer terms considering the system operating constraints. Whereas, power management strategies optimize the operation of the system for much shorter terms in order to achieve certain objectives. Both energy and power management strategies involve optimal allocation of the available resources and control implementations based on respective objectives. Several microgrid management strategies have been presented in literature, including energy management strategy of microgrid in grid-connected and islanded mode of operation [61], coordination of energy storage and demand response resources for microgrid emergency operation [63], power management strategy for microgrid autonomous operations using energy storage and demand response [64], cooperative control of energy storage and microsources for power management in microgrids during islanded operations [65], microgrid autonomous operation during and subsequent to islanding process [66], and real-time centralized demand response strategy for primary frequency regulation of microgirds [67]. Demand side management techniques such as- demand response, smart loads, and intelligent energy systems are discussed in [68]. A distributed agent based methodology for real-time power management and control of microgrid is presented in [69]. Multi-agent system for real-time operation of a microgrid in real-time digital simulator is presented in [70]. A multi-agent based

approach for energy resource scheduling in microgrids in presented in [71]. Multi-agent based approach for energy management in microgrids using demand response and distributed storage is presented in [72].

Ref. [61] presents a coordinated double-layer approach for microgrid energy management. The proposed approach consists of schedule layer and dispatch layer. The schedule layer utilizes forecasting data to formulate an economic operation scheme for microgrid operation, whereas the dispatch layer uses real-time data to set the outputs of the controllable microsources. The variability associated with the uncontrollable microsources based on renewable energy resources is resolved through the provision of having adequate active power reserve in the schedule layer and utilizing this reserve in the dispatch layer.

An emergency demand response scheme for microgrid emergency autonomous operation based on local frequency measurement is proposed in [63]. The proposed emergency demand response strategy utilizes controllable loads and electric vehicles (EVs) in microgrid power management during emergency operations. A power management methodology combining the aforementioned demand response and available controllable microsource is also presented in [63]. Simplified dynamic models were used in dynamic simulations to verify the effectiveness of the proposed power management strategy for microgrid emergency operation.

A multi-timescale power management strategy is presented in Ref. [64]. The proposed strategy consists of two layers operating in different time frames to account for the intra-interval dynamics of highly dynamic power system components such as- electric water heaters (EWH) and battery energy storage systems (BESS). Two different control strategies for EWH control as well as two different demand response strategies were proposed. Performance of the proposed power management strategy is compared for the two different demand response strategies proposed as well as for the case with no demand response in the system.

Cooperative control strategy for utilizing energy storage system (ESS) and microsources during microgrid emergency islanding operation is presented in [65]. A

two layer control structure is proposed; where, the primary control action is provided by the ESS and secondary control action is implemented by microgrid management system (MMS). Primary control is realized using constant frequency and constant voltage control in ESS; whereas, controls in microgrid management system acts as the secondary control which is designed to drive the power output from ESS to zero.

Ref. [66] investigates the typical electromagnetic transients in microgrids caused by pre-planned and unplanned islanding events, and illustrates the use of appropriate control of DG units to minimize the impact of transients and maintain the stability of the microgrid system after islanding. The presented case study indicates that microgrids with synchronous generator based DGs are capable of maintaining angular stability in the islanded system, primarily through its active power control. However, electronically interfaced DGs should be equipped with fast and independent active and reactive power controls. Control and power management scenarios with all inverter based DGs and/or multiple inverter based DGs along with other types of DGs are not discussed.

A centralized demand response (DR) strategy for primary frequency regulation in microgrids in discussed in [67]. The proposed DR strategy consists of three modes of operations and utilizes two different control strategies (i.e. adaptive hill climbing control and step by step control) for the DR resources. Case study results were presented to demonstrate the effectiveness of the proposed strategy in different operating scenarios in microgrid.

Ref. [68] presents a detailed overview of the demand side management techniques such as- demand response, smart responsive loads, and intelligent energy systems. Various demand side management tools including energy efficiency, energy controllers, demand response, distributed spinning reserves, demand shifting are discussed. Two demonstration projects are also discussed in Ref. [68].

A multi-agent system (MAS) for comprehensive power management functions in microgrids is presented in Ref. [69]. Microgrid power management and control framework based on distributed agents were investigated as well as the development of

a simulation environment to emulate the real-time operation of microgrid agents and their controlled assets were also discussed. Performance of the proposed methodology is investigated under various system operating conditions (such as- spot market price change, loss of solar PV unit etc.) during grid-connected mode of operations. However, the proposed methodology was implemented only for grid-connected mode of operations.

Multi-agent system based real-time microgrid power management strategy consisting of generation scheduling and demand side management is proposed in [70]. The generation schedule coordination agent combines a two stage scheduling- 1) day-ahead scheduling for hourly power setting for DERs from a day ahead energy market and 2) real-time scheduling for coordination between the day ahead scheduling and real-time system operating conditions. Demand side management agent is responsible for load shifting in day ahead scheduling and load shedding in real-time scheduling. Although, the proposed approach enables a common platform for all microgrid components to interact with each other and optimize the microgrid system operations in grid-connected mode, applicability of the proposed approach and/or methodology in islanded mode of operation were not investigated.

A multi-agent based approach for resource scheduling of an islanded power system with microgrid and lumped load is proposed in Ref. [71]. The resource scheduling process consists of three stages- 1) resource scheluling for satisfying individual microgrid's demand, 2) exporting power to the power system and compete in energy market, and 3) rescheduling of each microgrid's resources to meet the internal microgrid demand as well overall system demand in an optimal way.

An agent based energy management system to facilitate power trading between microgrids having demand response resources and distributed energy storage is proposed in [72]. The proposed approach utilizes thr diversity in consumer load consumption patterns and energy availability of DERs to reduce peak demand and cost of electricity.

Moreover, reactive power planning under high penetration of wind energy is presented in [73], coupon based demand response (CBDR) strategy considering wind power uncertainty is presented in [74], strategic scheduling of energy storage for load serving entities in locational marginal pricing (LMP) market is presented in [75], evaluation of LMP intervals and Strategic CBDR bidding strategies consider wind energy are proposed in [76, 77].

Power management strategies for grid-connected operation of microgrids are extensively studied in the literature. However, power management strategy integrating various generation, energy storage, and demand response resources is of utmost importance for microgrid emergency autonomous operations. Moreover, the power management strategy for autonomous microgrid operation should offer flexibility in integrating new microgrid resources in the management framework without significantly increasing computational burden and processing time.

Chapter 3

A Parallel Decision Tree Based Methodology for Islanding Detection of Distributed Generations

This chapter presents a passive islanding detection methodology for distributed generations (DGs) based on decision trees (DTs). In the proposed approach, a set of critical system attributes is utilized to capture the underlying signatures of a wide variety of system events on these critical system attributes through the utilization of DT based pattern recognition tool for DG islanding detection. The proposed methodology employs multiple optimal DTs in a parallel network for DG islanding detection. The use of multiple optimal DTs in parallel enables effective utilization of different combinations of critical system attributes over a wide range of power mismatch scenarios to enhance the reliability and accuracy of the proposed islanding detection scheme. Detailed case study on a grid-connected microgrid model based on IEEE 13 bus distribution system demonstrate the effectiveness of the proposed method in detection of islanding events. Moreover, performance of the

proposed methodology is validated on OPAL-RT/RT-LAB based real-time digital simulator using a software-in-loop (SIL) simulation environment. Case study results indicate that the proposed method can detect islanding events with high accuracy and reliability.

In the proposed approach, multiple optimal DTs developed from subsets within a comprehensive set of critical system attributes are employed in a parallel network of DTs for detection of islanding events. Employing multiple optimal DTs in parallel enhances the accuracy and reliability of the islanding detection process through minimization of variable masking problem associated with DTs and enabling better utilization of different combinations of critical system attributes over a broad range of power mismatch scenarios in the islanded system. The set of critical system attributes is selected to provide a systematic approach for capturing essential characteristics of the system, to reduce NDZ, and enhance islanding detection accuracy in the presence of multiple types of DGs under different system operating conditions (OCs). The proposed approach can be implemented for inverter based DGs as well as synchronous generator based DGs.

The chapter is organized as follows. Decision Tree (DT) principles are presented in brief in Section 3.1. The proposed methodology is presented in Section 3.2. Section 3.3 describes the test system model. Sections 3.4 present case study results and analysis. Finally, conclusions are presented in Section 3.5.

3.1 Decision Tree Principles

Decision trees (DTs) belong to a class of supervised machine learning techniques capable of extracting useful information from large data sets and provide assistance in classification of input vectors into discrete categories [78]. The classification and regression trees (CART) introduced by Breiman et al. [79] can be employed as a decision support tool for the classification of unseen events. The classification algorithm combines hyperplanes parallel to coordinate axes to approximate multiple

separation boundaries for splitting a complex decision process into a collection of simple decision processes [78].

DTs are developed from a learning set (LS) and a test set (TS). Trained with a learning set (LS) consisting of input-output pairs, DTs are capable of extracting underlying relationship (decision rules) between the inputs (critical attributes called predictors) and outputs (class). These decision rules serve as a predefined logical paths in the classification process and can be utilized for classification of unseen inputs.

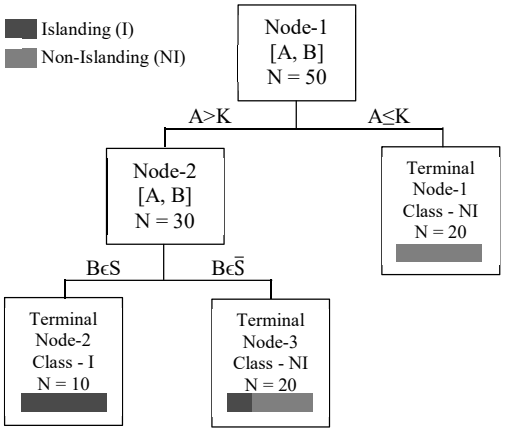

Figure 3.1: DT example.

The training process initiates with Root Node which contains the complete learning set (LS). Each of the Internal Nodes tests a critical attribute (CA) and each Arc corresponds to an attribute value. The learning process is achieved by recursively splitting the learning set (LS) into two purer subsets according to the critical splitting rule (CSR) at each of the internal nodes. A critical splitting rule (CSR) is the optimal splitting rule with the minimum over all GINI impurity index among all of the possible splitting rules [78, 79]. The GINI impurity index [78, 79] is

a measure of impurity of a node and is defined as follows:

$$g(t) = \sum_{j \neq i} c(i|j)p(i|t)p(j|t) \tag{3.1}$$

where $p(i|t)$ and $p(j|t)$ are the probabilities of *class* i and *class* j at *node* t respectively. $c(i|j)$ is the cost of classifying a *class* j case as a *class* i case. The terminal Node represents the predicted class of an input vector. TS containing the vector of predictors representing unseen cases are used to evaluate the developed DT classifiers. A commonly used performance index is mis-classification cost [55], which is calculated as:

$$R^{ts} = \frac{1}{N^{ts}} \sum_{i,j} c(i|j).N_{ij}^{ts} \tag{3.2}$$

where N^{ts} is the total number of cases in TS, $c(i|j)$ is the cost of misclassifying a *class* j case as *class* i case and N_{ij}^{ts} is the number of *class* j cases in TS which are predicted as *class* i cases. The cost of misclassifying an islanding case as a non-islanding one is often made larger than that of misclassifying a non-islanding case, because of the impacts associated with missing an islanding event. The correctness rate of classifying *class* i cases is calculated as [55]:

$$CR_i^{ts} = \frac{N_{ii}^{ts}}{N_i^{ts}} \times 100\% \tag{3.3}$$

where N_i^{ts} and N_{ii}^{ts} are the total number of *class* i cases and correctly classified *class* i case in TS. The correctness rate of classifying islanding and non-islanding cases are known as dependability index (DI) and security index (SI), which along with the mis-classification cost are used as indices for selection of optimal DT classifiers. The developed DTs are ranked based on the two following criteria: (1) minimum misclassification cost, such that $DT_i^* = min(R_i^{ts}), \forall i$ and (2) highest DI and SI, such that, $DT_i^* = max(SI_i)max(DI_i), \forall i$. In this paper, five best performing or

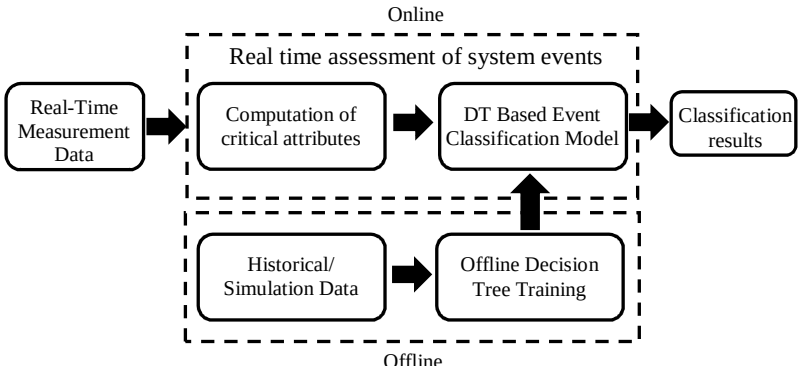

Figure 3.2: Conceptual model of the proposed islanding detection methodology.

optimal DTs are selected according to the aforementioned criteria. DT classifiers offer robustness, ease of interpretation and implementation compared to other intelligence based approaches such as- Support Vector Machine (SVM) and Random Forest (RF) classifiers.

3.2 Proposed Methodology

The proposed passive islanding detection methodology involves five main steps: (1) dataset generation for DT training, (2) offline DT training, (3) parallelization of optimal DTs, (4) periodic DT update, and (5) online implementation.

3.2.1 Dataset Generation for DT Training

The learning set (LS) for DT training is generated using extensive offline simulations of a wide variety of system events. Each of the system events are simulated under operating conditions (OCs) representative of past and forecasted operational states of the system. For each event under different OCs, detailed electromagnetic simulation is performed, and measurements of voltage and current are obtained at target DG locations (at PCC of the DG unit with distribution network). Predictors (critical system attributes) utilized in the classification of system events are extracted from the obtained measurements and each event is assigned a class, islanding (I) or non-islanding (NI) representing the type of the event. In order to ensure satisfactory

performance of DT classifiers, LS should contain a wide variety of training examples representing essential characteristics of the system. The following is a categorical list of system events considered in offline simulations.

- All possible tripping of circuit breakers leading to formation of islands.
- Islanding events in area-EPS and/ or loss of power on PCC bus at the target DG locations.
- Loss of line in area-EPS transmission and/ or distribution network.
- Abrupt load changes in area-EPS and/ or target DG locations.
- Capacitor bank switching events in area-EPS.

These events have been simulated under various operating states of area-EPS and distribution network or microgrid which include operations with normal, minimum and maximum loading conditions. Different loading conditions at the PCC bus and various operating states of target DG units have also been considered in development of the training dataset.

3.2.2 Offline Decision Tree Training

In the proposed methodology, parallel combination of multiple optimal DTs is used for the detection of DG islanding events. The DTs built in the proposed scheme are classification trees, which are developed from the training dataset containing n-dimensional feature vectors containing predictor values and corresponding class values. Developed DTs can predict the class of an unseen event from the n-dimensional vector of predictors presented to it for classification.

The mathematical formulation for the proposed approach can be illustrated as:

$$X_i = \left\{x_1^i, x_2^i, x_3^i, ..., x_{15}^i\right\}; i = 1, 2, 3, ..., N \tag{3.4}$$

$$F = [X_1, X_2, ..., X_N]^T \tag{3.5}$$

$$Y = [y^1, y^2, ..., y^N]^T \tag{3.6}$$

where X_i is the vector of predictors containing predictor values for i^{th} event, F is the matrix containing vectors of predictor values for each of the N system events, Y contains the class values (i.e. $y_i = 0$ for *non-islanding* events and $y_i = 1$ for *islanding* events) corresponding to each vector of predictors X_i for each of the N system events. The complete data model (E) for DT classifier training can be expressed as follows:

$$E = [F\ Y] = \begin{bmatrix} x_1^1 & x_2^1 & x_3^1 & .. & x_{15}^1 & y^1 \\ x_1^2 & x_2^2 & x_3^2 & .. & x_{15}^2 & y^2 \\ : & : & : & .. & : & : \\ x_1^N & x_2^N & x_3^N & .. & x_{15}^N & y^N \end{bmatrix} \tag{3.7}$$

The proposed method relies on a comprehensive set of predictors extracted from local measurements of voltages and currents at target DG location and recognition of system event specific signatures associated with these predictors through the application of DT classifiers for the detection of islanding events. The set of predictor is selected to capture the essential characteristics of each system events. In the proposed approach, a total of 15 predictors extracted from voltage and current measurements are utilized. Table 3.1 lists the set of predictors used in the classification process.

3.2.3 Parallelization of Multiple Optimal DTs

Classification performance from a solitary DT may suffer from data over-fitting and variable masking problems. Employing a parallel network of multiple optimal DTs for system event classification enables better utilization of different combinations of critical system attributes over a wide range of system operating conditions. Parallel DT networks have been successfully utilized in the past for problems such as user authentication based on keystroke pattern recognition [80]. Hence, a combination of multiple optimal DTs is utilized in this paper in order to improve the reliability and accuracy of the classification process. In this approach, multiple DTs are trained

Table 3.1: Predictors Used in Classification of System Events

Predictors	*Description*
$x_1^i = \Delta V_i$	Voltage deviation for i^{th} event (Volts)
$x_2^i = \left(\frac{\Delta V}{\Delta t}\right)_i$	Rate-of-change of voltage for i^{th} event (Volts/cycle)
$x_3^i = \Delta f_i$	Frequency deviation for i^{th} event (Hz)
$x_4^i = \left(\frac{\Delta f}{\Delta t}\right)_i$	Rate-of-change of frequency for i^{th} event (Hz/sec)
$x_5^i = \Delta I_i$	Change in current for i^{th} event (A)
$x_6^i = \left(\frac{\Delta I}{\Delta t}\right)_i$	Rate-of-change of current for i^{th} event (A/cycle)
$x_7^i = \left(\frac{V_-}{V_+}\right)_i$	Voltage unbalance for i^{th} event
$x_8^i = V_{THDi}$	Total harmonic distortion in voltage for i^{th} event
$x_9^i = I_{THDi}$	Total harmonic distortion in current for i^{th} event
$x_{10}^i = \left(\frac{{V_a}^3}{{V_a}^1}\right)_i$	Relative amplitude of 3^{rd} harmonics of voltage
$x_{11}^i = \left(\frac{{V_a}^5}{{V_a}^1}\right)_i$	Relative amplitude of 5^{th} harmonics of voltage
$x_{12}^i = \left(\frac{{I_a}^2}{{I_a}^1}\right)_i$	Relative amplitude of 2^{nd} harmonics of current
$x_{13}^i = \left(\frac{{I_a}^3}{{I_a}^1}\right)_i$	Relative amplitude of 3^{rd} harmonic of current
$x_{14}^i = \left(\frac{{I_a}^5}{{I_a}^1}\right)_i$	Relative amplitude of 5^{th} harmonic of current
$x_{15}^i = \theta_{{Ia}^3 i}$	Phase of 3^{rd} harmonics of current for i^{th} event

with various combinations of predictors which are subsets selected from full set of predictors. Optimal DTs selected based on the criteria presented in Section 3.1 are employed in parallel instead of entrusting the DT with the best performance. Individual DTs in the parallel network should be sufficiently different from each other in order to avoid the variable masking problem. Hence, the predictors presented in Table 3.1 are grouped and DTs are developed with predictors from each of the groups.

In the proposed approach, five optimal DTs are employed in parallel. The overall classification accuracy p of the parallel DT network is determined as [80]:

$$p = 1 - \prod_{i=1}^{5}(1 - p_i) \tag{3.8}$$

$$p = 1 - (1 - p_1).(1 - p_2).(1 - p_3).(1 - p_4).(1 - p_5) \tag{3.9}$$

where p_i is the classification accuracy of the i^{th} DT and $1 - p_i$ is the misclassification rate of i^{th} DT in the parallel DT network. The final classification result is the class value of the majority of the DTs in the parallel network.

Multiple DTs developed with different combinations of predictors may be able to accurately classify those cases which are misclassified by some of the individual DTs in the combination. Hence, a parallel combination of multiple optimal DTs can be applied to obtain a comprehensive and accurate classification result. Furthermore, employing a parallel combination of multiple optimal DTs for real-time classification of system events for islanding detection will neither incur significant processing-time to the overall operational time nor add significant computation burden to the overall process.

3.2.4 Periodic DT Update

Developed DT classifiers can be periodically updated through the incorporation of changing system states in the DT building process. Performances of the developed DT classifiers are evaluated during each operation time horizon. If significant changes in system operating conditions (in generation status, load levels, system topology etc.) exist and existing DTs do not perform satisfactorily under new OCs, then offline event simulations are carried out with the new OCs and new DTs are trained with extended learning set (LS) containing the new cases alongside the original cases. The updated DT classifiers are then used in the parallel DT network for online applications for the

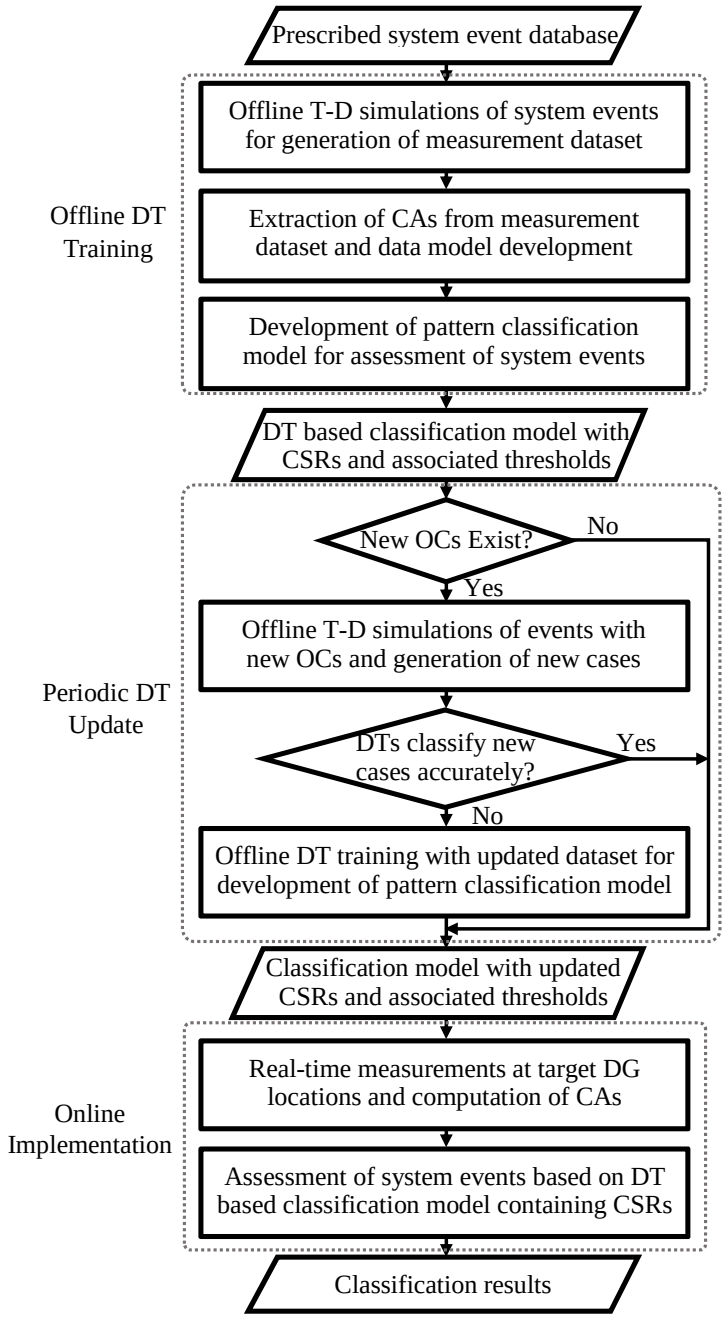

Figure 3.3: Outline of the DT classifier development and implementation steps in the proposed methodology.

upcoming operational period. Fig. 3.3 presents the flow diagram of the DT classifier development approach utilized in the proposed methodology.

3.2.5 Online Implementation

Measurements of voltages and currents at target DG locations are obtained in real time. Vector of predictors utilized in the classification process are computed and compared with the CSRs of the DTs in the parallel network. Classification results from each of the DTs are combined and necessary security measure is appropriated if an islanding event is detected. Fig. 3.4 represents the online implementation methodology of the proposed approach.

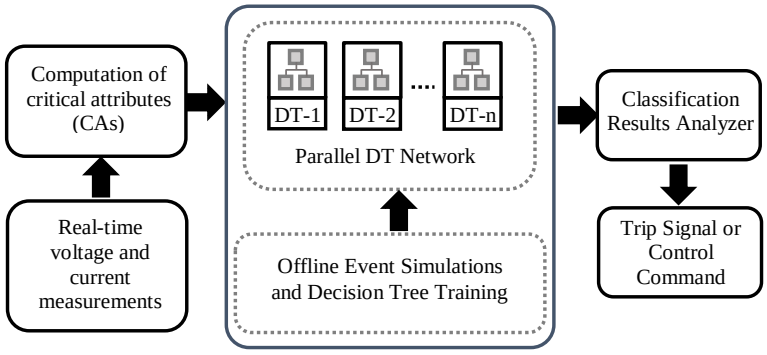

Figure 3.4: Outline of the implementation of the proposed islanding detection methodology.

3.3 Test System Model

IEEE 13 node distribution system model [81] modified with the addition of distributed generations (DGs) and battery energy storage system (BESS) is used in the case study for evaluation of the proposed islanding detection scheme. The test system, presented in Fig. 3.5, consists of a 3.125 MVA emergency diesel generator, two PV farm with the capacities of 200 kW and 400 kW at an irradiance of 1000 W/m^2 and a 150 kWh BESS along with associated controls. The IEEE 13 node feeder system is operated at 4.16 kV with unbalanced loads (both single phase and three phase loads) and

shunt capacitor banks to model a representative distribution system. The utility grid is modeled as the 2-area, 4-generator system described in [82]. The utility grid is operated at 230 kV and interconnected with the microgrid via 230kV/25kV and 25kV/4.16kV step-down transformers. The 2-area system has a relatively small size but is able to exhibit typical power system dynamics. Thus, interactions between the main grid and distribution system/ DG can be examined. The distribution network/ microgrid model is connected to area-1 of the two area system.

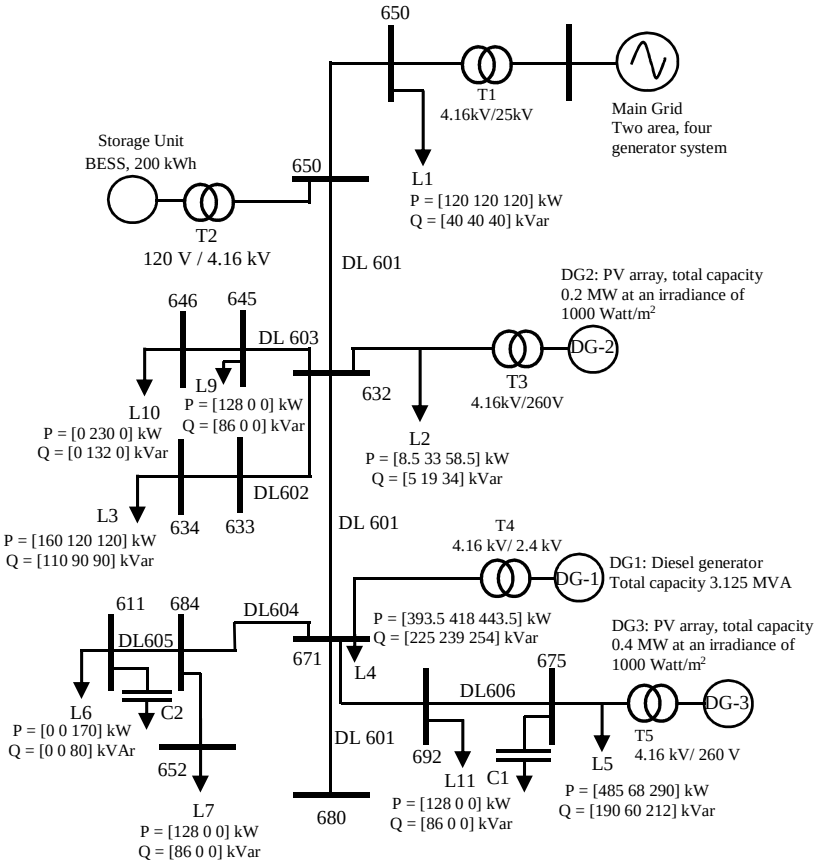

Figure 3.5: Microgrid test system model.

Table 3.2: Two Area System Model Overview

	Area-1	*Area-2*
Generations	G-1: 700 MW, 185 MVAr G-2: 700 MW, 235 MVAr	G-3: 719 MW, 176 MVAr G-4: 700 MW, 202 MVAr
System Loads	967 MW, 100 MVAr	177 MW, 100 MVAr
Shunt Capacitors	200 MVAr.	350 MVAr.

3.4 Case Study

The proposed method is evaluated on the test system described in Section 3.3. Detailed aspects of the case study including generation of measurement dataset, post-processing of measurement data, development of DT based classification model, and real-time simulation for performance assessment are presented in this section.

3.4.1 Offline Simulation of System Events

In this case study, a total of 234 system events under 13 different system operating conditions (OCs) have been used to generate the measurement dataset at target DG location (PCC bus of target DG unit with distribution network/microgrid). The OCs are selected based on combinations of load patterns in area-EPS, distribution network/microgrid and local loads at target DG locations, and production levels DGs to represent different levels of power imbalances between generation and demand in the islanded system. The following events have been considered in the offline system event simulations for generation of training dataset for DT classifiers.

- Tripping of circuit breaker at distribution substation to island the distribution system/ microgrid from the main grid.
- Loss of distribution lines leading to formation of power islands within the distribution network.

- Three phase faults in distribution network with instantaneous fault clearing time causing formation of islands.
- Formation of islands caused by loss of transmission lines between area-1 and area-2 of two area system.
- Three-phase load changes: 50% $\leftrightarrow$ 80%, 80% $\leftrightarrow$ 100%, 50% $\leftrightarrow$ 90%, 100% $\leftrightarrow$ 120%.
- Single-phase load changes: 50% $\leftrightarrow$ 60%, 70% $\leftrightarrow$ 90%, 40% $\leftrightarrow$ 100%, 100% $\leftrightarrow$ 120%.
- Shunt capacitors switching on or off.
- Loss of generations by DGs other than the target DG unit.
- Loss of generation units in either area-1 or area-2 of two area system.

A total of 18 system events under each of the selected OCs were simulated resulting in a total of 234 offline simulations. Voltage and current measurements were obtained at a sampling rate of 1920 Hz yielding 32 sample points per cycle. All variables measured at PCC of the target DG unit refer to the high voltage side of the DG interconnection transformer. Critical attributes (CAs) were extracted from obtained measurement dataset and classification model for the islanding detection relay at target DG location is developed. The simulations were performed in MATLAB/ Simulink platform.

3.4.2 Measurement Data Processing

Measurement data from six-cycles following the initiation of each event is utilized for computation of predictor variables. A sliding one-cycle window spanning 32 sampling points is employed for computation of the predictors. The window shifts four sampling points (1/8 cycle) between two consecutive computation steps. The set of predictor

variables obtained from each computation step along with the corresponding desired class value is termed as a *case*. Each event represented by the six-cycle measurement data yields 41 of such *cases*. Each event is classified as either *non-islanding* or *islanding*, represented by class values of 0 and 1 respectively. Hence, a comprehensive characterization of each system event is obtained using the *cases* represented by the time-dependent predictor values. The complete training dataset contains 234 events or 9594 cases among which 182 events or 7462 cases (78%) were classified as *non-islanding* and remaining 52 events or 2132 cases (22%) were classified as *islanding*.

3.4.3 Predictor Selection for Parallel Decision Trees

The predictors used in the proposed islanding detection methodology includes CAs extracted from post-event voltage and current measurements. The set of CAs presented in Table 3.1 is selected to capture essential information to characterize the system events for islanding detection. The set of CAs are further grouped into subsets in order to minimize correlation between the developed DT classifiers to enhance reliability and accuracy of the proposed parallel DT based scheme. Table 3.3 presents the predictor groups used in the proposed methodology. Group-1 and Group-2 contain CAs extracted from voltage and current measurements respectively, Group-3 contains the predictors that characterize the harmonic contents of the measured post-event voltages and currents, and Group-4 contains the complete set of CAs extracted from both voltage and current measurements. Training datasets are generated for each group of predictors consisting of the corresponding predictor and class values for each of the training cases. Finally, the developed training datasets are utilized for offline DT building process and classification model development.

Table 3.3: Different Groups of Predictors Used in DT Training

No.	Descriptions
Group-1	Predictors extracted from voltage measurements
	$x_1, x_2, x_3, x_4, x_7, x_8, x_{10}, x_{11}$
Group-2	Predictors extracted from current measurements
	$x_3, x_4, x_5, x_6, x_9, x_{12}, x_{13}, x_{14}, x_{15}$
Group-3	Predictors characterizing harmonic contents in measurements
	$x_8, x_9, x_{10}, x_{11}, x_{12}, x_{13}, x_{14}, x_{15}$
Group-4	Predictors extracted from voltage and current measurements
	$x_1, x_2, x_3, x_4, x_5, x_6, x_7, x_8, x_9, x_{10}, x_{11}, x_{12}, x_{13}, x_{14}, x_{15}$

3.4.4 Decision Tree Training and Testing Demonstration

Based on the developed training datasets, DT classifiers were constructed using *Simple CART* decision tree algorithm in Waikato Environment for Knowledge Analysis (WEKA) [83] data mining platform. DT classifiers are trained separately for each of the target DG locations under consideration. Initially, the DT training process involves all of the predictor variables in a predictor group for classification of each of the cases. The trained DTs utilize only a relevant set of predictors that have higher merits towards the overall classification process. Thus, predictors in the group with comparatively lower merit in the overall classification process are filtered out.

A total of five DT classifiers with optimal performances are employed in parallel for the classification of system events. For each of the predictor groups, multiple DTs were developed and performance of each DT classifiers are evaluated using k-fold cross validation method in WEKA. K-fold cross validation method partitions the original dataset into K subsets. The method performs K iterations with (K-1) subsets as training sets and a single subset as the validation set. Each of the K subsets are used as the validation set once in the process. In $(K+1)^{th}$ iteration, the complete set is used as training set and validation set. Accuracy results over (K+1) iterations are averaged

to obtain the final accuracy of the classifier. In this paper, 10-fold cross validation is performed to evaluate the classifier performances. DT classifier performances are evaluated based on overall classification accuracy, dependability index (DI), security index (SI) and misclassification cost. Five DT classifiers with optimal performances are selected for the parallel DT network for each of the target DG locations.

For each of the DGs in the microgrid, the parallel combination of multiple optimal DTs is developed from the four groups of predictors presented in Table 3.3. The parallel combination of DT classifiers is developed with three best performing DTs developed with predictors from Group-1, Group-2, and Group-3 only, and two best performing DTs developed from the predictors from Group-4. Table 3.4, Table 3.5, and Table 3.6 present the classification performance of the five best performing DTs for DG-1, DG-2, and DG-3, respectively.

Table 3.4: DT Classifier Performance Evaluation [10-Fold Cross Validation Method]-Target DG Location DG-1

Tree Code	Predictor Variables	Classifier Accuracy	Actual Class	Total Cases	Classified as	
					I	*NI*
DT-1	$x_1, x_2, x_3,$ x_4, x_7, x_8	99.53	*I*	2132	2123	9
			NI	7462	36	7426
DT-2	$x_2, x_5, x_6,$ x_{10}, x_{13}, x_{15}	98.93	*I*	2132	2110	22
			NI	7462	81	7381
DT-3	$x_1, x_2, x_7,$ x_{10}, x_{11}	98.73	*I*	2132	2106	26
			NI	7462	96	7366
DT-4	$x_5, x_{12}, x_{13},$ x_{14}, x_{15}	97.54	*I*	2132	2080	52
			NI	7462	184	7278
DT-5	$x_8, x_{10}, x_{11},$ x_{13}, x_{14}, x_{15}	95.42	*I*	2132	2035	97
			NI	7462	342	7120

Table 3.5: DT Classifier Performance Evaluation [10-Fold Cross Validation Method]-Target DG Location DG-2

Tree Code	Predictor Variables	Classifier Accuracy	Actual Class	Total Cases	Classified as	
					I	*NI*
DT-1	$x_1, x_2, x_5,$ x_{10}, x_{11}	99.74	*I*	2132	2128	4
			NI	7462	21	7441
DT-2	$x_3, x_4, x_7,$ x_8, x_9	99.11	*I*	2132	2115	17
			NI	7462	68	7394
DT-3	x_1, x_2, x_3, x_8	98.86	*I*	2132	2109	23
			NI	7462	86	7376
DT-4	$x_3, x_6, x_{12},$ x_{13}, x_{14}	97.72	*I*	2132	2086	46
			NI	7462	173	7289
DT-5	x_{10}, x_{11}, x_{12} x_{13}, x_{14}, x_{15}	96.15	*I*	2132	2051	81
			NI	7462	288	7174

Table 3.6: DT Classifier Performance Evaluation [10-Fold Cross Validation Method]-Target DG Location DG-3

Tree Code	Predictor Variables	Classifier Accuracy	Actual Class	Total Cases	Classified as	
					I	*NI*
DT-1	$x_1, x_2, x_5,$ x_{10}, x_{11}	99.67	*I*	2132	2126	6
			NI	7462	26	7436
DT-2	$x_3, x_4, x_7,$ x_8, x_{15}	99.25	*I*	2132	2118	14
			NI	7462	58	7404
DT-3	$x_1, x_2, x_3,$ x_8, x_{10}	98.95	*I*	2132	2113	19
			NI	7462	82	7380
DT-4	$x_3, x_4, x_6,$ x_{13}, x_{15}	97.32	*I*	2132	2077	55
			NI	7462	202	7260
DT-5	$x_{10}, x_{11}, x_{12},$ x_{13}, x_{14}, x_{15}	96.07	*I*	2132	2049	83
			NI	7462	294	7168

The decision trees from *DT-1* to *DT-5* for each of the DGs are all sufficiently different from each other although some of the braches share the same CSRs. DT classifiers developed from *Group-4* predictors have the highest classification accuracy. This is mainly because of the fact that, these DTs utilize the largest set of predictor variables characterizing voltage and current variations as well as harmonic contents. DT classifiers developed from *Group-3* predictors are the least accurate ones over the entire range of operating conditions (OCs) used in training and testing the DT classifiers. These DT classifiers only utilize predictor variables which characterizes harmonic contents in the voltage and currents at target DG locations. Moreover, as results from Table 3.4, Table 3.5, and Table 3.6 indicate that the set of five best performing DTs is different from each other. Hence, building DT classifiers for each of the DGs in the microgrid with local measurements at point of common couplings (PCC) of the DG units would perform better in detecting islanding events than building more generalized DT classifiers for different DGs (i.e. synchronous and inverter based DGs) in the microgrid. For any system event, classification results from each of the five DTs are obtained and a final classification is made based on the majority classification results.

In the DT building process, cost parameter for misclassifying an islanding event as non-islanding event is made twice than that of classifying a non-islanding event as islanding event. This is done to account for the fact that misclassification of an islanding event has more detrimental impact on system security and safety than misclassification of a non-islanding event. In this case study, cost parameter for misclassification of an islanding event and non-islanding event is set at 1 and 0.5 respectively. Hence, for all of the developed DT classifiers, number of misclassification of non-islanding events is larger than that of islanding events. Table 3.7, Table 3.8, and Table 3.9 present the overall misclassification cost, dependability index (DI), and security index (SI) for DG-1, DG-2, and DG-3, respectively.

Table 3.7: DT Classifier Performance Evaluation [Dependability and Security Indices] - Target DG Location DG-1

Tree Code	Predictor Variables	Misclassification Cost	Dependability Index (DI)	Security Index (SI)
DT-1	$x_1, x_2, x_3, x_4, x_7, x_8$	0.0028	99.58	99.52
DT-2	$x_2, x_5, x_6, x_{10}, x_{13}, x_{15}$	0.0065	98.97	98.91
DT-3	$x_1, x_2, x_7, x_{10}, x_{11}$	0.0077	98.78	98.71
DT-4	$x_5, x_{12}, x_{13}, x_{14}, x_{15}$	0.0150	97.56	97.53
DT-5	$x_8, x_{10}, x_{11}, x_{13}, x_{14}, x_{15}$	0.0279	95.45	96.42

Table 3.8: DT Classifier Performance Evaluation [Dependability and Security Indices] - Target DG Location DG-2

Tree Code	Predictor Variables	Misclassification Cost	Dependability Index (DI)	Security Index (SI)
DT-1	$x_1, x_2, x_5, x_{10}, x_{11}$	0.0015	99.81	99.72
DT-2	x_3, x_4, x_7, x_8, x_9	0.0053	99.20	99.08
DT-3	x_1, x_2, x_3, x_8	0.0069	98.92	98.85
DT-4	$x_3, x_6, x_{12}, x_{13}, x_{14}$	0.0138	97.84	97.68
DT-5	$x_{10}, x_{11}, x_{12}, x_{13}, x_{14}, x_{15}$	0.0235	96.20	96.14

Table 3.9: DT Classifier Performance Evaluation [Dependability and Security Indices] - Target DG Location DG-3

Tree Code	Predictor Variables	Misclassification Cost	Dependability Index (DI)	Security Index (SI)
DT-1	$x_1, x_2, x_5, x_{10}, x_{11}$	0.0020	99.72	99.65
DT-2	$x_3, x_4, x_7, x_8, x_{15}$	0.0045	99.34	99.22
DT-3	$x_1, x_2, x_3, x_8, x_{10}$	0.0063	99.11	98.90
DT-4	$x_3, x_4, x_6, x_{13}, x_{15}$	0.0163	97.42	97.29
DT-5	$x_{10}, x_{11}, x_{12}, x_{13}, x_{14}, x_{15}$	0.0238	96.11	96.06

Fig. 3.6 - Fig. 3.17 presents the dependability index (DI) and security index (SI) under various real and reactive power mismatch scenarios for each of the five DT classifiers for all three DGs. Fig. 3.8 and Fig. 3.9 show the dependability index (DI) for each of the five DT classifiers developed for DG-2 in cases of active power mismatch scenarios ranging from 0-50 percent and reactive power mismatch scenarios ranging from 0-40 percent. Obtained comparison results indicate that the performances of the developed DT classifiers depends on the predictor variables used to build the DTs and the system operating conditions (OCs). For example, DT-5, although being the least accurate among the developed DT classifiers for DG-2, has the best classification performance under zero percent active power mismatch scenarios. This is because of the fact that DT-5 is developed with predictors that characterizes harmonic contents of voltage and current measurements, and are more accurate under low generation-demand mismatch scenarios, where other predictors based on deviations in magnitude and rate-of-change of voltage and current are not that accurate in characterizing the system events. Hence, effective utilization of different combinations of critical attributes (CAs) over a broad range of power mismatch scenarios is possible in the proposed approach.

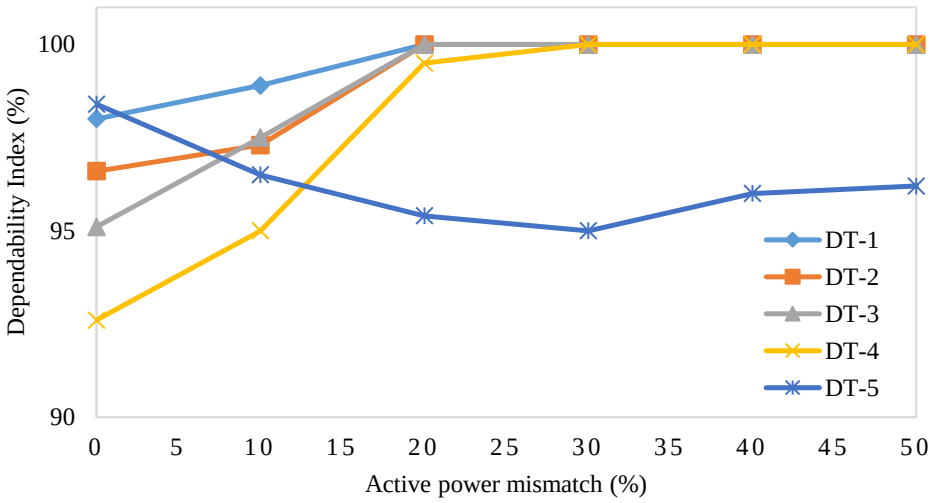

Figure 3.6: Performance comparison of the developed DT classifiers for DG-1 based on dependability index (DI) for active power mismatch scenarios in the range of 0-50 percent.

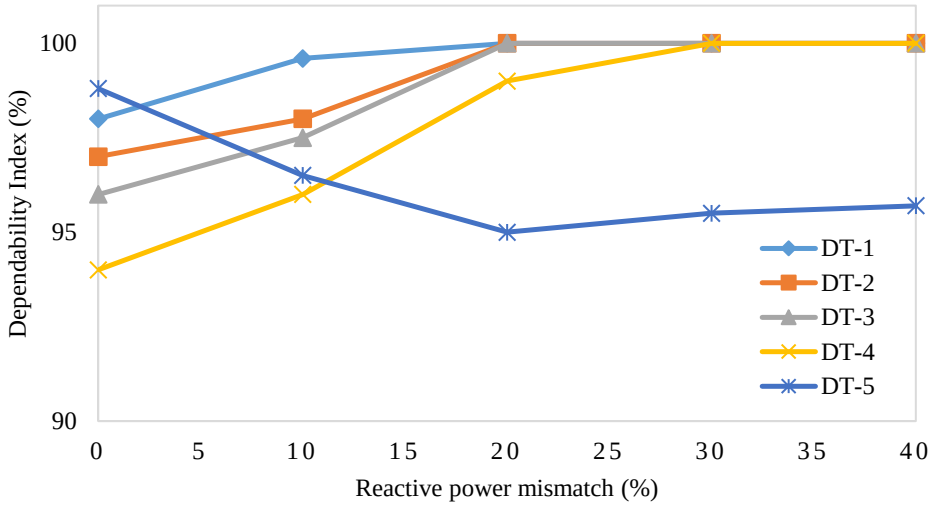

Figure 3.7: Performance comparison of the developed DT classifiers for DG-1 based on dependability index (DI) for reactive power mismatch scenarios in the range of 0-40 percent.

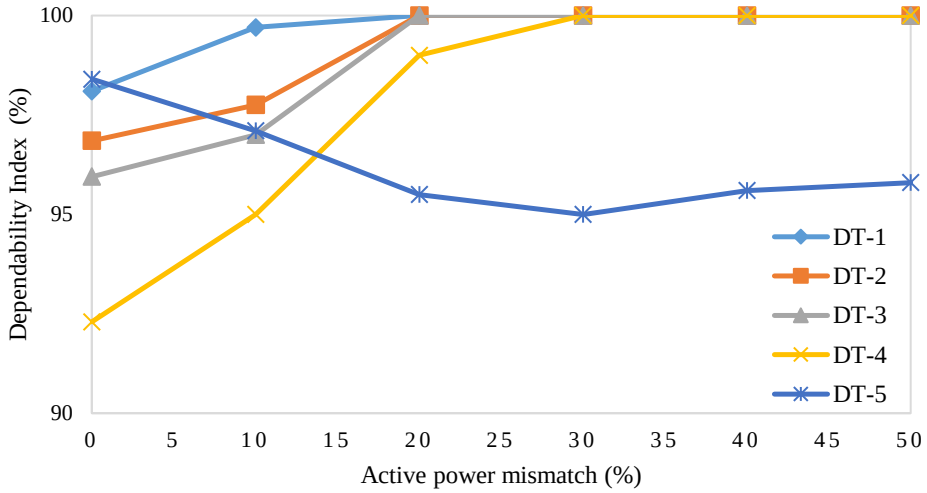

Figure 3.8: Performance comparison of the developed DT classifiers for DG-2 based on dependability index (DI) for active power mismatch scenarios in the range of 0-50 percent.

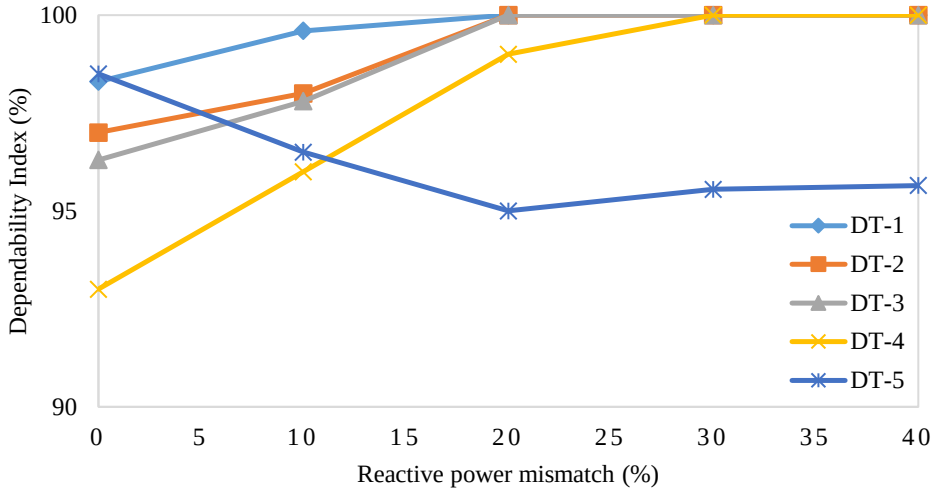

Figure 3.9: Performance comparison of the developed DT classifiers for DG-2 based on dependability index (DI) for reactive power mismatch scenarios in the range of 0-40 percent.

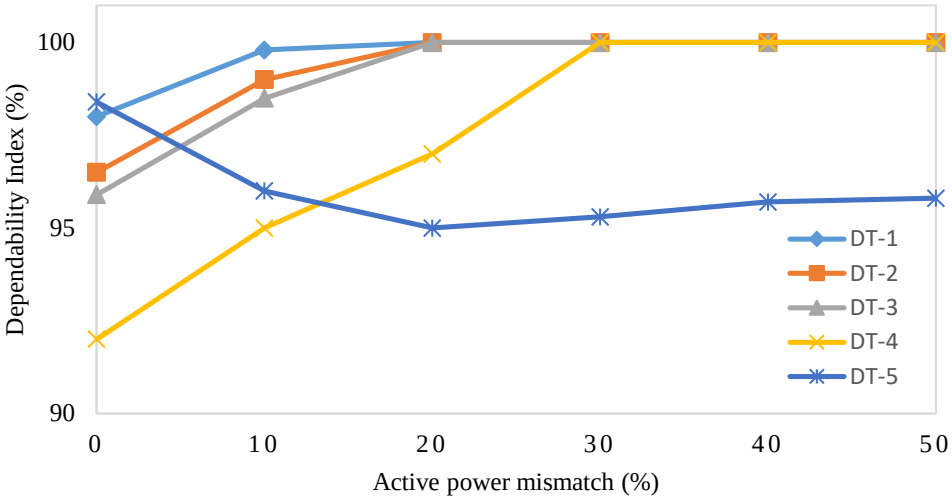

Figure 3.10: Performance comparison of the developed DT classifiers for DG-3 based on dependability index (DI) for active power mismatch scenarios in the range of 0-50 percent.

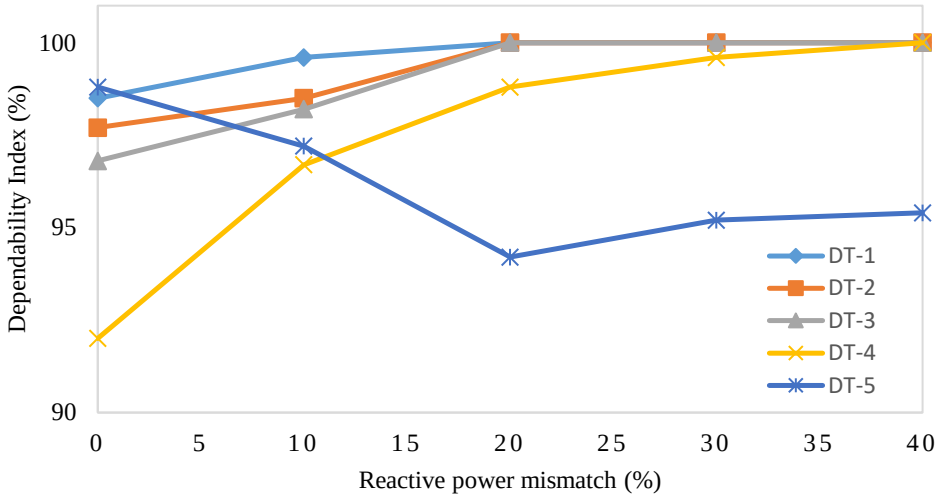

Figure 3.11: Performance comparison of the developed DT classifiers for DG-3 based on dependability index (DI) for reactive power mismatch scenarios in the range of 0-40 percent.

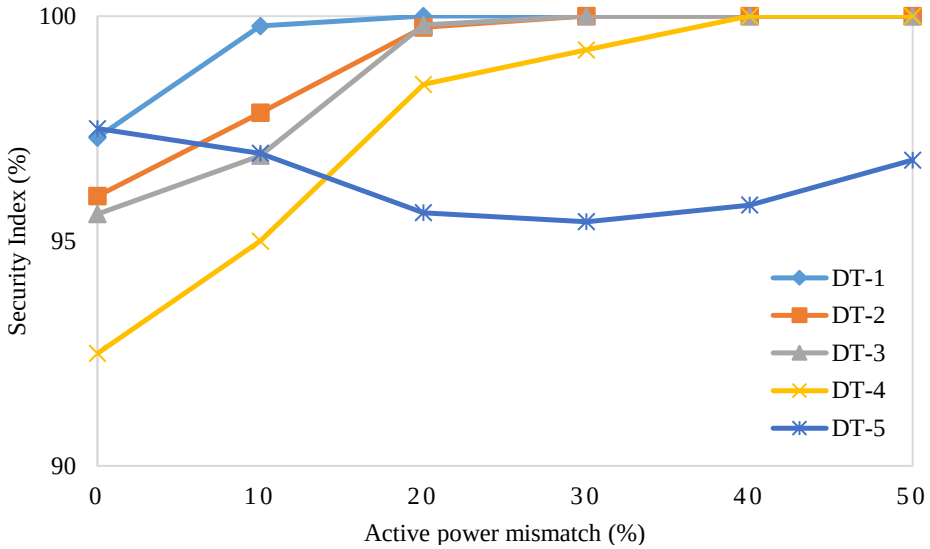

Figure 3.12: Performance comparison of the developed DT classifiers for DG-1 based on security index (SI) for active power mismatch scenarios in the range of 0-50 percent.

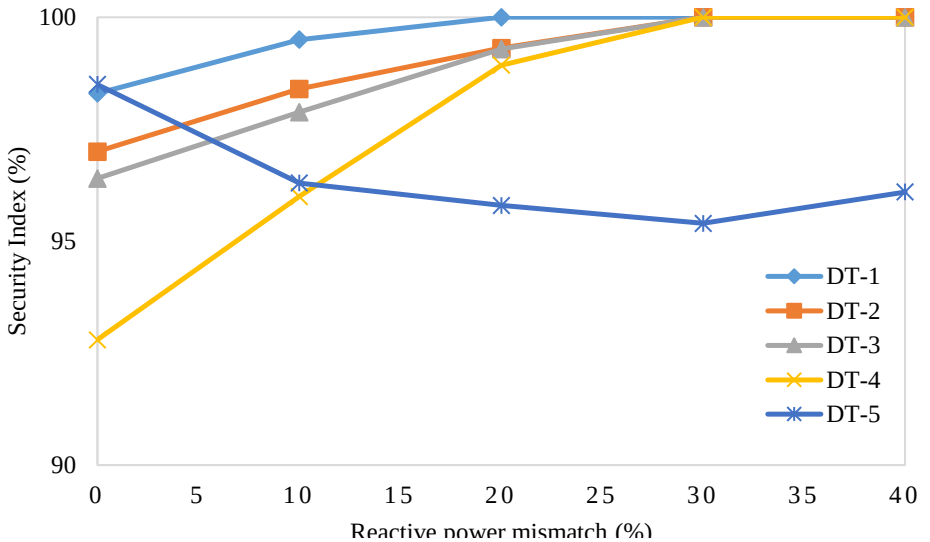

Figure 3.13: Performance comparison of the developed DT classifiers for DG-1 based on security index (SI) for reactive power mismatch scenarios in the range of 0-40 percent.

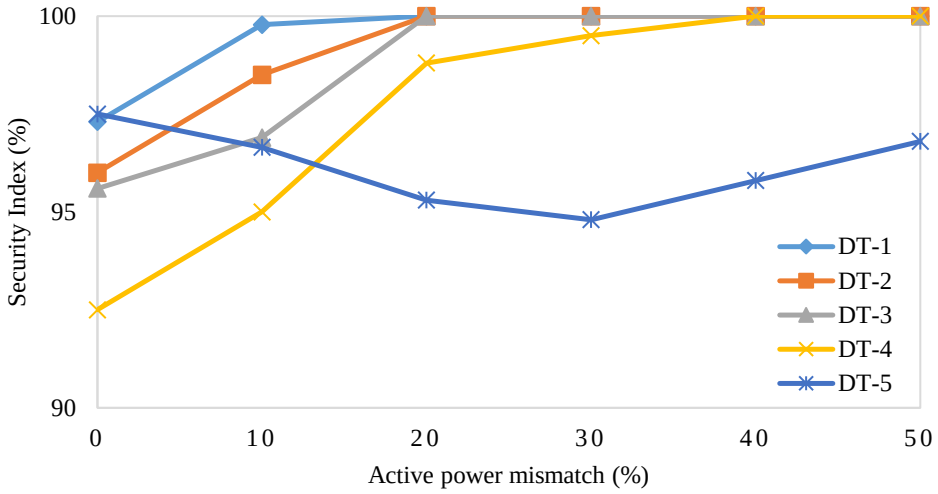

Figure 3.14: Performance comparison of the developed DT classifiers for DG-2 based on security index (SI) for active power mismatch scenarios in the range of 0-50 percent.

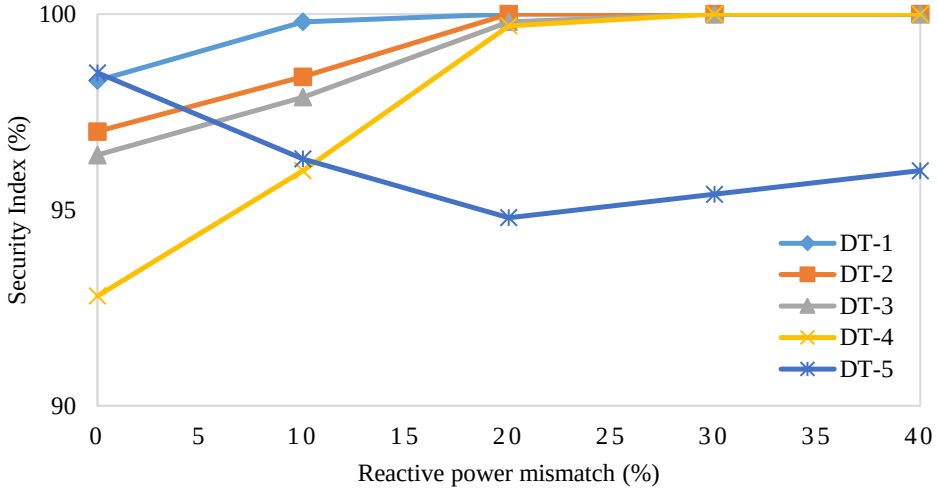

Figure 3.15: Performance comparison of the developed DT classifiers for DG-2 based on security index (SI) for reactive power mismatch scenarios in the range of 0-40 percent.

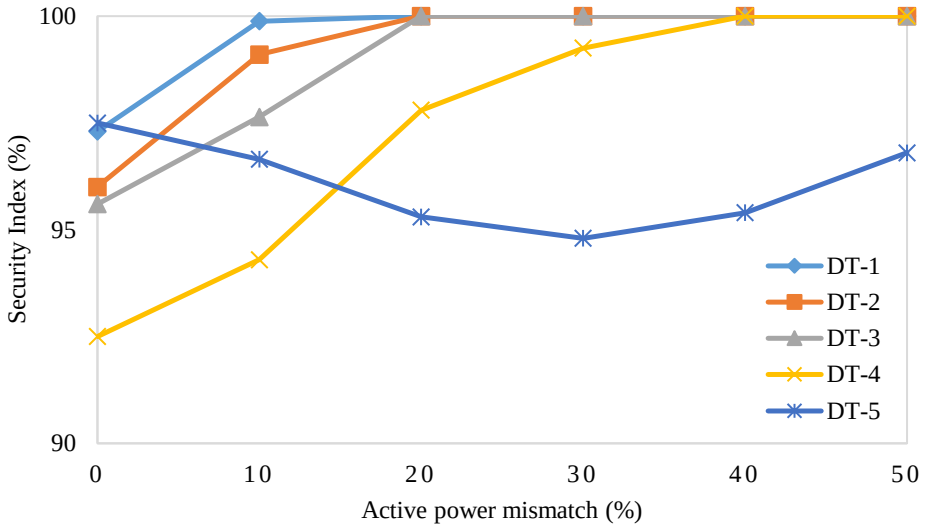

Figure 3.16: Performance comparison of the developed DT classifiers for DG-3 based on security index (SI) for active power mismatch scenarios in the range of 0-50 percent.

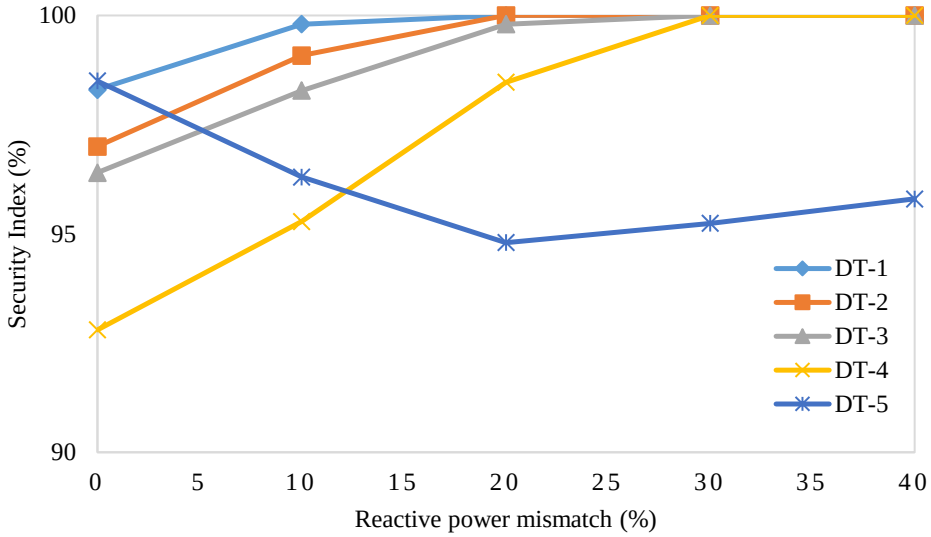

Figure 3.17: Performance comparison of the developed DT classifiers for DG-3 based on security index (SI) for reactive power mismatch scenarios in the range of 0-40 percent.

Fig. 3.14 and Fig. 3.15 show the security index (SI) of the developed DT classifiers for DG-2 under active power mismatch ranging from 0-50 percent and reactive power mismatch ranging from 0-40 percent. Obtained results show a trend similar to the dependability index (DI) results presented in Fig. 3.8 and Fig. 3.9. Hence, combining multiple optimal DTs in a parallel DT network enhances the overall classification accuracy over a wide range of active and reactive power mismatch scenarios. Moreover, the proposed approach enables easier implementation as compared to other black-box data mining algorithms with comparable classification accuracy such as- Random Forest (RF) classifiers. Fig. 3.18 and Fig. 3.19 present the DT structures for DT-1 and DT-2 for target DG location DG-2.

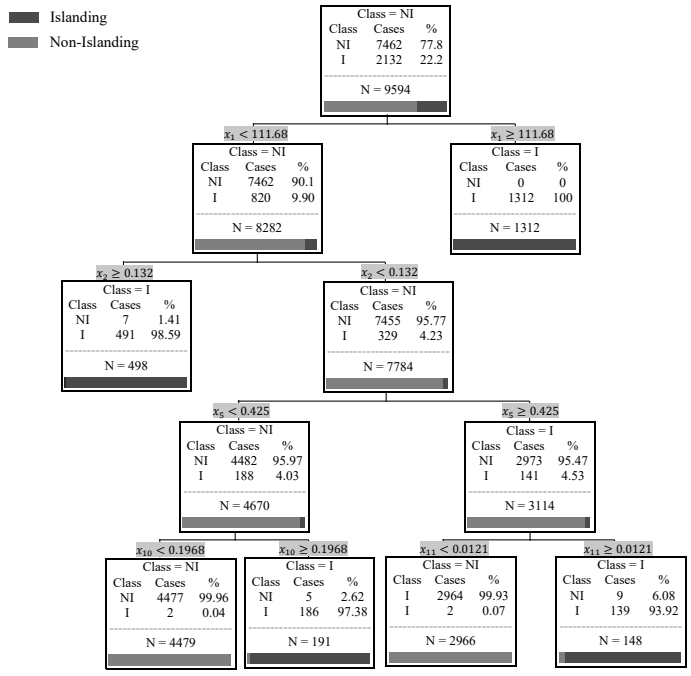

Figure 3.18: DT-1 for target DG location DG-2.

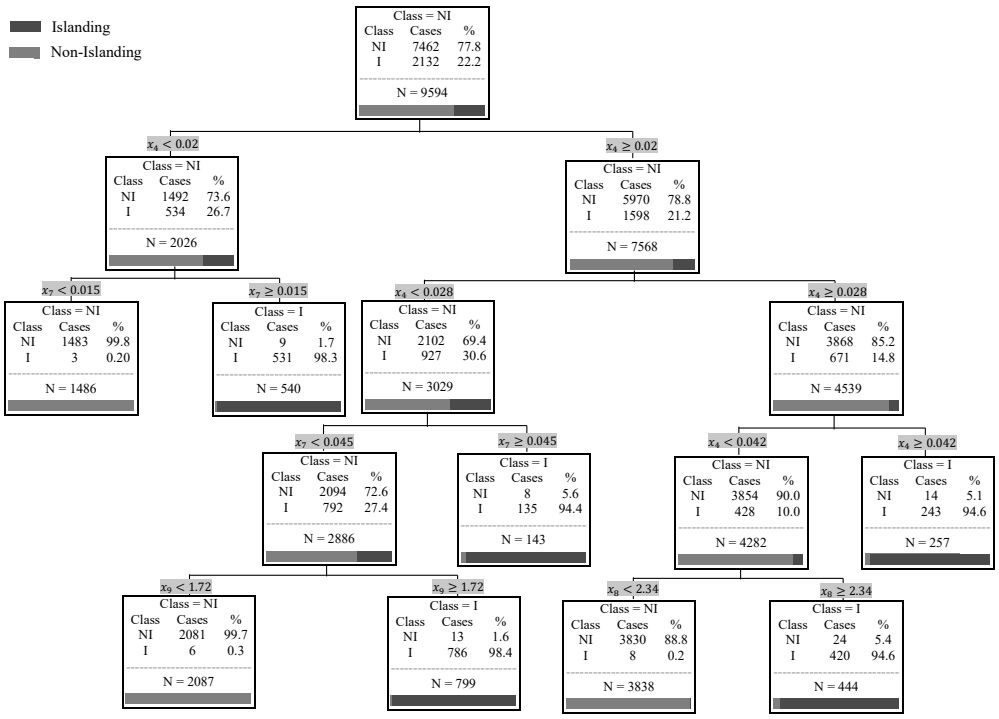

Figure 3.19: DT-2 for target DG location DG-2.

3.4.5 Real-Time Implementation

The proposed islanding detection methodology is implemented in a software-in-loop (SIL) test bed using OPAL-RT real-time digital simulation platform. OPAL-RT uses multiple multi-core processors for parallel processing and interfaces with MATLAB/Simulink via RT-LAB software environment. Power system models are split into several subsystems in RT-LAB environment and each subsystem is assigned to one of the cores in the OPAL-RT digital simulator. A schematic diagram for the real-time implementation of the proposed islanding detection methodology is presented in Fig. 3.20.

The microgrid model presented in Section 3.3 is simulated in OPAL-RT platform using RT-LAB software environment. The proposed parallel decision tree based islanding detection methodology is implemented as a separate subsystem which receives the local measurement data at target DG locations, extracts the features

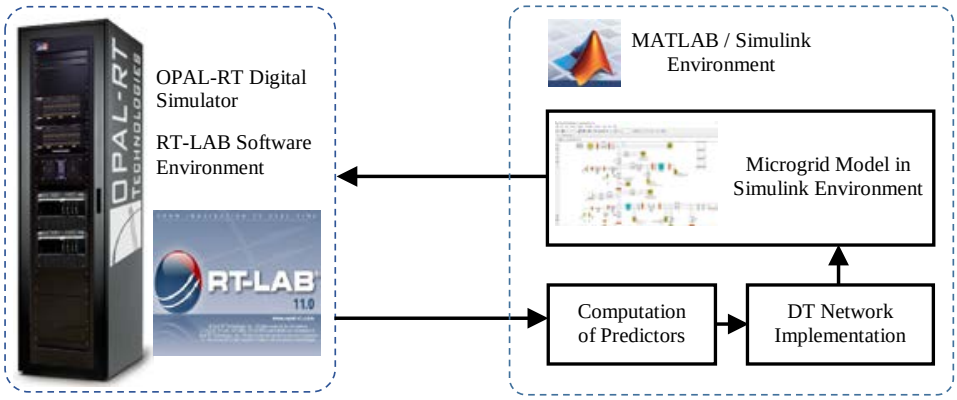

Figure 3.20: Schematic of OPAL-RT/ RT-LAB implementation.

presented in Table 3.1, and classification results are obtained from the parallel DT networks.

A test set containing 72 system events (2952 cases) were used in the performance assessment of the proposed parallel DT based islanding detection methodology. An overview of the performance of the individual DT classifiers for DG-2 is presented in Table 3.10 and overall classification performance of the parallel DT network for target DG location DG-2 is presented in Table 3.11. In order to eliminate missed detections and false alarms caused by misclassification of a case by DT classifiers, proposed methodology relies upon three consecutive classification outputs from the parallel DT network instead of one classification result. Hence, for any event to be classified as an islanding event, parallel DT network has to classify that event as an islanding event for three consecutive classification cycles. This criterion helps in reducing the chances of missed detections or false alarms even if the parallel DT network has misclassified some of the individual cases.

3.4.6 Comparative Analysis of IDMs

Performance of the proposed technique is compared with several intelligent based approaches as well as rate-of-change of frequency (ROCOF) based relays. Training and testing datasets utilized to evaluate the intelligent based classifiers in WEKA

Table 3.10: DT Classifier Performance Evaluation - Target Location DG-2

Tree Code	Classifier Accuracy	DI	SI	Actual Class	Total Cases	Classified as	
						I	*NI*
DT-1	99.73	99.54	99.78	*I*	656	653	3
				NI	2296	5	2291
DT-2	99.56	99.39	99.61	*I*	656	652	4
				NI	2296	9	2287
DT-3	99.53	99.39	99.56	*I*	656	652	4
				NI	2296	10	2286
DT-4	99.36	99.08	99.43	*I*	656	650	6
				NI	2296	13	2283
DT-5	98.88	98.17	99.08	*I*	656	644	12
				NI	2296	21	2275

Table 3.11: Overall system event classication performance of parallel DT network - Target Location DG-2

Event Class	Total Events	Classified as		Classification Accuracy	Dependability/ Security Index
		I	*NI*		
I	16	16	0	100	100
NI	56	0	56	100	100

contained 9594 *cases* and 2952 *cases* respectively. The ROCOF relays were designed with a three-cycle time window and with threshold settings of 0.1 Hz/s and 0.5 Hz/s. The islanding detection methodologies were compared based on the overall classification accuracy, dependability index (DI), and security index (SI). Random Forest (RF) classifier and the proposed parallel DT based approaches are the most accurate methods on the test set used in the study. Whereas, the ROCOF relays are the least accurate ones. While, RF classifiers offer robustness and accurate classification of system events, the implementation of such classifiers poses serious challenges owing to the black-box nature of the RF classifiers. Whereas, DT classifiers offer easier implementation using the decision rules and thresholds values, hence more suitable for practical applications.

Table 3.12: Comparative Evaluation of Islanding Detection Methodologies

Methodology	Accuracy	DI	SI
Parallel DT Network	100	100	100
Random Forest (RF)	100	100	100
Support Vector Machine (SVM)	88.27	84.57	90.12
Naive-Bayes Classifier	93.62	87.04	96.91
ROCOF (0.1 Hz/s)	79.85	73.24	86.45
ROCOF (0.5 Hz/s)	75.38	68.45	82.30

3.5 Summary

This chapter presents a passive islanding detection methodology for distributed generations (DGs) using decision trees (DTs). The proposed approach utilizes critical system parameters extracted from local measurements of post-event voltage and current at target DG locations in order to characterize the system events, and employs parallel decision tree networks to detect islanding events by characterizing the variations associated with the extracted parameters. Utilization of multiple optimal DTs in a parallel network allows minimization of variable masking problems associated with DT classifiers and enables effective utilization of critical system attributes over a broad range of power mismatch scenarios. The DT classifiers are trained with time-representative predictor values characterizing system events over six-cycles following the initiation of the events, which enhances the DT based classification model development and thereby, enhancing the classification accuracy. Performance of the proposed approach is evaluated based on simulation studies as well as real-time implementation on OPAL-RT/RT-LAB platform using a microgrid test system model under a wide range of power mismatch scenarios as well as in the presence of multiple DGs. Use of parallel DT network for DG islanding detection improves the performance over employing the DT classifier with best performance alone, as indicated by the presented training and testing demonstration on the microgrid test system. The proposed parallel DT based approach provides a

transparent data mining model based on decision trees as opposed to other black-box data mining solutions with comparable classification performance such as the Random Forest (RF) technique. Hence, the proposed approach enables easier implementation. Moreover, being a passive islanding detection technique, the proposed approach can be utilized for inverter based DGs as well as synchronous generator based DGs.

Chapter 4

Islanding Detection Methodology Combining Decision Trees and Sandia Frequency Shift for Inverter Based Distributed Generations

Distributed generations (DGs) for grid-connected applications require an accurate and reliable islanding detection methodology (IDM) for secure system operation. This chapter presents an islanding detection methodology for grid-connected inverter based DGs. The proposed method is a combination of passive and active islanding detection techniques for aggregation of their advantages and elimination /minimization of the drawbacks. In the proposed IDM, the passive method utilizes critical system attributes extracted from local voltage measurements at target DG location as well as employs decision tree based classifiers for characterization and detection of islanding events. The active method is based on Sandia frequency shift (SFS) technique and is initiated only when the passive method is unable to differentiate islanding events from other system events. Thus, the power quality degradation introduced in the system by active islanding detection techniques can be minimized. Furthermore, combination

of active and passive techniques allows detection of islanding events under low power mismatch scenarios eliminating the disadvantage associated with the use of passive techniques alone. Moreover, the proposed method also provides an effective means to automate the threshold setting tasks based on DTs and measurement data at target DG locations. The Harmony Search Algorithm (HSA) [84], which is a metaheuristic, population-search optimization method, is applied to optimize the performance of the SFS method. Harmony search algorithm, which is a meta-heuristic optimization algorithm, offers computational efficiency in comparison with classical optimization techniques. Moreover, HSA being a meta-heuristic population search algorithm provides a problem-independent optimization technique as compared to other heuristic optimization techniques, which allows through exploration of the solution space and achieves a better solution by not being trapped into a local optimum without obtaining a global optimum solution. Case studies on a grid-connected photovoltaic (PV) farm and a microgrid model consisting of multiple inverter based DGs are performed to verify the effectiveness of the proposed method under IEEE Std. 1547 [11], IEEE Std. 929 [85], and UL1741 [86] test conditions with different load quality factors and power mismatch scenarios. Detailed case study results demonstrate the effectiveness of the proposed method in detection of islanding events under various power mismatch scenarios, load quality factors and in presence of single or multiple grid-connected inverter based DG units.

The chapter is organized as follows. The principles of the proposed hybrid IDM are presented in Section 4.1. Section 4.2 describes the test system. Sections 4.3 and 4.4 present case study results. In Section 4.5, performance of the proposed methodology is compared with other IDMs based on detection accuracy, dependability and security indices. Finally, a summary is presented in Section 4.6.

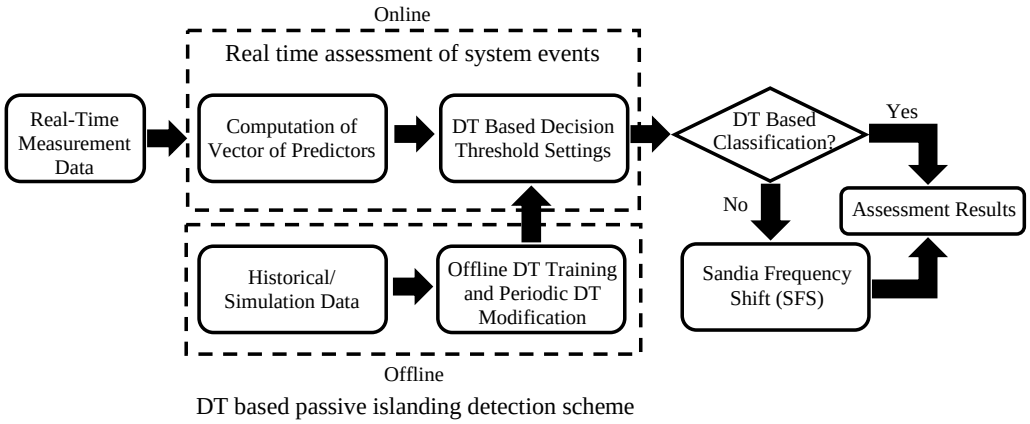

Figure 4.1: Conceptual model of the proposed islanding detection methodology.

4.1 Proposed Methodology

The conceptual model of the proposed hybrid IDM is presented in Fig. 4.1. The proposed method is composed of two main components: 1) passive islanding detection based on decision trees (DTs) and 2) active islanding detection based on Sandia frequency shift (SFS) technique. The proposed passive islanding detection is based on variations in system parameters extracted from voltage measurements, whereas, the active islanding detection is based on frequency perturbations. Hence, variations in system frequency and system indices based on voltage measurements are both considered for accurate and reliable detection of islanding events. This section presents an overview of the proposed methodology.

4.1.1 DT Based Passive IDM

The passive scheme is based on extraction of system parameters by post-processing voltage waveforms obtained from measurements at target DG locations, and detection of event specific signatures on these system parameters through the application of DT based pattern recognition technique. Table 4.1 lists all four system parameters or features (also called predictors) used in the DT based passive scheme.

Table 4.1: System Parameters used in Passive Islanding Detection

$x_1^i = \Delta V_i$	Voltage deviation under i^{th} event (Volts)
$x_2^i = \left(\frac{\Delta V}{\Delta t}\right)_i$	Rate-of-change of voltage under i^{th} event (Volts/cycle)
$x_3^i = \left(\frac{V_{-seq}}{V_{+seq}}\right)_i$	Voltage unbalance under i^{th} event
$x_4^i = V_{THDi}$	Total harmonic distortion in voltage under i^{th} event

These features are selected since inverter based DGs generally operate at unity power factor. Hence, islanding events may lead to possible deficiency in reactive power and subsequent voltage variations which can be utilized for islanding detection. Moreover, islanding scenarios may also lead to variations in network topology and DG loading conditions, which may lead to variations in voltage unbalance and total harmonic distortions in voltage. In the proposed scheme, the DT based passive method consists of four major components: 1) Offline DT training, 2) DT based threshold setting, 3) periodic DT modification, and 4) online implementation.

Offline DT Training

The DTs built in this proposed scheme are classification trees built from training dataset consisting of feature vectors and corresponding class values. Properly trained DTs can predict the class of an unseen event (i.e. non-islanding or islanding events) from the feature vector presented to it for classification. The feature vector consists of system parameter values utilized in the classification process. The mathematical formulation for the proposed approach can be illustrated as:

$$X_i = \left\{x_1^i, x_2^i, x_3^i, x_4^i\right\}; i = 1, 2, 3, ..., N \tag{4.1}$$

$$F = [X_1, X_2, ..., X_N]^T \tag{4.2}$$

$$Y = [y^1, y^2, ..., y^N]^T \tag{4.3}$$

where X_i is the feature vector containing feature values for i^{th} event, F is the matrix containing feature vectors for each of the N system events, and Y contains the class values (i.e. $y_i = 0$ for non-islanding events and $y_i = 1$ for islanding events) corresponding to the feature vectors X_i for each of the N system events. The complete data model (E) for DT classifier training can be expressed as follows:

$$E = [F\ Y] = \begin{bmatrix} x_1^1 & x_2^1 & x_3^1 & x_4^1 & y^1 \\ x_1^2 & x_2^2 & x_3^2 & x_4^2 & y^2 \\ : & : & ... & : & : \\ x_1^N & x_2^N & x_3^N & x_4^N & y^N \end{bmatrix} \tag{4.4}$$

The training dataset containing feature vectors and corresponding class values are obtained from extensive offline simulation of system events. A wide variety of system disturbances leading to islanding and non-islanding events are considered in offline simulations for acquiring essential system characteristics (i.e. characteristic variations in voltage magnitude, voltage unbalance, and total harmonic distortions for each of the system events). Moreover, these events are simulated under various operating states of area-EPS and target DG unit.

DT Based Threshold Setting

The DT based classification model yields a set of decision rules associated with the classification process. Decision rules are essentially decision boundaries in the data model which differentiates islanding events from non-islanding events. Threshold values for system parameters used in the classification process are extracted from the decision rules obtained from offline DT building process.

Passive islanding detection methods usually suffer from detection inaccuracies in low generation and load mismatch scenarios (where generation and demand are approximately balanced) due to the low variation in voltage magnitude and system frequency during an islanding event. Thus, in the proposed approach, DT based

threshold settings are utilized to trigger the active IDM based on SFS technique during low generation and load mismatch scenarios. In the proposed scheme, two sets of threshold values were generated: 1) Lower threshold setting (TH_L), which differentiates normal operations from other system events (i.e. load switching, capacitor switching, islanding events etc.), and 2) upper threshold setting (TH_U), which differentiates islanding events from other system events (i.e. normal system operation, load and capacitor switching events etc.). As the lower threshold setting (TH_L) is designed to differentiate between normal system operation and all other system events (i.e. load and capacitor switching events, faults and islanding events etc.), DTs are trained with the entire training dataset containing wide range of power mismatch scenarios (both low power mismatch scenarios in the range of 0-20 percent and high power mismatch scenarios in the range of 20-30 percent in the case study presented in this chapter) to obtain the lower threshold values. In contrast, upper threshold setting (TH_U) is designed to differentiate between islanding events and all other system events (i.e. normal system operation, load and capacitor switching events etc.) under large power mismatch scenarios. Hence, DTs are trained with training dataset containing large power mismatch scenarios (in the range of 20-30 percent in the case study presented in this chapter). So, in essence, lower threshold setting (TH_L) is the set of maximum values of critical system parameters under various system operating conditions below which all of the system events are classified as "normal operation", whereas, upper threshold setting (TH_U) is the set of minimum values of critical system parameters above which all of the system events are classified as "islanding" events. Therefore, an event is classified by DTs as non-islanding (i.e. normal system operation) only if the selected feature values are below the lower threshold settings, TH_L. Whereas, an event is classified as an islanding event only when the feature values are above the upper threshold settings, TH_U. If the feature values are between TH_L and TH_U, DT based classification model may not be completely accurate in classification of system events (low generation and demand mismatch scenarios); thus, the active IDM based on Sandia frequency shift (SFS) is

initiated to differentiate islanding events from other system events (such as load and capacitor switching events). So, active IDM is operating only when the DT based passive scheme cannot differentiate between islanding events and other system events, hence the proposed method minimizes the power quality degradation caused by the active IDM as well as minimizes the erroneous detections by passive IDM alone under low mismatch scenarios.

Periodic DT Modification

The DTs developed offline can be modified periodically by incorporating changing system states in DT training. If significant changes in various system operating conditions such as load levels, generation status etc. occur, then performance of existing DTs will be evaluated under new operating conditions (OCs). If DTs do not classify the new cases accurately, then offline event simulations will be carried out with new operating conditions (OCs) in order to generate training cases with new OCs for DT training. DTs are trained with the enhanced training set containing the new cases alongside the original cases, and updated threshold settings are obtained and implemented for real-time classification of system events.

Online Implementation

Voltage measurements at target DG location are obtained in real-time. Feature vectors containing system parameters are computed, averaged over three cycles, and compared with the threshold settings; and classification results are obtained. Fig. 4.2 presents the complete flowchart of the proposed DT based passive scheme.

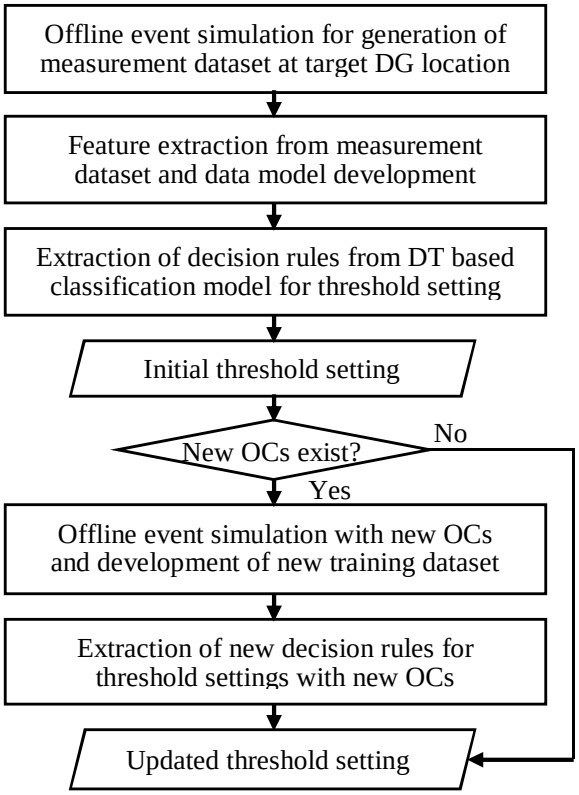

Figure 4.2: Flowchart of the proposed passive islanding detection scheme.

4.1.2 Active IDM Based on Sandia Frequency Shift

Sandia frequency shift (SFS) method [19] is essentially an active frequency drift (AFD) [18] islanding detection method with positive feedback. SFS method injects small perturbations in inverter output current and uses positive feedback to destabilize system frequency. In grid-connected mode, injected perturbations produce insignificant variations in system frequency. Whereas, in islanded mode, significantly larger frequency variations are caused by the injected perturbations. Perturbations are injected in inverter output current as one zero time (t_z) segment per line semi-cycle. The ratio of zero time (t_z) to half of the period of voltage waveform (T_v) as expressed in (5), is called chopping fraction (cf). Positive feedback formulated as linear function of deviation in frequency of PCC voltage is applied to chopping fraction (cf) which causes frequency to deviate from nominal value in absence of the

grid. Mathematically, computation of chopping fraction with positive feedback can be expressed as follows:

$$cf = \frac{2t_z}{T_v} = cf_0 + k(f - f_0) \tag{4.5}$$

where cf_0 is the chopping fraction when there is no frequency error, k is the accelerating gain, f is the system frequency and f_0 is the nominal value of system frequency in grid-connected mode. Insertion of the zero time (t_z) segment in inverter current advances the phase of fundamental component of inverter current with respect to voltage at PCC giving rise to a phase error and thereby causing frequency to drift away from the nominal value in absence of the grid. Inverter phase angle (θ_{inv}) for SFS method can be computed as:

$$\theta_{inv} = \frac{\omega t_z}{2} = \frac{\pi cf}{2} = \frac{\pi}{2}(cf_0 + k(f - f_0)) \tag{4.6}$$

The load phase angle is a function of system frequency (f), load resonant frequency (f_r) and load quality factor (Q_f) [24].

$$\theta_{load} = -\tan^{-1}\left[Q_f\left(\frac{f_r}{f} - \frac{f}{f_r}\right)\right] \tag{4.7}$$

Inverter phase angle (θ_{inv}) and load phase angle (θ_{load}) must be equal for stable islanded operation. Hence, the equilibrium point can be obtained by equating two phase angles as:

$${f_r}^2 + \frac{f\tan\left[\pi\left(cf_0 + k(f - f_0)\right)/2\right]f_r}{Q_f} - f^2 = 0 \tag{4.8}$$

NDZ of SFS method depends on SFS parameters (cf_0 and k) and load parameters (Q_f and f_r). In order to eliminate NDZ, the equilibrium point defined by the phase criterion in (8) must be an unstable equilibrium point which is obtained when the

following criterion in (9) is satisfied [24].

$$\frac{d\theta_{load}}{df} < \frac{d\theta_{inv}}{df} \tag{4.9}$$

The instability criterion in (9) translates into the following condition for instability in terms of accelerating gain k:

$$k > max \frac{2\left[Q_f\left(\frac{f_r}{f^2}\right) + \left(\frac{1}{f_r}\right)\right]}{\pi\left[1 + {Q_f}^2\left(\left(\frac{f_r}{f}\right) - \left(\frac{f}{f_r}\right)\right)\right]} \tag{4.10}$$

In this study, harmony search algorithm (HSA) [84] is used to find optimal values of k under different loading conditions (i.e. different values of Q_f and f_r). Main constraints in the optimization problem are $0 < Q_f \leq Q_{fmax}$, $f_{min} < f \leq f_{max}$ and $f_r > 0$ [24]. Optimal values of k are utilized in different loading conditions to achieve optimal SFS performance.

4.1.3 Outline of the Proposed Methodology

The outline of the proposed hybrid islanding detection method is presented in Fig. 4.3, which summarizes the discussions presented in subsections 4.1.1 and 4.1.2.

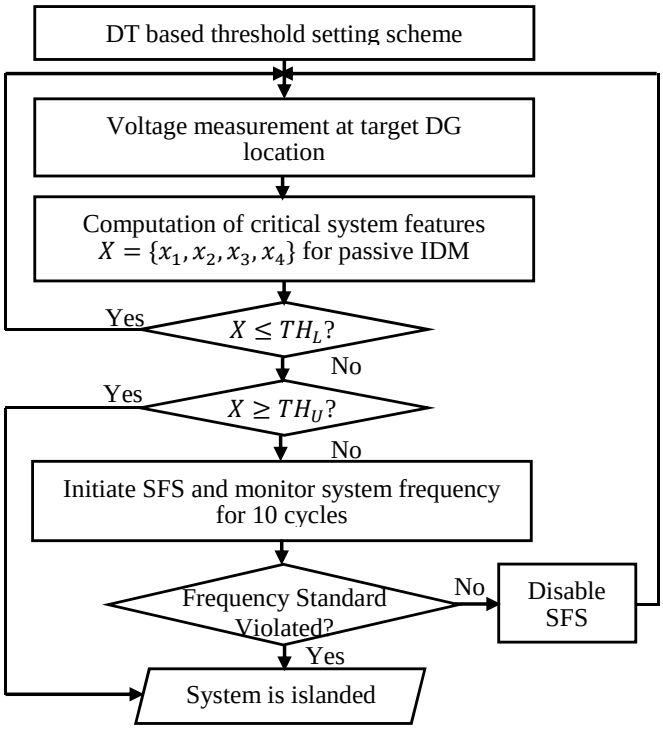

Figure 4.3: Outline of the proposed hybrid islanding detection method.

4.2 Test System Models

Performance of the proposed IDM for inverter based DGs is evaluated using two different test systems. Test System-I, presented in Fig. 4.4, consists of a 200 kW inverter based DG (PV farm) and loads connected to the utility grid. The utility grid is modelled as a 25 kV distribution feeder connected to a 120 kV equivalent transmission network. The PV model consists of two PV units each delivering a maximum power of 100 kW at an irradiance of 1000 W/m^2. PV power conditioning system consists of two DC-DC boost converters (equipped with Perturb and Observe MPPT controllers) which increase the voltage output from PV arrays to 500V and a voltage source converter (VSC) which converts the 500V DC to 260V AC at unity power factor. The system load is modeled as parallel RLC branch.

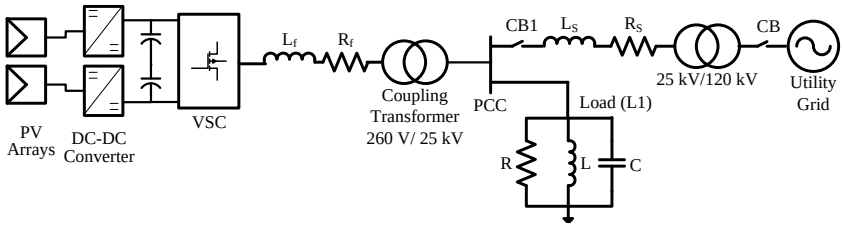

Figure 4.4: Single line diagram of test system-I.

Test system-II, presented in Fig. 4.5, is a grid-connected microgrid based on IEEE 13 bus distribution feeder model [81] consisting of three DGs and a battery energy storage system. The microgrid is operated at 4.16 kV/60 Hz and inter-connected with a 230 kV equivalent transmission via a 230 kV/25 kV step-down transformer. The transmission network is modelled as the two area, four generator system described in [82]. Loads in the system are modeled as constant PQ loads. This test system is utilized to evaluate the performance of the proposed methodology under various real and reactive power mismatch scenarios in the presence of multiple inverter based DGs.

Fig. 4.6 presents the SFS implementation using phase angle transformation where the reference values of d-axis and q-axis current components i_{dref} and i_{qref} are transformed to obtain new references for d-q axis current components ${i_{dref}}^*$ and ${i_{qref}}^*$ using the phase angle transformation matrix.

Fig. 4.7 presents the implementation of the DT based passive IDM. The DT based passive scheme generates the initiation signal for the SFS scheme when parameter values are in the range of, $TH_L < x_i < TH_U$ for three consecutive cycles. Otherwise, if the parameter values are, $x_i \geq TH_U$ for three consecutive cycles, a trip signal is generated by the DT based scheme in order to isolate the DG from the system.

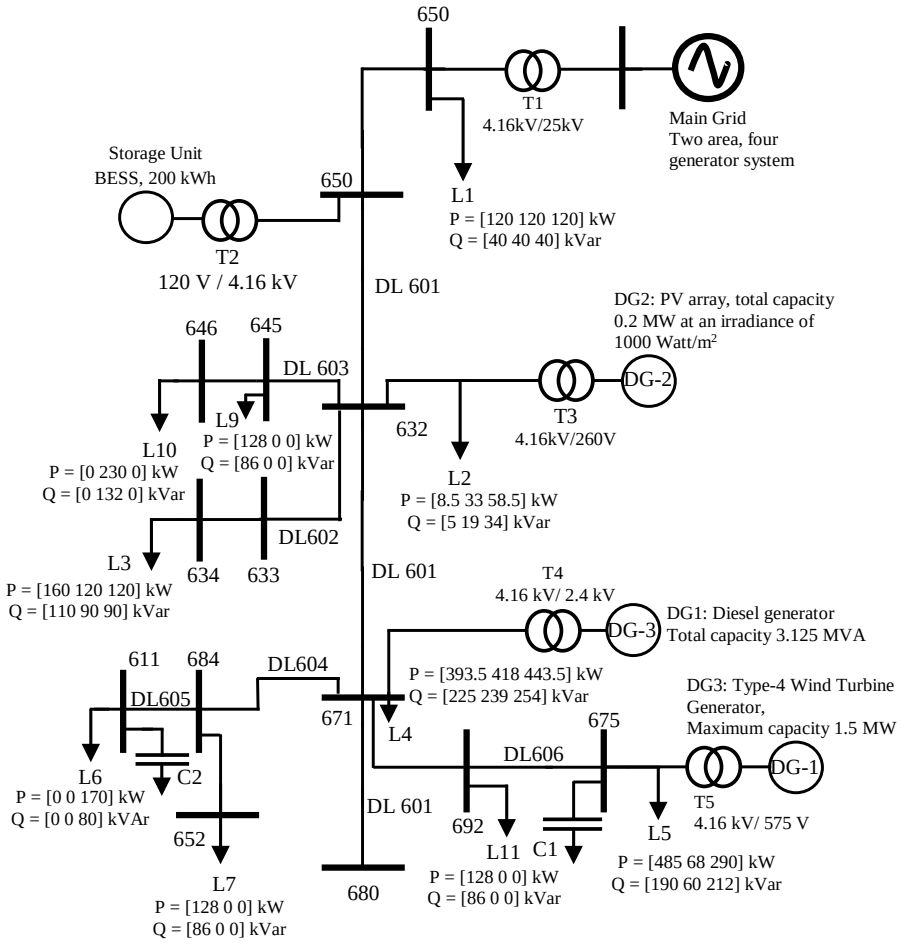

Figure 4.5: Microgrid test system model based on IEEE 13 bus distribution system.

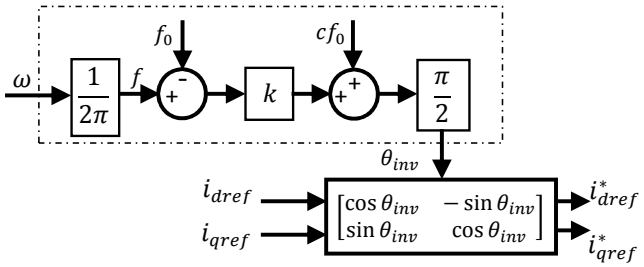

Figure 4.6: Implementation of SFS scheme in DG interface control.

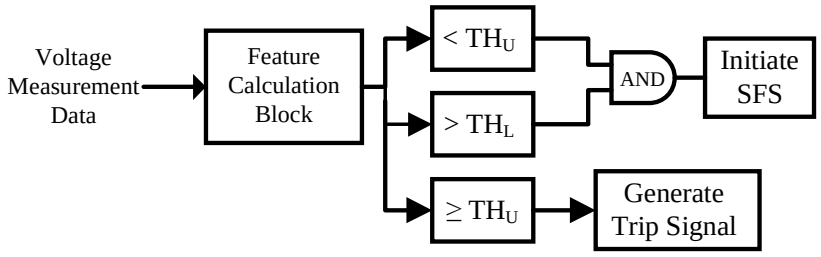

Figure 4.7: Implementation of DT based passive scheme.

Fig. 4.8 presents the complete DG interface control block diagram with the proposed hybrid islanding detection method.The DG control interface is essentially a constant DC-link voltage control structure which controls the reference value of d-axis current component in order to maintain the DC-link voltage at a constant level. Since the DG operates at unity power factor, the reference value of q-axis current is set to zero.

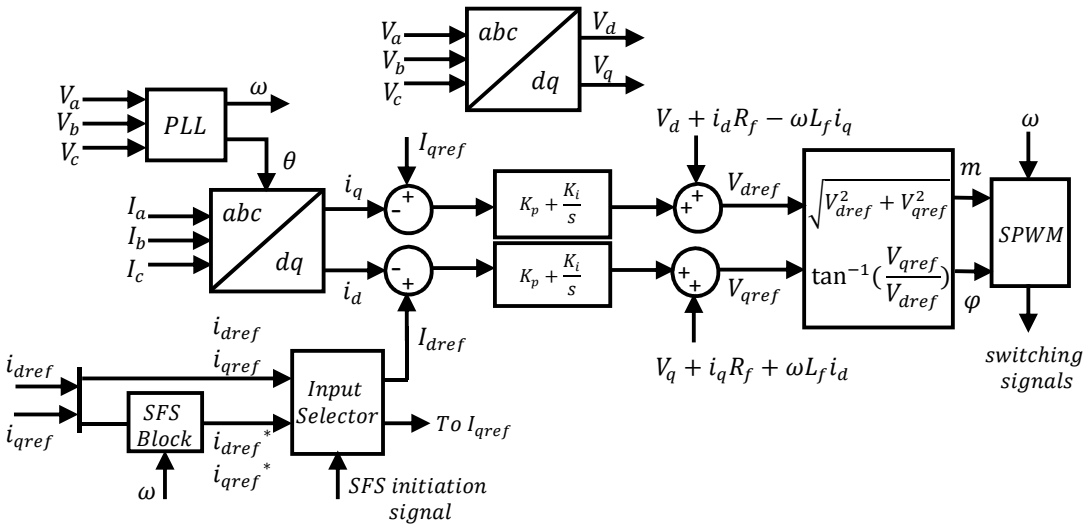

Figure 4.8: Implementation of the proposed hybrid islanding detection method in DG interface control architecture.

4.3 Simulation Results on Test System-I

For test system-I, 150 system events under various system operating conditions (OCs) were simulated offline to generate the measurement dataset at target DG location. Simulations are performed in MATLAB/Simulink platform. System parameters are extracted from obtained measurement dataset and data model for setting the threshold values for the passive islanding relay is developed. Based on the data model, DTs are constructed using J48 decision tree algorithm in Waikato Environment for Knowledge Analysis (WEKA) [83] data mining platform. Decision rules and corresponding threshold values are extracted for implementation of the passive scheme in the proposed islanding detection method.

Two sets of DTs were constructed for extracting lower and upper threshold settings. The lower threshold settings were obtained by training the DT classifiers using all 150 cases generated through system event simulations under both low and high real/reactive power mismatch scenarios between the DG production levels and local load demands. Various combinations of real power mismatch ranging from 0 to 30 percent and reactive power mismatch ranging from -10 to 10 percent were considered in developing the training data set.

DT classifiers were trained with 85 training cases corresponding to various combinations of real power mismatch greater than 20 percent and reactive power mismatch in the range of 5 to 10 percent for obtaining the upper threshold settings. The lower threshold setting differentiates normal system operation from other system events such as- islanding, load and capacitor switching events etc., whereas, the upper threshold setting differentiates the islanding events from other system events such as- normal operations, load and capacitor switching events etc. Table 4.2 presents the threshold settings for the passive islanding relay for the test system under consideration.

Table 4.2: Threshold Setting for Passive IDM in Test System-I

Feature	Threshold Values(TH_L)	Threshold Values(TH_U)
Voltage deviation (ΔV)	58.468	243.40
Rate-of-change of voltage ($\Delta V/\Delta t$))	3.6420	48.635
Voltage Unbalance (VU)	0.0045	0.9055
Total harmonic distortion (V_{THD})	0.4590	2.2435

The SFS method is initiated when system parameter values are between TH_L and TH_U (i.e. $TH_L < x_i < TH_U$). Performance of SFS method depends on the value of accelerating gain (k) which helps in destabilizing the system frequency during islanding events. Higher values of k leads to faster detection times and smaller NDZ, but causes increased number of false trips and higher degradation in power quality. In this work, optimal values of k for different loading conditions and quality factors are obtained using Harmony Search Algorithm (HSA)[84]. The optimization results are presented in Table 4.3. SFS method is implemented in conjunction with over frequency and under frequency protection (OFP/UFP) relays. The OFP/UFP scheme is implemented in accordance with IEEE Std. 929-2000 which recommends any non-islanding inverter to cease to energize the utility lines within 6 cycles when the frequency is outside the range of 59.3-60.5 Hz [85].

Table 4.3: Thresholds for Accelerating Gain (k) Parameter in SFS Method for Different Load Quality Factors

Q_{fmax}	$k_{threshold}$
1	$k > 0.02143$
2	$k > 0.04279$
2.5	$k > 0.05356$
3	$k > 0.06428$
4	$k > 0.08413$
5	$k > 0.10347$

Performance of the proposed method is evaluated based on simulation of system events under various test conditions recommended in IEEE Std. 1547 [11], IEEE Std. 929 [85], and UL1741 [86]. The load and capacitor switching events were simulated by switching a 1MW/50kVAR load and a 70kVAR capacitor bank connected to the grid, respectively. Islanding events were simulated by opening the circuit breaker CB to isolate the DG from utility grid. The accelerating gain parameter (k) and initial chopping fraction (cf_0) in SFS scheme are set to 0.085 and zero respectively. Results from four test case scenarios are presented in this section in order to demonstrate the performance of the proposed method.

4.3.1 Test Case Scenario I

Load L1 is adjusted to 100% of rated active power output of the DG unit ($P_{L1} = P_{DG}$) and zero reactive power ($Q_{L1} = 0$; unity power factor). Parameter values for islanding event at t=5s, $x_1 = 86.75V$, $x_2 = 11.62V/cycle$, $x_3 = 0.812$, and $x_4 = 0.769\%$. Hence, SFS method is initiated as the parameter values are in the range $TH_L < x_i < TH_U$ and islanding is detected by OFP/UFP relay as system frequency deviates past the over frequency limit of 60.5 Hz. For load and capacitor switching events, the set of parameter values are $x_1 = 98.59V$, $x_2 = 18.17V/cycle$, $x_3 = 0.2412$, $x_4 = 1.305\%$, and $x_1 = 29.4V$, $x_2 = 5.107V/cycle$, $x_3 = 0.007$, $x_4 = 4.61\%$, respectively. In both cases, at least one of the parameter values are in the range $TH_L < x_i < TH_U$, hence SFS is activated. As the DG is grid-connected, injected perturbations do not cause significant deviations in system frequency. Fig. 4.9 and Fig. 4.10 present the system voltage and frequency profiles for system events in test case scenario-I.

4.3.2 Test Case Scenario II

Load L1 is set to 110% of rated active power of the DG unit ($P_{L1} = 1.1P_{DG}$) and reactive power is set to 1% of rated DG active power (Q_{L1} is positive; lagging power

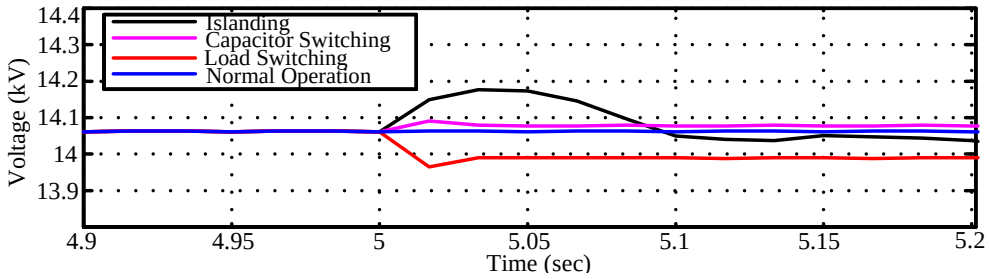

Figure 4.9: Voltage at PCC for system events in test case scenario-I.

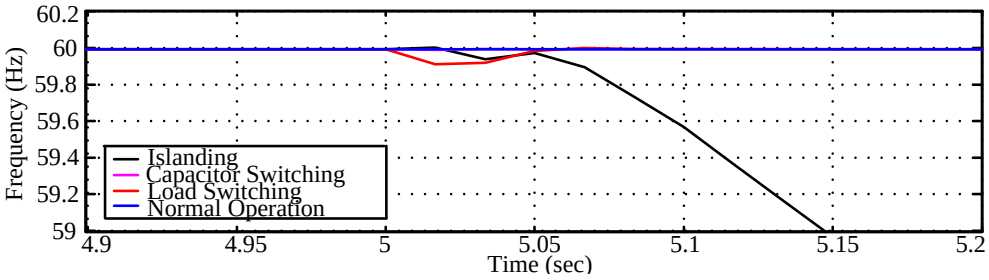

Figure 4.10: System frequency for system events in test case scenario-I.

factor load). In case of islanding event at t=5s, $x_1 = 191.02V$, $x_2 = 38.57V/cycle$, $x_3 = 0.271$, and $x_4 = 1.181\%$. Since, not all parameters are beyond TH_U, SFS is initiated and islanding is detected as the frequency deviates beyond over frequency set point. For load and capacitor switching events, $x_1 = 100.62V$, $x_2 = 18.25V/cycle$, $x_3 = 0.242$, $x_4 = 1.31\%$; and $x_1 = 27.24V$, $x_2 = 5.23V/cycle$, $x_3 = 0.007$, $x_4 = 4.58\%$, respectively. Hence, SFS method is initiated and perturbations are injected. As the DG is in grid-connected mode, system frequency does not deviate beyond permissible limits. Fig. 4.11 and Fig. 4.12 present the system voltage and frequency profiles for system events in test case scenario-II.

4.3.3 Test Case Scenario III

Load L1 is 125% of rated active power of the DG unit ($P_{L1} = 1.25P_{DG}$) and reactive power is set to 15% of the rated DG active power output (Q_L1 is positive, lagging

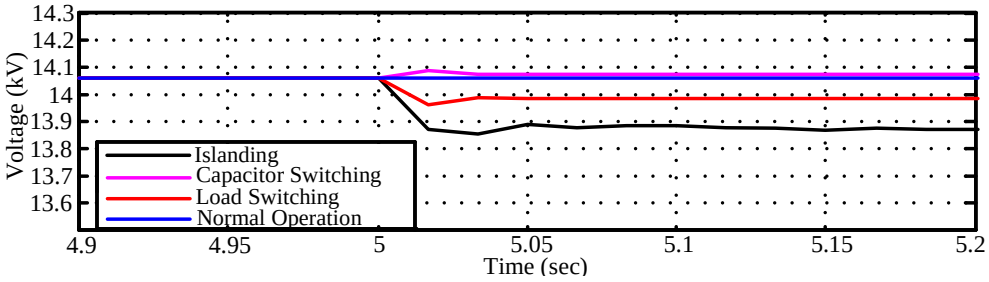

Figure 4.11: Voltage at PCC for system events in test case scenario-II.

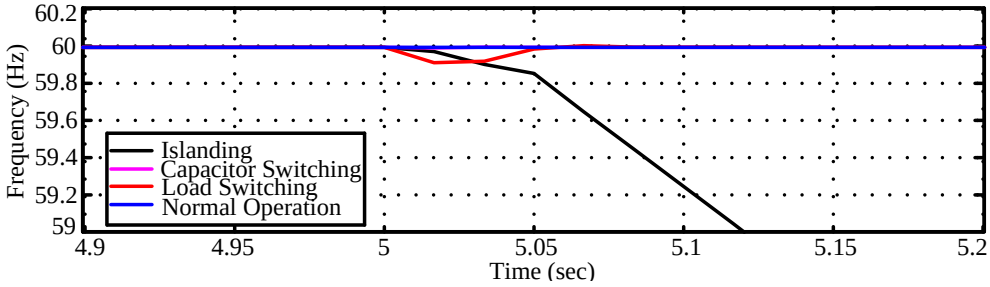

Figure 4.12: System frequency for system events in test case scenario-II.

power factor load). For islanding event at t=5s, $x_1 = 1965.26V$, $x_2 = 559.2V/cycle$, $x_3 = 5.97$, and $x_4 = 6.88\%$; which are all above threshold setting THU. Hence islanding is detected by the DT based passive scheme. For load and capacitor switching events, $x_1 = 112.78V$, $x_2 = 18.25V/cycle$, $x_3 = 0.241$, $x_4 = 1.31\%$; and $x_1 = 14.59V$, $x_2 = 5.27V/cycle$, $x_3 = 0.0068$, $x_4 = 4.54\%$, respectively. Hence, SFS method is initiated and perturbations are injected. As the DG is grid-connected, system frequency does not deviate beyond permissible limits. Fig. 4.13 and Fig. 4.14 present the system voltage and frequency profiles for system events in test case scenario-III.

4.3.4 Test Case Scenario IV

In this scenario, performance of the proposed method is evaluated for loads with a wide range of quality factors (Q_f). IEEE Std. 1547 [11], IEEE Std. 929 [85], and

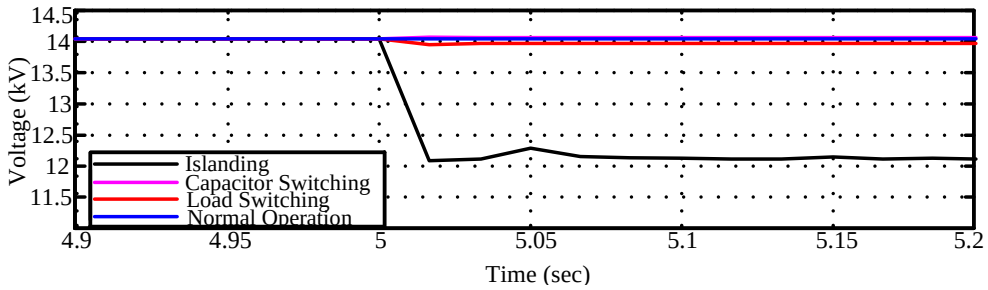

Figure 4.13: Voltage at PCC for system events in test case scenario-III.

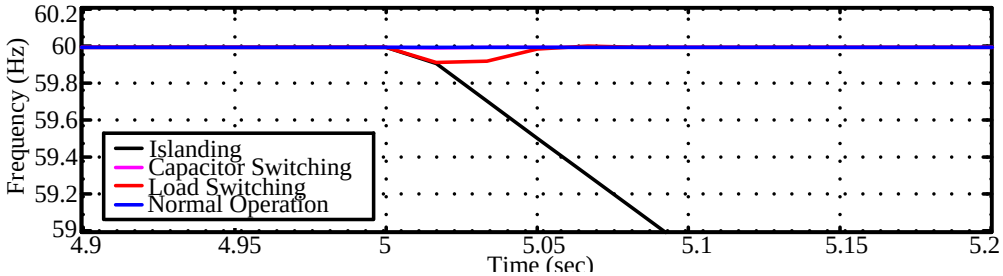

Figure 4.14: System frequency for system events in test case scenario-III.

UL1741 [86] recommend test conditions with $Q_f = 1$, $Q_f 2.5$, and $Q_f 1.8$, respectively. Hence, islanding detection performance of the proposed method is evaluated for loads with Q_f ranging from 1 to 5 with load L1 adjusted to 100% of rated active power output of DG unit ($P_{L1} = P_{DG}$). The load configurations for different Q_f values are presented in Table 4.4. Fig. 4.15 presents the system frequency for islanding events under different load quality factors (Q_f). It is evident from Fig. 4.15 that, frequency deviations beyond the OFP/UFP thresholds become much slower with increasing load quality factor (Q_f) which is mainly because of the fixed value of the accelerating gain k used in the analysis. The accelerating gain k is set at 0.085, which is higher than the optimal threshold value of k for loads with a maximum Q_f value of 4, as presented in Table 4.3. Thus, the system frequency deviates beyond the OFP/UFP thresholds within 0.2 seconds from the initiation of the islanding event for loads with Q_f values upto 4. Whereas, the frequency deviation in case of loads with $Q_f = 5$ is much slower.

Hence, utilization of optimal k values for different load quality factors (Q_f) allows minimization of NDZ and enhance the overall detection time in the proposed IDM.

Table 4.4: Load RLC Parameters for Different Load Quality Factors
[Load Resonant Frequency (f_0) = 60 Hz]

Q_f	$R(k\Omega)$	$L(H)$	$C(\mu H)$
1	2.965	7.86	0.89
2	2.965	3.39	1.79
2.5	2.965	3.15	2.24
3	2.965	2.62	2.69
4	2.965	1.97	3.58
5	2.965	1.58	4.48

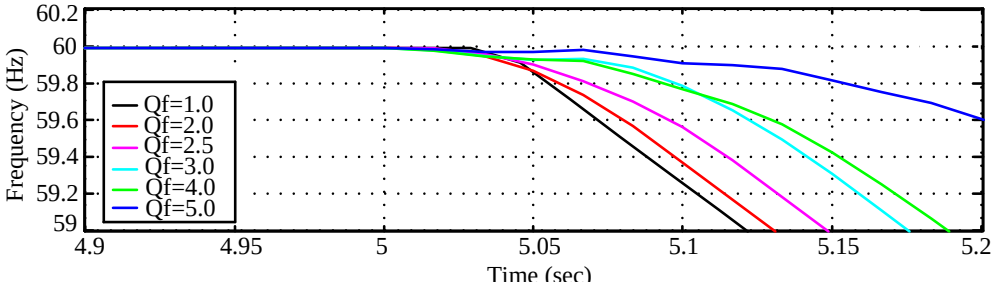

Figure 4.15: System frequency for islanding events for different load quality factors (Q_f) in test case scenario-IV.

4.4 Simulation Results on Test System II

Test system-II presents the performance of the proposed islanding detection methodology in the presence of multiple DGs, especially in the presence of multiple inverter based DGs. The microgrid model contains three DGs- an emergency diesel generator and two inverter based DGs (i.e. a PV plant and a type-4 full converter wind generator). For test system-II, measurement data set for offline DT training is generated using a total of 320 system events under 16 different system operating conditions (OCs) at target DG location (PCC bus of target DG unit with distribution

network/microgrid). The OCs are selected based on combinations of load patterns in area-EPS, distribution network/microgrid and target DG unit, and generation profile of DGs to represent different levels of power imbalances between generation and demand in the islanded microgrid system. The following events have been considered in the offline simulations for generation of training dataset for DT classifiers.

- Tripping of circuit breaker at distribution substation to island the distribution system/ microgrid from the main grid.
- Loss of distribution lines leading to formation of power islands within the distribution network.
- Three phase faults in distribution network with instantaneous fault clearing time causing formation of islands.
- Formation of islands caused by loss of transmission lines between area-1 and area-2 of two area system.
- Three-phase load changes: 50% $\leftrightarrow$ 80%, 80% $\leftrightarrow$ 100%, 50% $\leftrightarrow$ 90%, 100% $\leftrightarrow$ 120%.
- Single-phase load changes: 50% $\leftrightarrow$ 60%, 70% $\leftrightarrow$ 90%, 40% $\leftrightarrow$ 100%, 100% $\leftrightarrow$ 120%.
- Shunt capacitors switching on or off.
- Loss of generations by DGs other than the target DG unit.
- Loss of generation units in either area-1 or area-2 of two area system.

A total of 20 system events under each of the selected OCs were simulated resulting in a total of 320 offline time domain simulations. All variables measured at PCC of the target DG unit refer to the high voltage side of the DG interconnection transformer. Critical attributes (CAs) were extracted from obtained measurement

dataset and classification model for the islanding detection relay at target DG location is developed. The simulations were performed in MATLAB/ Simulink platform.

Two sets of DTs were constructed in WEKA [83] for extracting the lower threshold setting (TH_L) and upper threshold setting (TH_U) at the target DG location. For extracting the lower threshold settings (TH_L), DTs were trained with all 320 cases generated from system events simulated under real power mismatch in the range of 0 to 30 percent and reactive power mismatch in the range of -10 to 10 percent. For upper threshold settings (TH_U), 140 cases were used from system events simulations under high real and reactive power mismatches in the range of 20 to 30 percent and 5 to 10 percent, respectively. Table 4.5 presents the threshold settings for the passive islanding relay for test system-II considering DG-2 as the target DG location.

Table 4.5: Threshold Setting for Passive IDM in Test System-II (Target DG Location is DG-2)

Feature	Threshold Values(TH_L)	Threshold Values(TH_U)
Voltage deviation (ΔV)	65.75	595.57
Rate-of-change of voltage ($\Delta V/\Delta t$))	3.720	90.891
Voltage Unbalance (VU)	0.0058	0.85
Total harmonic distortion (V_{THD})	0.46	6.38

In order to prevent the degradation of performance of active frequency drifting IDM (i.e. Sandia Frequency Shift) resulting from averaging effects in multi-inverter systems, all the inverters in the system should have the same frequency drift directions (drift up/down). Although, performance degradation resulting from parameter settings and measurement errors can happen, but the overall effect on the islanding detection capability in the system is negligible as discussed in Ref. [87]. For test system-II, SFS method is implemented with frequency drift down setting in both the inverter based DGs. Simulation results from three test cases with various power mismatch scenarios (considering DG-2 as the target DG location) are presented to

demonstrate the performance of the proposed method in the presence of multiple inverter based DGs. Load and capacitor switching events were simulated by switching load L9 at bus 645 and capacitor bank C2 at bus 611, respectively. SFS parameters k and cf_0 are set to 0.085 and zero, respectively.

4.4.1 Test Case Scenario I

Load L4 is adjusted to 100% of rated active power output of DG-2 ($P_{L4} = P_{DG2}$) and zero reactive power ($Q_{L4} = 0$; unity power factor). Loads L1 and L2 are adjusted to set the overall microgrid loading at 100% of the aggregated rated active power output from DG-1 and DG-2 ($P_{\mu G} = \sum P_{DG}$). For microgrid islanding and DG-2 islanding events at $t = 5s$, set of parameters are $x_1 = 125.05V$, $x_2 = 19.03V/cycle$, $x_3 = 1.56$, $x_4 = 0.864\%$; and $x_1 = 93.42V$, $x_2 = 18.03V/cycle$, $x3 = 1.0428$, $x4 = 0.83\%$, respectively. Hence, SFS is initiated and frequency deviation beyond permissible limit is detected by OFP/UFP scheme. For DG-1 islanding, load and capacitor switching events, sets of parameters are $x_1 = 20.53V$, $x_2 = 8.03V/cycle$, $x_3 = 0.0397$, $x_4 = 0.5725\%$; $x_1 = 116.24V$, $x_2 = 17.98V/cycle$, $x_3 = 0.24$, $x_4 = 1.26\%$; and $x_1 = 9.72V$, $x_2 = 5.84V/cycle$, $x_3 = 0.0072$, $x_4 = 4.15\%$, respectively. Hence, although SFS is initiated for each of these events, system frequency does not deviate beyond the permissible limits as a result of DG-2 being grid-connected. Fig. 4.16 and Fig. 4.17 present the system voltage and frequency profiles for system events in test case scenario-I.

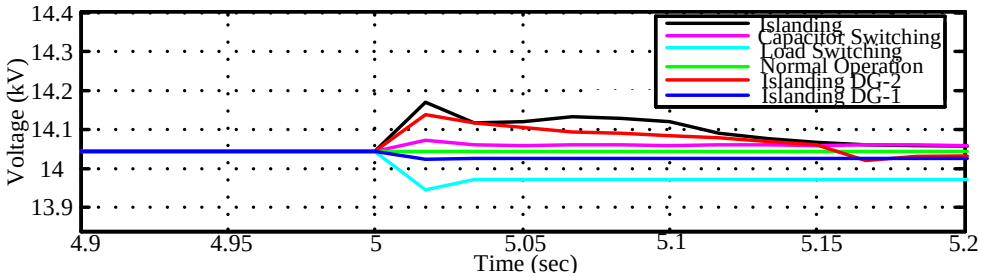

Figure 4.16: Voltage at PCC for system events in test case scenario-I.

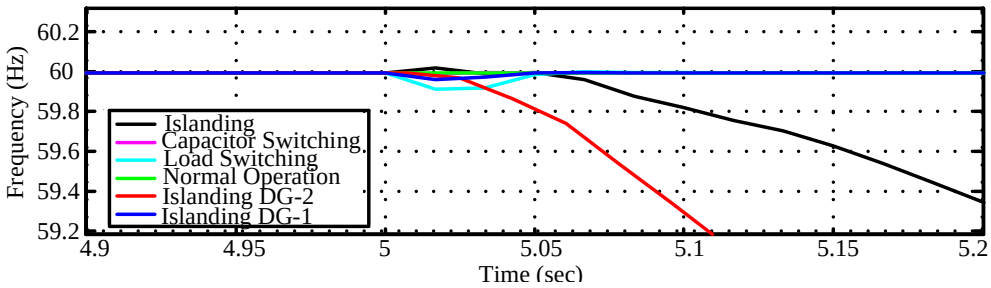

Figure 4.17: System frequency for system events in test case scenario-I.

4.4.2 Test Case Scenario II

Load L4 is 110% of rated active power of DG-2 ($P_{L4} = P_{DG2}$) and reactive power is 1% of rated active power of DG-2 (Q_{L4} is positive, lagging power factor). Loads L1 and L2 are adjusted to set the overall microgrid loading at 110% of the aggregated rated active power output of DG-1 and DG-2 ($P_{\mu G} = 1.1 \sum P_{DG}$). For microrid and DG-2 islanding events at $t = 5s$, the sets of parameters are $x_1 = 97.74V$, $x_2 = 32.58V/cycle$, $x_3 = 1.52$, $x_4 = 1.26\%$; and $x_1 = 106.35V$, $x_2 = 35.46V/cycle$, $x_3 = 1.38$, $x_4 = 1.08\%$, respectively. Since the parameters are in the range of $TH_L < x_i < TH_U$, SFS is initiated and islanding is detected by OFP/UFP scheme. For DG-1 islanding, load and capacitor switching events, the sets of parameters values are $x_1 = 21.76V$, $x_2 = 8.09V/cycle$, $x_3 = 0.04$, $x_4 = 0.572\%$; $x_1 = 124.03V$, $x_2 = 17.98V/cycle$, $x_3 = 0.237$, $x_4 = 1.253\%$; and $x_1 = 26.21V$, $x_2 = 5.32V/cycle$, $x_3 = 0.0043$, $x_4 = 4.07\%$, respectively. Hence, SFS is initiated for each of these events but system frequency remains within permissible limits as DG-2 is grid-connected. Fig. 4.18 and Fig. 4.19 present the system voltage and frequency profiles for system events in test case scenario-II.

4.4.3 Test Case Scenario III

Load L4 is at 125% of rated active power of DG-2 ($P_{L4} = 1.25P_{DG2}$) and reactive power is set to 15% of rated active power of DG-2 (Q_{L4} is positive; lagging power factor

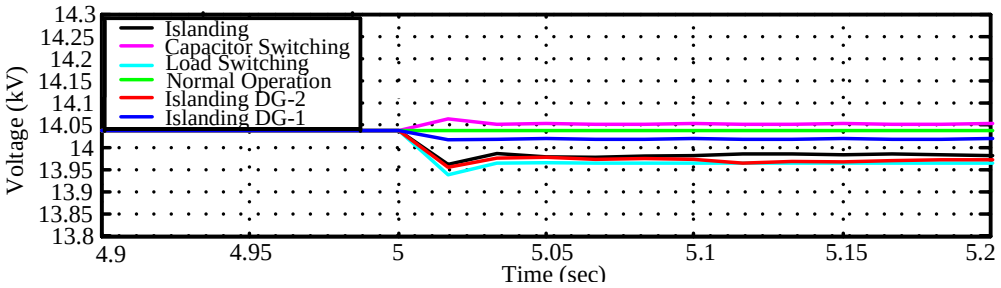

Figure 4.18: Voltage at PCC for system events in test case scenario-II.

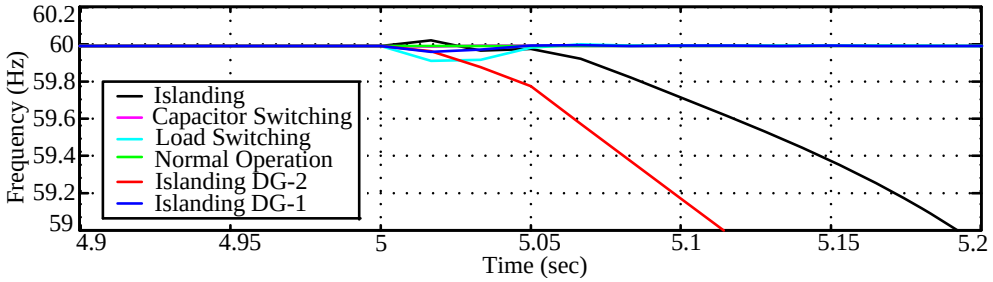

Figure 4.19: System frequency for system events in test case scenario-II.

load). Loads L1 and L2 are adjusted to set the overall microgrid loading at 125% of the aggregated rated active power output from DG-1 and DG-2 ($P_{\mu G} = 1.25 \sum P_{DG}$). For microgrid and DG-2 islanding events, the sets of parameters are $x_1 = 940.8V$, $x_2 = 656.08V/cycle$, $x_3 = 2.65$, $x_4 = 6.78\%$; and $x_1 = 1915.5V$, $x_2 = 553.37V/cycle$, $x_3 = 5.48$, $x_4 = 6.72\%$, respectively. Since all system parameters exceed TH_U for both events, islanding is detected by the DT based passive islanding relay. For DG-1 islanding, load and capacitor switching events, the sets of parameters are $x_1 = 67.25V$, $x_2 = 7.93V/cycle$, $x_3 = 0.042$, $x_4 = 0.57\%$; $x_1 = 161.51V$, $x_2 = 17.73V/cycle$, $x_3 = 0.242$, $x_4 = 1.242\%$; and $x_1 = 53.03V$, $x_2 = 5.07V/cycle$, $x_3 = 0.0055$, $x_4 = 3.956\%$; respectively. Hence, SFS is initiated, but system frequency remains within permissible limits as DG-2 is grid-connected. Fig. 4.20 and Fig. 4.21 present the system voltage and frequency profiles for system events in test case scenario-III.

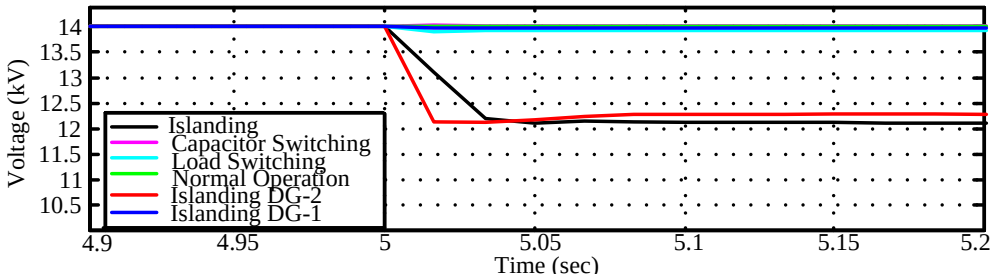

Figure 4.20: Voltage at PCC for system events in test case scenario-III.

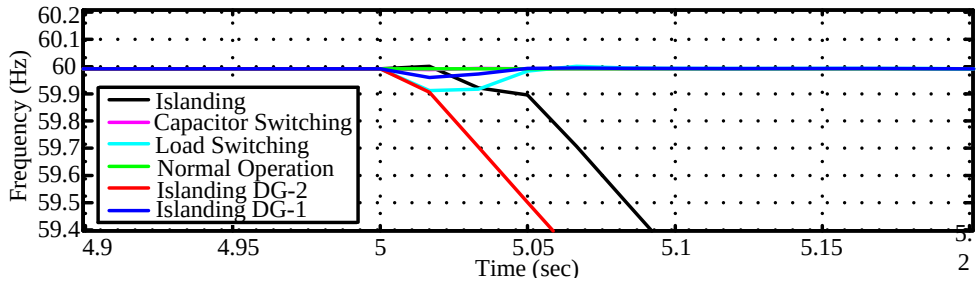

Figure 4.21: System frequency for system events in test case scenario-III.

For both case studies, test case scenarios I, II, and III demonstrate the performance and operation of the proposed method under low, moderate, and high power mismatch scenarios, respectively. Islanding detection speed for the proposed approach is observed to be approximately between 4 cycles or 0.07 seconds (detection by passive islanding relay) and 13 cycles or 0.22 seconds (detection by the combination of passive islanding relay and SFS). This is within the detection time window specified in IEEE Std. 1547 [11].

4.5 Comparative Analysis of IDMs

Performance of the proposed technique is compared with several intelligent based passive IDMs as well as rate-of-change of frequency (ROCOF) and rate-of-change of voltage (ROCOV) based relays. Test system-II is utilized as test system. Training and testing datasets utilized to evaluate the intelligent based classifiers in WEKA contained 320 cases. The ROCOF relays were designed with a three-cycle time

window and with threshold settings of 0.1 Hz/s and 0.5 Hz/s. The ROCOV relay was also set with a three cycle-time window with threshold value of 0.07 V/s. The islanding detection methodologies were compared based on overall classification accuracy, dependability index (DI), and security index (SI). Dependability index (DI) and Security index (SI) are the classification accuracy of the islanding events and non-islanding events respectively.

In the proposed methodology, threshold settings for the DT based passive IDM are designed to provide classification of islanding events (for high generation and load mismatch scenarios) as well as classification of normal system operations (under all generation and load mismatch scenarios). For low generation and load mismatch scenarios, where passive IDM usually suffer from classification inaccuracies, SFS technique is utilized for islanding detection. The NDZ of the SFS technique can be eliminated/minimized by optimizing the SFS parameters. Hence the proposed methodology is capable of detecting islanding events with high accuracy and reliability.

Table 4.6 presents the comparative evaluation of the islanding detection methodologies based on overall classification accuracy, dependability index (DI), and security index (SI).

Table 4.6: Comparative evaluation of islanding detection methodologies

Methodology	Accuracy	DI	SI
Combination of DT and SFS	100	100	100
Decision Tree Classifier	98.76	98.84	98.68
Support Vector Machine (SVM)	86.54	83.68	89.40
Naive-Bayes Classifier	91.28	87.24	95.32
ROCOF (0.1 Hz/s)	78.65	74.38	82.92
ROCOF (0.5 Hz/s)	72.13	64.72	79.52
ROCOV (0.07 V/s)	68.08	36.16	100

4.6 Summary

This chapter proposes an islanding detection technique for grid-connected inverter based DGs. The proposed methodology is a combination of DT based passive islanding detection technique and optimized Sandia frequency shift (SFS) method. Harmony search algorithm (HSA) is utilized in optimization of the SFS parameters for minimizing NDZ. Performance of the proposed scheme is evaluated with two different test systems under a wide range of power mismatch scenarios as well as in the presence of multiple inverter based DGs. The major contributions of the chapter can be summarized as follows:

- The proposed approach offers accuracy and robustness in islanding detection under various system operating conditions, load configurations and in the presence of multiple inverter based DGs. Results from detailed case studies performed on two test systems validate the performance of the proposed approach.

- The proposed technique utilizes the SFS method only when the DT based passive islanding relay cannot differentiate islanding events from other system events. Thus periodic disturbance injections are avoided and power quality degradation in the system is minimized.

- The proposed method eliminates the detection inaccuracies resulting from using passive islanding detection methods alone under low generation and demand mismatch scenarios.

- The proposed scheme enhances islanding detection time and minimizes false trips through adaptive combination of DT based passive IDM and SFS technique.

- The proposed method provides an effective means to automatize the threshold setting tasks based on DTs and measurement data at target DG locations. Thus inaccuracies caused by improper threshold settings can be eliminated. Moreover, the periodic DT modification feature enables integration of changing system conditions in the islanding detection process.

Hence, the proposed hybrid islanding detection technique, which combines the passive and active methodologies, can provide fast and accurate detection of islanding events. Future works may include enhancement of the periodic DT update feature enabling the modification of the threshold settings based on changing system scenarios with minimal supervision, and also, implementation and testing of the proposed method on real microgrid testbeds or using hardware-in-loop environments.

Chapter 5

A Decision Tree Based Approach for Controlled Islanding of Microgrids

This chapter presents a decision tree based systematic approach for controlled islanding of grid-connected microgrids. The objective of the proposed approach is to develop an adaptive controlled islanding methodology to be implemented as a preventive control component in emergency control strategy for microgrid operations. A contingency-oriented decision tree classifier is trained with event database generated from offline simulations of system events. The trained decision tree classifier is capable of identifying system events that warrant controlled islanding of microgrids as a preventive control measure. Real time voltage and current measurements are utilized in conjunction with the trained decision tree classifier for online decision support on controlled islanding strategy of microgrids. A microgrid test system model consisting of multiple distributed generations and energy storage systems is employed to demonstrate the performance of the proposed approach.

The proposed approach aims at the implementation of the DT based controlled islanding methodology as a preventive control component within the emergency

control framework for microgrids. In the proposed approach, a contingency-oriented DT classifier trained with learning set (LS) obtained from extensive offline simulations is employed for detection of system events that require controlled islanding of microgrids a preventive measure. The proposed controlled islanding strategy is initiated upon the detection of contingency events posing system security concerns. Detailed case study on grid-connected microgrid model consisting of inverter interfaced DGs (PV farms), battery energy storage system (BESS) and local loads is performed to demonstrate the performance of the proposed methodology.

The chapter is structured as follows. Principles of the proposed decision tree assisted controlled islanding methodology is presented in Section 5.1. Section 5.2 describes the test system model. In Section 5.3, case study results are presented, and performance of the proposed method is discussed. Finally, a summary is presented in Section 5.4.

5.1 Decision Tree Based Controlled Islanding Methodology

The conceptual model of the proposed methodology is presented in Fig. 5.1. In the proposed approach, the DT assisted controlled islanding strategy is employed as a means for preventive control with the primary objectives being localization of system disturbances through controlled separation at the point of common coupling (PCC), and enhancement of supply reliability and availability through controlled autonomous operation microgrids. Fast and reliable detection of any system disturbances posing security concerns is critical towards successful controlled islanding operations. In this regard, DT classifiers are proposed for online detection and classification of system events for initiation of controlled islanding strategy for microgrids. DT classifiers built from extensive offline training are implemented for real time detection and classification of system events. A brief overview of the proposed DT based controlled islanding methodology is presented in this section.

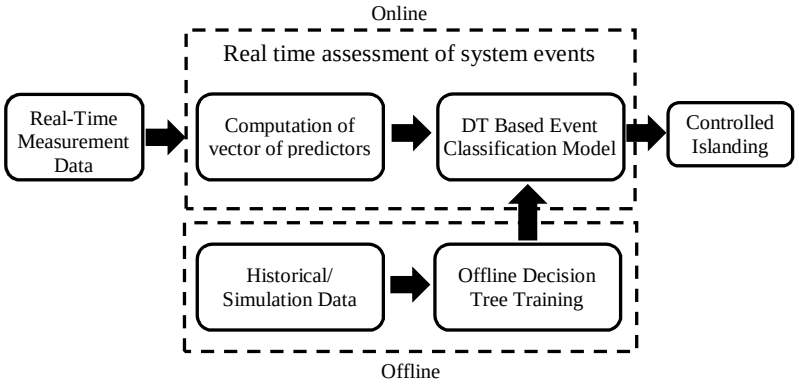

Figure 5.1: Conceptual model of the proposed controlled islanding methodology.

5.1.1 Decision Tree Based Classification of System Events

DTs are supervised machine learning techniques that serve as a statistical alternative to deterministic system models. Trained with a learning set (LS) consisting of input-output pairs, DTs are capable of extracting underlying relationship (decision rules) between the inputs (predictors) and outputs (class). These decision rules serve as a predefined logical paths generated from offline DT training and can be utilized for online classification of unseen system events. DTs generated from offline training with a representative LS consisting of wide variety of system events can be employed online for real time assessment and classification.

In the proposed approach, DTs are utilized for identification of contingency events that require preventive measures to ensure system security. The DTs built in the proposed scheme are classification trees which are built from a training dataset containing n-dimensional vector of predictors and corresponding class values. The developed DTs can predict the class of an unseen event from the n-dimensional vector of predictors presented to it for classification.

Power system contingencies often induces abrupt variations in electrical states (i.e. voltages and currents) of the system. The proposed method relies on extraction of a set of predictors from local measurements of voltages and currents, and recognition of event specific signatures associated with these predictors through the application of DT classifiers for identification of contingency events.

5.1.2 Mathematical Representation

The proposed approach can be mathematically illustrated as:

$$X_i = \left\{x_1^i, x_2^i, x_3^i, ..., x_{15}^i\right\}; i = 1, 2, 3, ..., N \tag{5.1}$$

$$F = [X_1, X_2, ..., X_N]^T \tag{5.2}$$

$$Y = [y^1, y^2, ..., y^N]^T \tag{5.3}$$

where X_i is the vector of predictors containing predictor values for i^{th} event, F is the matrix containing vectors of predictor values for each of the N system events, Y contains the class values (i.e. $y_i = 0$ for *safe* events and $y_i = 1$ for *unsafe* events) corresponding to each vector of predictors X_i for each of the N system events. The complete data model (E) for DT classifier training can be expressed as follows:

$$E = [F\ Y] = \begin{bmatrix} x_1^1 & x_2^1 & x_3^1 & .. & x_{15}^1 & y^1 \\ x_1^2 & x_2^2 & x_3^2 & .. & x_{15}^2 & y^2 \\ : & : & : & .. & : & : \\ x_1^N & x_2^N & x_3^N & .. & x_{15}^N & y^N \end{bmatrix} \tag{5.4}$$

The set of predictors is selected to capture the essential characteristics of each of the system events. Table 5.1 lists the set of predictor variables used in the classification process.

5.1.3 Offline Decision Tree Training

The learning set (LS) for DT training is generated through extensive offline simulations of a wide variety of system events. In order to ensure satisfactory performance of DT classifiers, LS should contain a large number of training examples representing all possible system events.

Table 5.1: Predictors Used in Classification of System Events

$x_1^i = \Delta V_i$	Voltage deviation for i^{th} event (Volts)
$x_2^i = \left(\frac{\Delta V}{\Delta t}\right)_i$	Rate-of-change of voltage for i^{th} event (Volts/cycle)
$x_3^i = \Delta f_i$	Frequency deviation for i^{th} event (Hz)
$x_4^i = \left(\frac{\Delta f}{\Delta t}\right)_i$	Rate-of-change of frequency for i^{th} event (Hz/sec)
$x_5^i = \Delta I_i$	Change in current for i^{th} event (A)
$x_6^i = \left(\frac{\Delta I}{\Delta t}\right)_i$	Rate-of-change of current for i^{th} event (A/cycle)
$x_7^i = \left(\frac{V_-}{V_+}\right)_i$	Voltage unbalance for i^{th} event
$x_8^i = V_{THDi}$	Total harmonic distortion in voltage for i^{th} event
$x_9^i = I_{THDi}$	Total harmonic distortion in current for i^{th} event
$x_{10}^i = \left(\frac{{V_a}^3}{{V_a}^1}\right)_i$	Relative amplitude of 3^{rd} harmonics of voltage for i^{th} event
$x_{11}^i = \left(\frac{{V_a}^5}{{V_a}^1}\right)_i$	Relative amplitude of 5^{th} harmonics of voltage for i^{th} event
$x_{12}^i = \left(\frac{{I_a}^2}{{I_a}^1}\right)_i$	Relative amplitude of 2^{nd} harmonics of current for i^{th} event
$x_{13}^i = \left(\frac{{I_a}^3}{{I_a}^1}\right)_i$	Relative amplitude of 3^{rd} harmonic of current for i^{th} event
$x_{14}^i = \left(\frac{{I_a}^5}{{I_a}^1}\right)_i$	Relative amplitude of 5^{th} harmonic of current for i^{th} event
$x_{15}^i = \theta_{Ia^3 i}$	Phase of 3^{rd} harmonics of current for i^{th} event

The following is a categorical list of possible system events for offline simulations.

- Symmetric faults: all possible three phase faults (bolted 3-phase faults, 3-phase faults with varying fault impedances) in microgrid and area EPS.
- Asymmetric faults: line-to-line, line-to-ground and line-line-to-ground faults in microgrid and area EPS.
- Load changes and capacitor switching events in microgrid, distribution system and transmission network.
- Probable system contingencies such as- loss of generation in area EPS, loss of transmission line or islanding formation in area EPS.

Moreover, these events are simulated under various operating states of area EPS and microgrid. For each of the simulated events, voltage and current measurements are obtained at PCC of microgrid and distribution network. The set of predictor variables are obtained through post-processing of the voltage and current measurements at PCC. Each of the simulated events are characterized by the set of predictors and an assigned class value (*safe* or *unsafe*). The classification DTs are trained to distinguish between contingency events and other system events. The trained DT classifier is employed for real time assessment and classification of system events.

5.1.4 Online Implementation

Voltage and current measurements at PCC of microgrid and distribution network are obtained in real time. Vectors containing the predictor values obtained through post-processing of voltage and current measurements are compared with the pre-defined threshold values associated with the decision rules (based on which DT based classification model is developed) and necessary control action is appropriated.

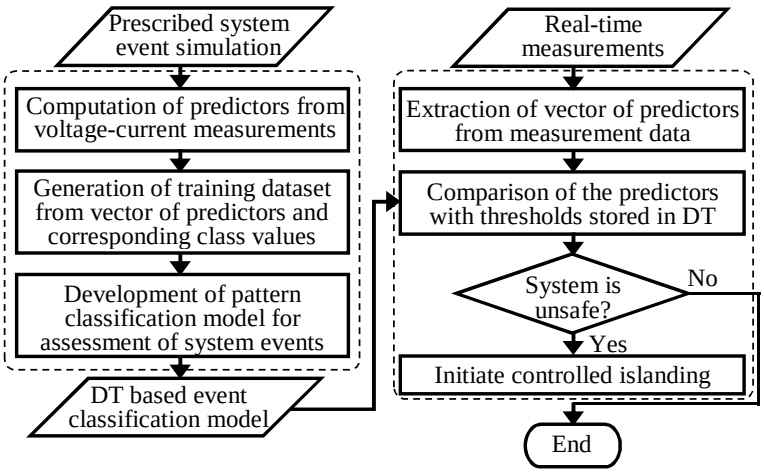

Figure 5.2: Flowchart of the proposed controlled islanding methodology.

5.2 Microgrid Configuration and Components

In order to accurately investigate the interactions between microgrid and utility grid, a 4 bus microgrid model consisting of two PV farms, a 200 kWh BESS and loads is adopted as the test system. The microgrid is operated at 25 kV/ 60 Hz and interconnected with the 230 kV transmission network through a 25 kV distribution feeder.

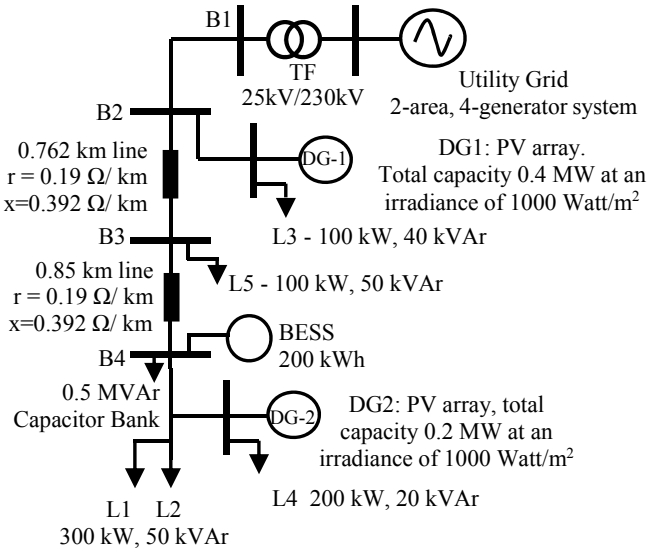

Figure 5.3: Microgrid test system model

The utility grid is modeled as 2-area, 4-generator system described in [82]. The system has a relatively small size but is able to exhibit typical power system dynamics. Thus, interactions between utility grid and microgrid can be studied. The distribution network containing the microgrid is connected to area-1 of the two area system.

In grid-connected mode, both DGs operate with grid-following controls maintaining nominal voltage and frequency of the grid. In islanded mode, DG-1 operates with V-f controls, and is responsible for voltage and frequency references of the islanded microgrid. Whereas, DG-2 operates with P-Q controls and injects fixed active/reactive powers at the voltage/frequency references established by DG-1. BESS does not operate in grid-connected mode, but operates with P-Q controls in

islanded mode of operation. The microgrid is cabale of autonomous operation by delivering the local demand, and maintaining voltage and frequency references.

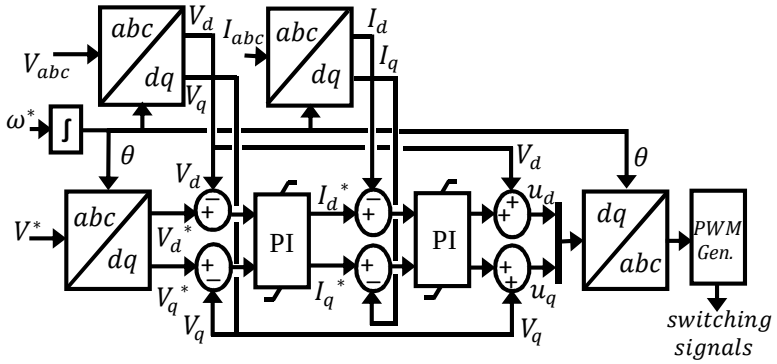

Figure 5.4: Grid-forming control architecture of voltage source inverter in DG-1 generating voltage (V^*) and frequency (ω^*) references in islanded mode.

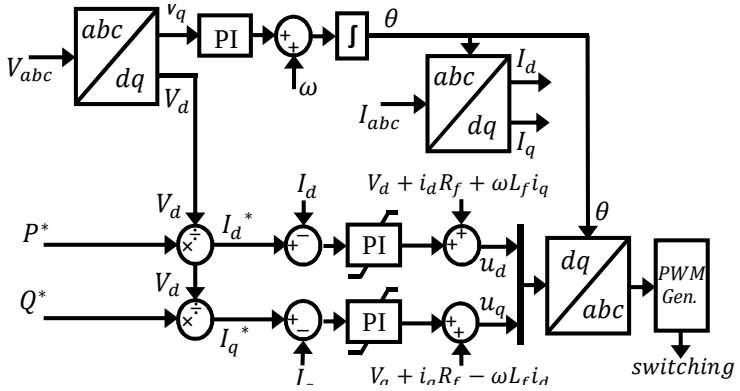

Figure 5.5: Grid-feeding control architecture of voltage source inverters providing predefined real (P^*) and reactive (Q^*) power outputs.

5.3 Case Study

Detailed overview of the main aspects of the case study performed on the test system model in presented in this section.

5.3.1 Offline Simulation of System Events

The following events have been considered in offline simulations for generation of training dataset for DT classifiers.

- Three-phase load changes: 50% $\leftrightarrow$ 80%, 80% $\leftrightarrow$ 100%, 50% $\leftrightarrow$ 90%, 100% $\leftrightarrow$ 120%.
- Single-phase load changes: 50% $\leftrightarrow$ 60%, 70% $\leftrightarrow$ 90%, 40% $\leftrightarrow$ 100%, 100% $\leftrightarrow$ 120%.
- Shunt capacitors switching on or off.
- Three-phase faults (with or without ground connections) with different levels of fault impedances.
- Single phase to ground faults and phase to phase faults (with or without ground connections) with different levels of fault impedances.
- Loss of generation in either area-1 or area-2 of transmission network.
- Formation of islands caused by loss of transmission lines between area-1 and area-2 of two area system, loss of lines in distribution network etc.

Each of the events was considered in microgrid and distribution network separately in offline simulations. A total of 92 system events were studied to generate the measurement dataset. Voltage and current measurements were obtained at a sampling rate of 1920 Hz yielding 32 sample points per cycle. The simulations were performed in Matlab/ Simulink platform.

5.3.2 Measurement Data Processing

Measurement data from six-cycles following the initiation of each event is utilized for computation of predictor variables. A sliding one-cycle window spanning 32 sampling points is employed for computation of the predictors. The window shifts four sampling points (1/8 cycle) between two consecutive computation steps. The set of

predictor variables obtained from each computation step along with the corresponding desired class value is termed as a *case*. Each event represented by the six-cycle measurement data yields 41 of such *cases*. Each event is classified as either *safe* or *unsafe*, represented by class values of 0 and 1 respectively. The complete training dataset contains 92 events or 3772 cases among which 52 events or 2132 cases were classified as *safe* and remaining 40 events or 1640 cases were classified as *unsafe*.

5.3.3 Decision Tree Training and Testing Demonstration

Based on the generated learning set (LS), DT classifiers were constructed using J48 decision tree algorithm in Waikato Environment for Knowledge Analysis (WEKA) [83] data mining platform. Initially, the DT training process involved all 15 predictors available for classification of each of the cases. The trained DTs utilized only a relevant set of predictors that have higher merit towards the overall classification process. Thus, predictors that have comparatively lower merit in the overall classification process is filtered out which reduces online computational time requirements. Average merit of each predictor in the classification of LS is presented in Table 5.2.

A total of five DT classifiers were developed for classifying the system events. Developed DT classifiers were evaluated using 10-fold cross validation method in WEKA. Table 5.3 summarizes the performances of five DT classifiers developed for the classification task.

Table 5.2: Average Merit of Predictors in DT Training

Predictor	Avg. Merit	Predictor	Avg. Merit	Predictor	Avg. Merit
x_1	92.38	x_6	72.78	x_{11}	78.92
x_2	74.61	x_7	84.63	x_{12}	69.86
x_3	71.98	x_8	82.84	x_{13}	72.74
x_4	67.34	x_9	94.82	x_{14}	80.92
x_5	86.67	x_{10}	77.05	x_{15}	82.49

Table 5.3: DT Classifier Performance Evaluation [10-Fold Cross Validation Method]

Tree Code	Predictor Variables	Classifier Accuracy	Actual Class	Total Cases	Classified as	
					Safe	*Unsafe*
DT-1	$x_1, x_4, x_5, x_7,$ x_8, x_9, x_{12}, x_{14}	99.61	*Safe*	2132	2121	11
			Unsafe	1640	4	1636
DT-2	x_3, x_4, x_6, x_7, x_8 $x_9, x_{11}, x_{12}, x_{14}$	99.36	*Safe*	2132	2116	16
			Unsafe	1640	8	1632
DT-3	x_4, x_5, x_6, x_7, x_8 $x_9, x_{10}, x_{12}, x_{14}$	99.26	*Safe*	2132	2114	18
			Unsafe	1640	8	1632
DT-4	x_3, x_4, x_6, x_7, x_8 $x_9, x_{10}, x_{11}, x_{15}$	99.22	*Safe*	2132	2114	18
			Unsafe	1640	9	1631
DT-5	$x_3, x_4, x_8, x_9,$ $x_{10}, x_{11}, x_{12}, x_{14}$	99.17	*Safe*	2132	2111	21
			Unsafe	1640	11	1629

DT-1 is selected for online implementation as it provides best classification performance among the developed DT classifiers. The tree has 31 branches (arcs) and 16 leaves (terminal nodes). *DT-1* classification results include 4 *missed operations* and 11 *false alarms*. The relatively large number of *false alarms* are caused by the misclassification cost settings used in development of DT classifiers. Misclassification cost parameter specifies the relative frequency of misclassification of *safe* to *unsafe* versus *unsafe* to *safe*. The misclassification cost for *unsafe* to *safe* is made twice than that for *safe* to *unsafe* in DT training. In order to eliminate *missed operations* and *false alarms* caused by misclassification of a *case* by DT classifier, proposed methodology relies upon five consecutive classification outputs from DTs instead of individual classification of the *cases*. Hence, for a contingency event to be classified as *unsafe*, DT classifier has to generate *unsafe* as classification output for five consecutive *cases*. This criterion helps in reducing the chances of *missed operations* or *false alarms* even if the DT classifier has misclassified some of the individual *cases*.

5.3.4 Online Performance Assessment

Online performance of the developed DT classifier is evaluated with a wide range of system events not used in DT training process. Two test case scenarios are presented to illustrate the online performance of the proposed methodology.

Case-I

The test system is operating at 80% of the base case loading scenario and a loss of generation in area-1 of the two area system is initiated at t=4s. The DT classifier correctly identifies the event as *unsafe* with a detection time of 0.031 seconds (approximately 2 cycles) and generates a trip signal to initiate the controlled islanding process.

For test case scenario-I, voltage and frequency deviations caused by the contingency event remain within the stipulated bounds recommended by IEEE Std. 1547 [11] for approximately 0.5 seconds following the initiation of the event. However, the DT classifier serves as an early warning mechanism and identifies the event within 0.031 seconds. Hence, controlled islanding of microgrid is initiated to ensure reliability and security of supply through autonomous operation.

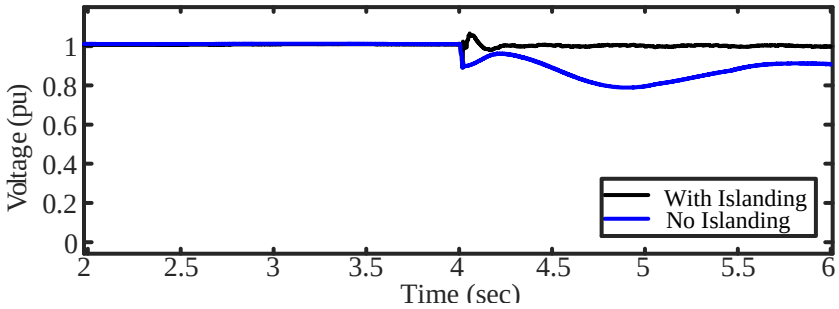

Figure 5.6: Voltage magnitude on PCC bus for test case scenario-I.

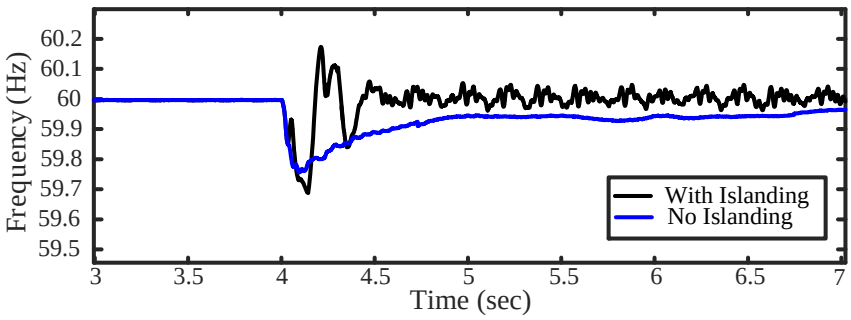

Figure 5.7: System frequency on PCC bus for test case scenario-I.

Case-II

Loss of a line in distribution network leading to the formation of power island containing the 25 kV distribution feeder, loads in the distribution network and the microgrid is considered at t=5s. Overall system loading is at 70% of the base case scenario. Formation of the island leads to a large mismatch between generation and demand in the islanded system which causes large voltage and frequency deviations. DT classifies the event as *unsafe* within 0.025 seconds. Initiation of controlled islanding aids in localizing the effects of the disturbance and restore secure operation of the microgrid.

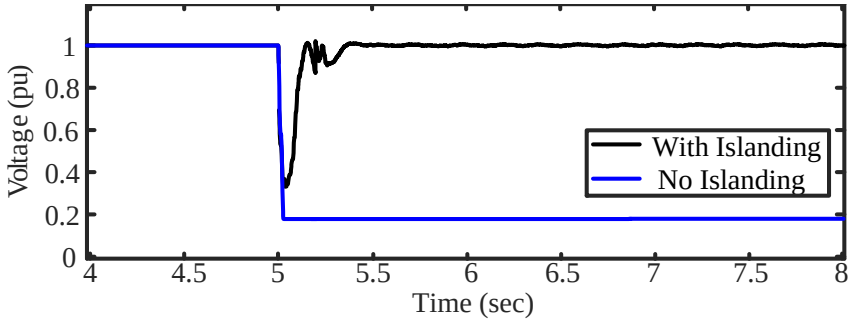

Figure 5.8: Voltage magnitude on PCC bus for test case scenario-II.

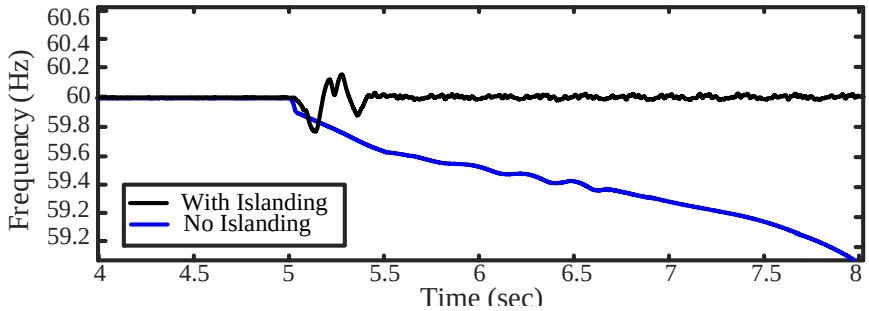

Figure 5.9: System frequency on PCC bus for test case scenario-II.

5.4 Summary

This chapter presents a decision tree based methodology for controlled islanding of utility-interconnected microgrids. The proposed approach employs DT classifiers trained with contingency-oriented dataset generated from offline simulations of an extensive array of system events for identification of events posing security concerns. Case study results on a grid-connected microgrid model demonstrate the effectiveness of the proposed method in fast and accurate assessment of a wide range of system events. For certain contingencies, DT classifier is capable of early identification of impending violation of operational security limits, thereby can be utilized in prevention of cascading degradations. Therefore, the proposed DT based event classification model can be implemented for initiation of controlled islanding of microgrids to ensure operational security, reliability, and power quality. Robustness of the proposed method can be further enhanced by adaptively expanding the training dataset and including more system operating scenarios.

Chapter 6

Power Management Strategy Combining Energy Storage and Demand Response for Microgrid Emergency Autonomous Operation

This chapter presents a power management strategy for microgrid emergency autonomous operation subsequent to unplanned islanding events. The proposed approach is composed of two coordinated scheduling stages operating in different time-frames to accommodate the uncertainty and variability associated with renewable generations as well as forecasting errors, and combines distributed generations, energy storage systems and demand side management techniques to ensure secure and stable microgrid autonomous operation. A scenario dependent rule-based approach is adopted for scheduling the microgrid resources which is computationally efficient and particularly suitable for microgrids with limited number of resources. Case study on a grid-connected microgrid test system based on IEEE 13 - node distribution feeder demonstrates the effectiveness of the proposed approach in microgrid frequency regulation following an unplanned islanding events.

The proposed strategy for microgrid emergency autonomous operation subsequent to unplanned islanding events integrates microgrid resources such as energy storage systems (ESS), demand response (DR) resources and controllable micro-sources (MS) to layout a comprehensive power management strategy for ensuring secure and stable microgrid operation through primary and secondary frequency regulation following an unplanned islanding event. The proposed strategy consists of two main modules: 1) look-ahead resource scheduling module and 2) emergency dispatch module. The resource scheduling module periodically defines the most adequate power management scheme considering the forecasted and available microgrid resources for the period of operation ahead. The emergency dispatch module utilizes real-time system data to check the availability of the scheduled resources and incorporates the necessary modifications to account for the intermittency and forecasting errors to the power management scheme recommended by the resource scheduling module. Detailed case study on a grid-connected microgrid consisting of wind and PV farm, diesel generator, ESS and responsive loads is performed to validate the performance of the proposed approach.

The chapter is structured as follows. Section 6.1 presents a brief overview of the resources critical towards MG emergency autonomous operation. The proposed power management strategy is presented in Section 6.2. Section 6.3 and Section 6.4 describes the test system model and case study results, respectively. Conclusions are presented in section 6.5.

6.1 Microgrid Emergency Autonomous Operation

The stability and security of microgrid operation in islanded mode is ensured by the effective coordination between available microgrid resources to maintain the power balance in the islanded system and minimize the system frequency deviation. Microgrid resources critical towards ensuring the power balance and frequency regulation include:

- ESS capacity and state-of-charge (SoC), contribute in primary frequency regulation in islanded MG.
- Controllable MS generation and reserve, which provide secondary frequency regulation.
- Demand resources, which ensure MG operation flexibility, and contribute in frequency regulation through utilization of interruptible and deferrable system loads.
- Generation from non-controllable MS, which acts as negative loads and contributes in minimization of generation-demand mismatch in the islanded MG.

Hence, appropriate power management strategies for microgrid autonomous operation subsequent to unplanned islanding events can be developed ahead of time through coordination of available microgrid resources. Microgrid power management strategies should allow fast characterization of MG operating conditions, ensure MG resource availability, enhance the speed of response, and minimize the frequency excursions.

6.2 Proposed Power Management Strategy

The proposed power management strategy consists of two main modules: 1) Look-ahead resource scheduling module and 2) Emergency dispatch module, which coordinate to enable power management solution in multi-timescale structure. The proposed approach allows dynamic coordination between the two modules to enhance solution accuracy and minimize computational time. For the development of the individual power management modules, scenario dependent rule-based approach is adopted, which enables management of MG resources based on a set of pre-defined rules. Rule-based power management strategies are computationally efficient, hence particularly well suited for real-time management applications of MG with limited

number of resources. Fig. 6.1 visualizes the conceptual model of the proposed power management strategy.

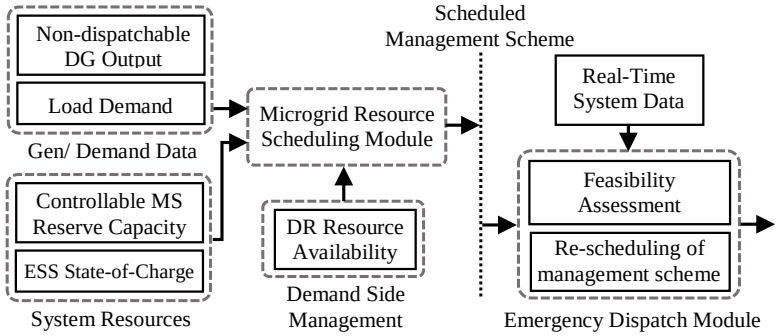

Figure 6.1: Conceptual model of the proposed power management strategy.

6.2.1 Look-Ahead Resource Scheduling Module

The look-ahead resource scheduling module (LSM) is responsible for scheduling the available microgrid resources for the upcoming operation interval, which is assumed to be the next 15 minutes period in the proposed approach. LSM utilizes information on available system resources (such as- controllable MS generation and reserve, ESS state-of-charge), and forecast data (such as- non-controllable DG generation and system demand) to schedule an effective power management scheme for preservation of power balance in case of any unplanned islanding event within the upcoming operation interval. The scheduling is achieved using a rule-base, which prioritizes the available resources to minimize operating cost and maintain power balance in the islanded microgrid.

Power Management Strategy in Scenario-I

Total demand (P_{DEMAND}) is higher than the aggregated generation (P_{GEN}) from controllable generation (P_{Gen}^{Ctrl}) and non-controllable generation (P_{Gen}^{N-Ctrl}) resources in the MG for the operation interval ahead; that is, $P_{DEMAND} > P_{GEN}$, where, $P_{GEN} =$

$P_{Gen}^{Ctrl} + P_{Gen}^{N-Ctrl}$. Hence, the mismatch in power, i.e., $\Delta P = P_{DEMAND} - P_{GEN}$, is required to be supplied by the primary frequency regulation resources, such as ESS and DR resources. As DR incurs no additional costs in MG operation, it is executed as the primary means to minimize ΔP. If implementation of the DR strategy is inadequate for restoring the power balance in the islanded microgrid (i.e., $P_{DR} < \Delta P$), then ESS is utilized to minimize the power mismatch (ΔP). However, utilization of ESS in primary frequency regulation is contingent upon the state-of-charge (SoC) of the ESS unit, which requires to be above the minimum allowable level SoC_{min}. If the mismatch in power persists (i.e., $\Delta P \neq 0$) after the utilization of ESS, then emergency load shedding scheme needs to be implemented to minimize ΔP to zero for primary frequency regulation.

The secondary frequency regulation is essentially performed through demand side management (i.e., demand response and emergency load shedding) and re-dispatching controllable MS. If DR resources (P_{DR}) are inadequate for compensating the mismatch in power, ΔP, then controllable MS are re-dispatched. In presence of multiple units of controllable MS with available reserve, the most economical MS are utilized to ensure cost-effective system operation. If available reserve capacity of controllable MS (P_{Res}^{Ctrl}) is sufficient to compensate for the power contributed by ESS and emergency load shedding scheme during primary frequency regulation, i.e., $P_{Res}^{Ctrl} \geq \Delta P - P_{DR}$, then shed loads are gradually connected to the system in steps and power drawn from ESS is replaced by the contributions from controllable MS. Otherwise, if $P_{Res}^{Ctrl} < \Delta P - P_{DR}$, then combination of controllable MS and ESS (provided $SoC > SoC_{min}$) is scheduled. In case, if shortage in generation persists, emergency load shedding scheme is utilized and excess load will remain disconnected.

Power Management Strategy in Scenario-II

In this case, total load demand (P_{DEMAND}) is lower than the aggregated generation (P_{GEN}) from controllable generation (P_{Gen}^{Ctrl}) and non-controllable generation

(P_{Gen}^{N-Ctrl}) resources in the MG for the operation interval ahead, i.e., $P_{GEN} > P_{DEMAND}$, where, $P_{GEN} = P_{Gen}^{Ctrl} + P_{Gen}^{N-Ctrl}$. In the proposed power management strategy, the mismatch in power, $\Delta P = P_{GEN} - P_{DEMAND}$, which is the excess generation in this case, is stored in the ESS, if the SoC is lower than the predefined maximum, SoC_{max}. Otherwise, if the excess generation cannot be stored in the ESS or if mismatch in power (ΔP) still persists after the utilization of the ESS, i.e. if $\Delta P \neq 0$, then DR strategy is implemented and availability of time-flexible DR resources (such as- EV or PHEV, pool pumps, washer and dryer etc.) for load shifting is explored for the upcoming operation interval. In case, if there is excess generation after the utilization of ESS and implementation of DR strategy, generation from non-controllable generation resources needs to be curtailed or dump loads can be used for dissipating the excess power. The scheduled power management scheme is validated through time-domain simulation of the islanded MG system to ensure stability during unplanned islanding events.

Fig. 6.2 presents the flowchart of the look-ahead resource scheduling module operation.

6.2.2 Emergency Dispatch Module

The emergency dispatch module (EDM) coordinates the scheduled power management scheme from LSM and real-time system measurements to account for the uncertainties introduced by the intermittent renewable resources and forecasting errors. EDM incorporates necessary adjustments in the scheduled power management scheme based on real-time measurements for secure and stable system operation. EDM functionalities are executed in a minute-ahead timeframe and schedules an emergency power management scheme for the upcoming minute of operation.

The availability of the scheduled resources are assessed based on the real-time data representing present system operating states. If the scheduled resources are all available and system operating conditions are unchanged, then the minute-ahead

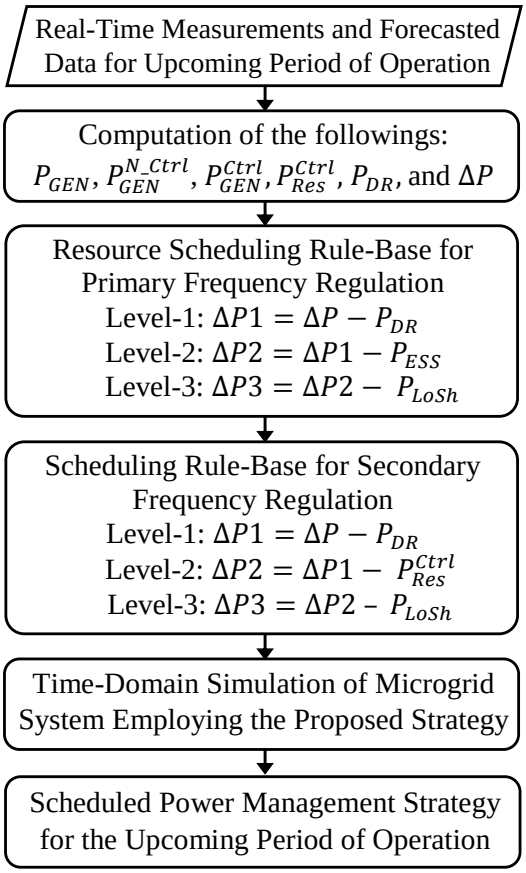

Figure 6.2: Flowchart defining the scheduling operation in LSM.

scheduling by EDM is performed in accordance with the power management scheme proposed by LSM.

Otherwise, the variations in resource availability is incorporated in the scheduling process by EDM to manage the variability in scheduled generations from non-controllable resources, forecasted demand, and DR resource availability. EDM reschedules the emergency microgrid resources based on their availability and associated cost. Hence, any deficiency/adequacy in generation is managed by deploying MG emergency resources in accordance with their associated cost effectiveness. As an example, if the scheduled DR resources (P_{DR}^{sch}) is higher than the available DR resources (P_{DR}^{sys}), then EDM looks to assign $\Delta P_{DR} = P_{DR}^{sch} - P_{DR}^{sys}$ to the MG resource

next in the priority list based on cost effectiveness and availability, which is the ESS. In case the ESS is unable to handle the excess power, then $\Delta P_{DR} - P_{ESS}$ is allocated to the emergency load shedding scheme for primary frequency regulation. The set points for the controllable MS are correspondingly adjusted given that enough reserve is available. Otherwise, the load shedding scheme is adopted to preserve the power balance. Similarly, if $P_{DR}^{sys} > P_{DR}^{sch}$, then $\Delta P_{DR} = P_{DR}^{sys} - P_{DR}^{sch}$ is curtailed from scheduled MG resource with the least priority, which is the emergency load shedding scheme. Hence, with $P_{DR}^{sys} > P_{DR}^{sch}$, load shedding is reduced by ΔP_{DR} and the set points for the ESS and controllable MS are also adjusted accordingly.

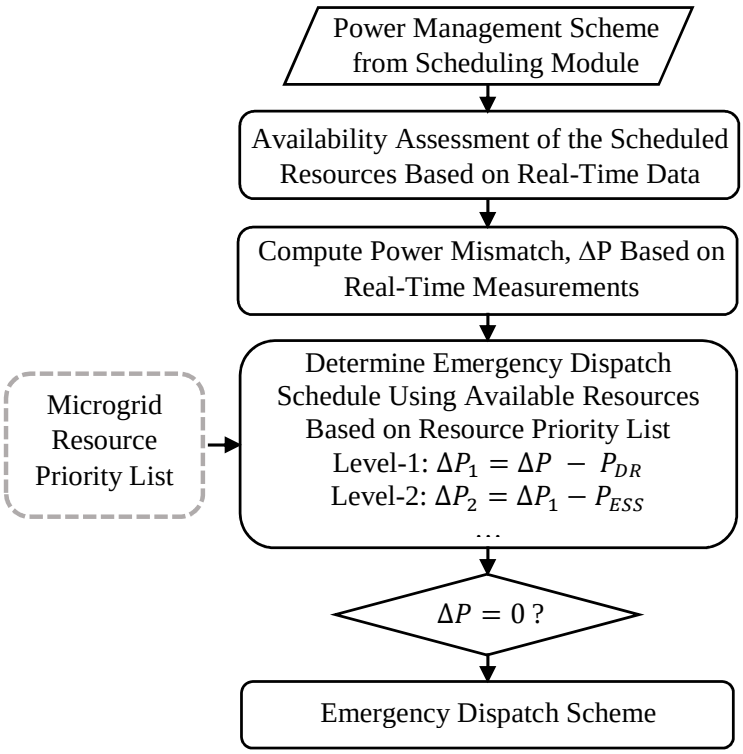

Figure 6.3: Flowchart defining the operation of emergency dispatch module.

6.2.3 Demand Response Strategy

Integration of demand side management (DSM) techniques such as- demand response (DR) in MG power management strategies enable a cost effective way to compensate or minimize the power mismatches caused by unplanned islanding events. The primary objective of any DR strategy is to acknowledge consumer priorities and minimize discomfort.

EV in MG Power Management

EVs offer flexibility in MG management and operation through load controllability and storage capability. Hence, management of EVs recognizing consumer requirements may provide an effective means of integrating EVs into MG emergency power management strategies. This chapter proposes a management strategy for EVs based on their battery SoC, which controls the EV charging and consequently the power consumption during MG emergency operation. Depending on the rated power, voltage and current, EV charging systems in North America are categorized into three groups as presented in Table 6.1 [88].

Table 6.1: Rated Power Levels, Voltage, Current and Charging Time for Different EV Charging Modes

Charging Mode	Maximum Power (kW)	Nominal Voltage (V)	Maximum Current (A)	Charging Time
AC Level-1	1.44	120 AC	12	6-8 hrs
AC Level-2	7.68	208-240 AC	32	2-4 hrs
DC Level-2	240	200-600 DC	400	10-20 min

The proposed EV management strategy is presented in Fig. 6.4. In the proposed approach, the load controller (LC) for EV units evaluates the battery SoC and the charging mode. The battery SoC is compared to an user defined threshold value SoC_{TH}. If $SoC > SoC_{TH}$, then the EV unit participates in the DR program by

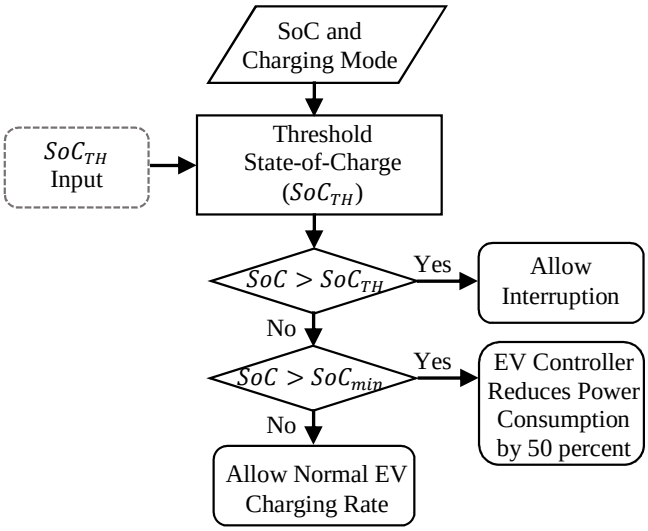

Figure 6.4: Flowchart of the proposed EV management strategy.

allowing interruptions during MG emergency operations. The use of SoC_{TH} allows users to dynamically adjust their contribution towards the DR program based on their necessity. On the other hand, if SoC is less than a predefined minimum level SoC_{min}, then normal EV charging rate is allowed by the EV controller. If the battery SoC is between SoC_{TH} and SoC_{min}, that is $SoC_{min} < SoC < SoC_{TH}$, then EV controller reduces power consumption by 50 percent by reducing the charging current in order to contribute to the demand response strategy. The EV controller continuously evaluates the charging mode and computes the estimated power consumption to determine the units availability for the DR program. LC for a group of EVs aggregates the information sent by individual EV controllers to estimate their availability for the DR strategy.

Responsive Residential Loads in MG Power Management

Residential loads are grouped into two major categories: critical (non-controllable) and responsive (controllable) loads. Only responsive residential loads participate in the DR program. Customers can prioritize each of their appliances to participate in the DR program as well as set operation preferences to minimize their discomfort.

Several DR strategy allowing the customers to prioritize and manage their responsive loads have been proposed in literature [89, 90]. The proposed power management strategy utilizes the aggregated DR resource availability information to schedule the power management scheme for unplanned islanding events. The load controllers monitor the power consumptions for each responsive load groups and aggregate the available DR resources under its control for the operation interval ahead. The microgrid central controller (MGCC) utilizes the aggregated DR resource availability information from each of the load controllers to estimate the amount of available DR resources for the upcoming operation interval, which is utilized by the look-ahead resource scheduling module to schedule the power management scheme.

6.3 Microgrid Configuration and Components

In order to accurately evaluate the proposed power management strategy, IEEE 13 node distribution feeder modified with the addition of distributed generations (DGs) and battery energy storage system (BESS), is used as the microgrid test system. The microgrid model presented in Fig. 6.5, consists of a 3 MVA emergency diesel generator, a 200 kWh battery energy storage system (BESS), two PV farms with maximum capacities of 800 kW and 500 kW respectively at an irradiance of 1000 W/m^2, and a wind farm with maximum capacity of 1.5 MW. The microgrid is operated at 4.16 kV/ 60 Hz.

The emergency diesel generator (DiGn) model consists of synchronous generator, speed governor, and excitation controller. DiGn is operated in standby mode, where it incurs a fixed amount of operating cost even at no load, which needs to be considered in the power management scheme for cost-effective system operation. The renewable generations are operated in P-Q control mode with MPPT controllers and associated power conditioning units. The battery energy storage system (BESS) is operated in P-Q control mode as well with the pre-specified set points selected by the power management strategy.

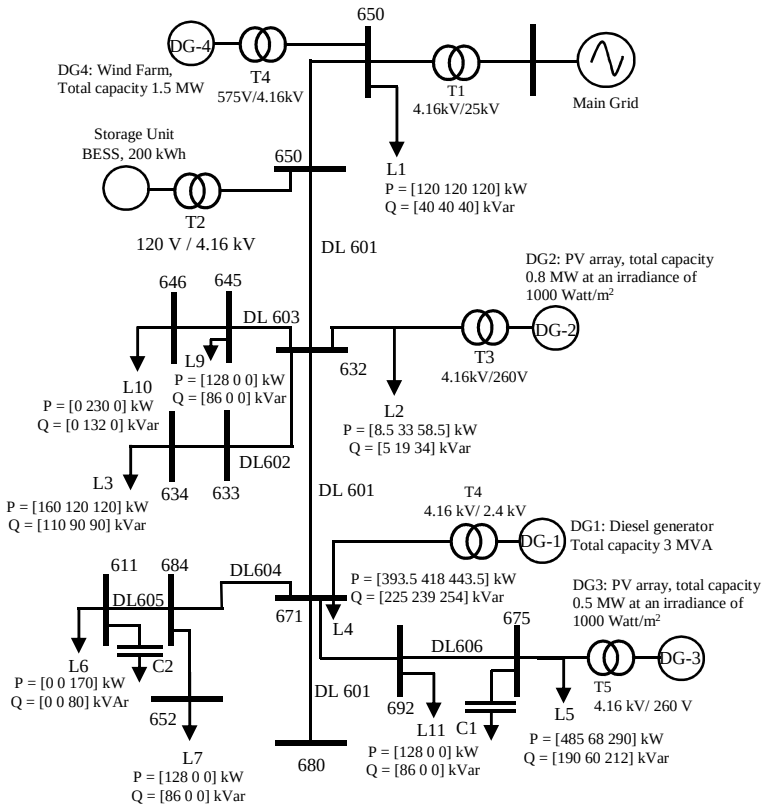

Figure 6.5: Test system model.

The loads are modeled as constant PQ loads. An EV population equivalent to 30 EVs are considered, among which 50 percent of the EVs are charged using AC level-1 charging with each consuming a maximum of 1.44 kW, 35 percent of the EVs are charged using AC level-2 charging with each consuming a maximum of 7.68 kW, and 15 percent of the EVs are charged with DC Level-2 charging with each consuming a maximum of 240 kW. The maximum system load corresponding to EV population is assumed to be 1 MW. The microgrid model is developed in *Matlab/Simulink* environment using *SimPowerSystems* toolbox.

6.4 Case Study Results

In order to demonstrate the effectiveness of the proposed power management strategy for microgrid emergency islanding operation, three test case scenarios are considered- 1) MG with adequate reserve capacity, 2) MG with inadequate reserve capacity, and 3) MG with excess renewable generation.

6.4.1 Case-I: MG Operation with Adequate Reserve Capacity

In this case, the demand at the beginning of the upcoming operation interval is 3.4 MW, which is the base case loading scenario for the considered MG system. The aggregated generation from renewable resources for the operation interval ahead is considered as 2.8 MW (i.e., $P_{Gen}^{N-Ctrl} = 2.8MW$; where $P_{PV1} = 0.8MW$, $P_{PV2} = 0.5MW$, and $P_{Wind} = 1.5MW$). Hence, MG is importing 0.6 MW (i.e. $\Delta P = 0.6MW$) through the point of common coupling (PCC). DiGn is operating in standby mode with a reserve capacity of 3 MW (i.e., $P_{Res-Gen}^{Ctrl} = 3MW$). Based on the characteristics of the considered operation interval (i.e., time of the day), 50 percent of the EV population (approximately 500 kW) is assumed to be connected to the system, and considering the EV management strategy presented in Sec III, it is assumed that the connected EV units participate in the DR strategy in various forms enabling a demand resource of 300 kW. The available demand resources from EVs and responsive residential loads are assumed to be 300 kW and 150 kW, respectively (i.e., $P_{DR}^{sch} = 450kW$). Hence, BESS and DiGn are scheduled to generate 150 kW for primary and secondary frequency regulation purposes.

The system operating conditions obtained by EDM in minute-ahead scheduling consist of power exchange at point of common coupling (PCC) of the MG, $\Delta P = 0.504MW$; generation from non-controllable sources, $P_{Gen}^{N-Ctrl} = 2.78MW$ (($P_{PV1} = 0.798MW$, $P_{PV2} = 0.482MW$, and $P_{Wind} = 1.5MW$ respectively). The availability of the aggregated DR resources is assumed unchanged. In order to compensate for the mismatch in power $\Delta P = 0.504MW$, EDM redefines the set points for BESS and

DiGn to 54 kW in the emergency dispatch scheme. An unplanned islanding event 30 seconds into the EDM period of operation is considered for simulation and the MG frequency response is presented in Fig. 6.6.

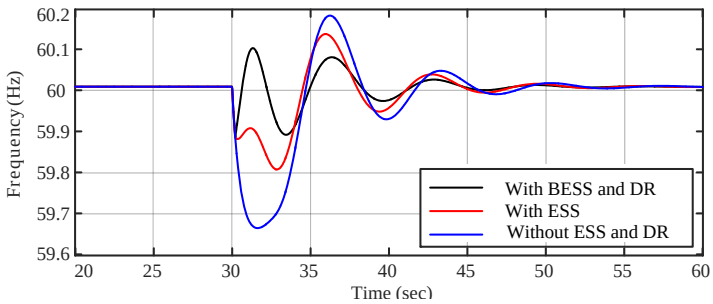

Figure 6.6: Microgrid frequency response in test case scenario-I following an unplanned islanding event at 30 second.

6.4.2 Case-II: MG Operation with Inadequate Reserve Capacity

The aggregated renewable generation for the upcoming operation interval is assumed to be 1.5 MW (i.e., $P_{Gen}^{N-Ctrl} = 1.5MW$) with the wind plant generating the entire share ($P_{Wind} = 1.5MW$) and PV farms are not operating. The MG is grid-connected at the beginning of the operational interval; hence, DiGn is operating in standby mode with a reserve capacity of 3 MW (i.e., $P_{Res-Gen}^{Ctrl} = 3MW$). MG is importing about 3.3 MW of active power from the utility grid at the beginning of the operation interval (i.e., $\Delta P = 3.3MW$); hence, the total MG load (P_{DEMAND}) for the operation interval under consideration is approximately 4.8 MW. The characteristics of the operation interval under consideration represent heavy system loading similar to evening peak hours of daily system operation. Based on the characteristics of the considered operation interval, the entire EV population (approximately 1 MW) is assumed to be connected to the system and considering the EV management strategy in Sec III, it is assumed that the connected EV units participate in the DR strategy in various forms enabling a demand resource of 650 kW. The aggregated demand

resources (i.e., including EVs and responsive residential loads) is assumed to be 1.5 MW (i.e., $P_{DR}^{sch} = 1.5MW$). Hence, an emergency load shedding scheme of 1.6 MW will be required alongside the support from the BESS unit (thus, $P_{LoSh} = 1.6MW$ and $P_{BESS} = 0.2MW$) for primary frequency regulation. The emergency diesel generator (DiGn) is scheduled to generate 1.8 MW for secondary frequency regulation purposes.

An unplanned islanding event 30 seconds into the fifth minute of the operation interval is considered for simulation. Prior to the islanding event, MG is importing 3.39 MW from the utility grid, $\Delta P = 3.39MW$. A variation in the wind power generation due to wind speed variability is considered, thus P_{Wind} is $1.41MW$ (i.e., $P_{Gen}^{N-Ctrl} = 1.41MW$). Other system operating states are assumed to be unchanged. Hence, EDM checks the availability of the other generation and demand resources in accordance with their priority. Since, all of the generation and demand resources are utilized to their capacity by LSM during the scheduling process, EDM assigns the deficiency in generation due to wind variability to the emergency load shedding scheme. Hence, P_{LoSh} is set to $1.69MW$ and DiGn reference point is set at 2.7 MW, that is $P_{Gen}^{Ctrl} = 1.89MW$. The MG frequency response in test case scenario-II is presented in Fig. 6.7.

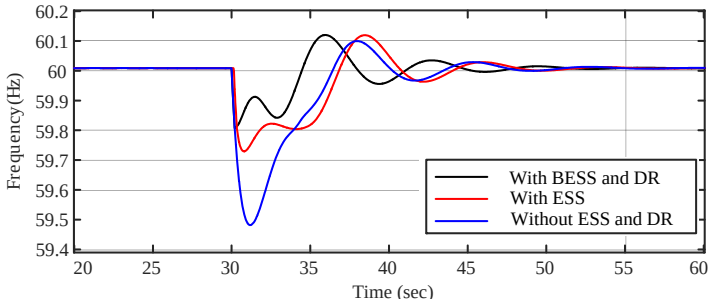

Figure 6.7: Microgrid frequency response in test case scenario-II following an unplanned islanding event at 30 second.

6.4.3 Case-III: MG Operation with Excess Generation

In this case, the aggregated renewable generations for the operation interval ahead is 2.8 MW (i.e., $P_{Gen}^{N-Ctrl} = 2.8MW$; where $P_{PV1} = 0.8MW$, $P_{PV2} = 0.5MW$, and $P_{Wind} = 1.5MW$). The demand at the beginning of the upcoming operation interval is set to 2.6 MW representing a low loading scenario in the MG. The BESS state-of-charge (SoC) at the beginning of the interval is SoC_{max}, thus the BESS cannot be utilized by the LSM for the storage of excess renewable generation. Hence, the scheduling module searches for time-flexible demand resources (i.e., both EVs and time-flexible residential responsive loads) in order to utilize the excess generation. The availability of the aggregated time-flexible demand resources is assumed to be 300 kW, out of which 200 kW will be utilized by the LSM. Both, BESS and the emergency load shedding scheme are not utilized in this case for primary frequency regulation and so as the DiGn for the secondary frequency regulation purposes.

A variation in the aggregated renewable generations amounting to 0.05 MW in order to account for the variability in wind speed and solar irradiation is considered in the real-time system operating conditions acquired by EDM. The other system operating states are assumed to be unchanged. Hence, $P_{Gen}^{N-Ctrl} = 2.75MW$, $P_{DEMAND} = 2.6MW$, and $P_{DR}^{sys} = 300kW$. EDM utilizes 150 kW of the available time-flexible demand resources for the primary frequency regulation purpose. The connection of dump loads are not required in this case. The MG frequency response is presented in Fig. 6.8.

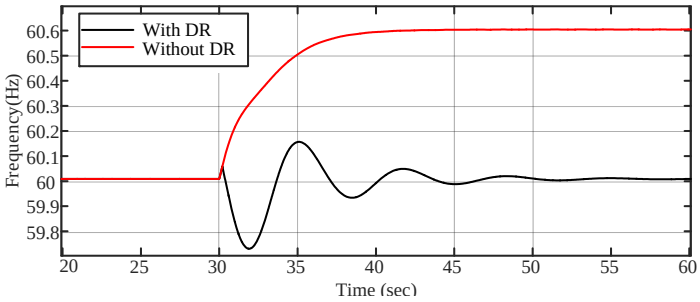

Figure 6.8: Microgrid frequency response in test case scenario-III following an unplanned islanding event at 30 second.

6.5 Summary

This chapter presents a scenario dependent rule-based cost effective power management strategy for secure and stable autonomous operation of microgrids consisting of distributed generations (DGs), energy storage systems (ESS) and demand response (DR) resources. The proposed strategy consists of two stages (look-ahead resource scheduling and emergency dispatch) operating in different timeframes to accommodate the variability and uncertainty introduced by the intermittent renewable resources and errors in forecasted data. The proposed approach incorporates demand side management (DSM) techniques such as- demand response through responsive residential loads and electric vehicles (EVs) in the power management for autonomous MG operations, which provides cost effective solutions compared to having expensive spinning and non-spinning reserves for system operations. This chapter also proposes a management strategy for EVs allowing users to vary their contributions towards the demand response programs. Case study on a grid-connected MG model based on IEEE 13 node distribution feeder demonstrates the effectiveness of the proposed approach in minimizing the frequency excursion during unplanned islanding events. Further developments will include enhancement of the rule-base through explicit incorporation of the cost parameters and improvement of the component models in MG and DR resources.

Chapter 7

Conclusions and Future Works

The major contributions and conclusions of the dissertation can be summarized as follows:

- A decision tree based controlled islanding approach is presented which utilizes decision tree based pattern recognition technique in order to detect system events for which preventive control is required to ensure microgrid supply continuity and reliability. The proposed approach aim for implementation of decision tree based detection of system contingency events for which preventive control is required as an emergency tool. The proposed approach is capable of an early warning mechanism for impending violations of microgrid security and hence, can be implemented as an emergency control tool in the control and protection environment of microgrid.

- A hybrid islanding detection method combining decision tree based data mining technique and Sandia frequency shift method is for inverter based distributed generations in microgrids is proposed, investigated and validated.

- The proposed hybrid islanding detection scheme is capable of accurate and reliable detection of islanding events under various power mismatch scenarios in the islanded microgrid. The proposed approach can also be utilized in

automated threshold setting and dynamic threshold update with changing system states. The proposed approach also enhances the detection time for the islanding events.

- A passive islanding detection method based on decision trees is also proposed. The proposed method utilizes a parallel combination of multiple optimal decision trees for reliable and accurate detection of islanding events and minimization of non-detection zones under various real and reactive power mismatch scenarios in the islanded microgrid. The proposed passive islanding detection methodology can be implemented for any type of distributed generations including synchronous machine based DGs and inverter based DGs.

- A power management strategy for primary and secondary frequency regulations considering demand response and energy storage system is also proposed. The proposed approach coordinates two scheduling modules operating in different timeframe in order to account for the variability introduced by the renewable generations, demand resource scheduling, etc. and also to enhance the response time in case of unplanned islanding events. The proposed approach is based on scenario dependent scheduling rules; hence, can be suitably implemented in real-time management environment for microgrids with limited number of generation resources and loads.

The future works to enhance the methodologies proposed in the dissertation may include the followings:

- The periodic DT update process in the DT based passive islanding technique is a manual process in the current implementation. Automation of the periodic DT update process in the DT based passive islanding technique would enhance the islanding detection schemes presented in this dissertation.

- Investigation of new scenarios and enhancement of training dataset by including new contingency events to improve the early detection mechanism offered by the proposed decision tree based controlled islanding methodology.

- Enhancement of the proposed power management strategy by investigating the economic aspects (such as real time pricing of the corresponding microgrid resources) in the scheduling process.

- Investigation of multi-agent based approach for power/ energy management applications in microgrids and operation of microgrids in electricity market environment.

Bibliography

[1] D. Don and M. A. Smith, "The U.S. Department of Energy's microgrid initiative," *The Electricity Journal*, vol. 25, pp. 84–94, Oct. 2012. 1, 3, 10, 11, 13

[2] U.S. Department of Energy, "The SMART GRID: An Introduction," Tech. Rep., 2010. 2

[3] R. Kempener, P. Komor, and A. Hoke, "Smart Grids and Renewables - A Guide for Effective Deployment," Tech. Rep. November, 2013. 2

[4] S. Backhaus, G. W. Swift, S. Chatzivasileiadis, W. Tschudi, S. Glover, M. Starke, J. Wang, M. Yue, and D. Hammerstrom, "Dc microgrids scoping study - estimate of technical and economic benefits," U.S. Department of Energy and Los Alamos National Laboratory, NM, Tech. Rep. LA-UR-15-22097, 2015. 3

[5] S. Adhikari, "Control of Solar Photovoltaic (PV) Power Generation in Grid-Connected and Islanded Microgrids," PhD Dissertation, University of Tennessee Knoxville, 2013. 4, 5, 6, 7

[6] B. Owens, "The Rise of Distributed Power," General Electric Company, Tech. Rep., 2014. 4, 5, 6, 7, 8

[7] (2016, July) U.S. Department of Energy Combined Heat and Power Website. [Online]. Available: https://www.energy.gov/eere/amo/combined-heat-and-power-basics 5, 6

[8] F. Katiraei, R. Iravani, N. Hatziargyriou, and A. Dimeas, "Microgrids management," *IEEE Power and Energy Magazine*, vol. 6, no. 3, pp. 54–65, 2008. 10

[9] D. E. Olivares, A. Mehrizi-Sani, A. H. Etemadi, C. A. Cañizares, R. Iravani, M. Kazerani, A. H. Hajimiragha, O. Gomis-Bellmunt, M. Saeedifard, R. Palma-Behnke, G. A. Jiménez-Estévez, and N. D. Hatziargyriou, "Trends in microgrid

control," *IEEE Transactions on Smart Grid*, vol. 5, no. 4, pp. 1905–1919, 2014. 14, 15, 16

[10] A. Bidram and A. Davoudi, "Hierarchical structure of microgrids control system," *IEEE Transactions on Smart Grid*, vol. 3, pp. 1963–1976, Dec. 2012. 14, 15, 16

[11] IEEE, "IEEE Application Guide for IEEE Std 1547(TM), IEEE Standard for Interconnecting Distributed Resources with Electric Power Systems," pp. 1–217, 2009. 18, 23, 24, 74, 89, 91, 99, 114

[12] T. Funabashi, K. Koyanagi, and R. Yokoyama, "Review of islanding detection methods for distributed resources," in *Proc. IEEE PowerTech conference*, vol. 2, Bologna, Italy, 2003, pp. 1–6. 24

[13] M. E. Ropp, K. Aaker, J. Haigh, and N. Sabbah, "Using power line carrier communications to prevent islanding [of PV power systems]," in *Proc. Twenty Eighth IEEE photovoltaic specialists conference-2000*, Alaska, USA, 2000, pp. 1675–1678. 24

[14] W. Bower and M. Ropp, "Evaluation of islanding detection methods for photovoltaic utility-interactive power systems," Sandia National Laboratory, NM, Tech. Rep. IEA PVPS T5-09: 2002, Mar. 2002. 24

[15] M. Ciobotaru, R. Teodorescu, and F. Blaabjerg, "On-line grid impedance estimation based on harmonic injection for grid-connected PV inverter," in *IEEE International Symposium on Industrial Electronics*, no. 1, 2007, pp. 2437–2442. 25

[16] J. Warin and W. H. Allen, "Loss of mains protection," in *Proc. ERA Conf. Circuit Protection for Industrial and Commercial Installation*, London, UK, 1990, pp. 4.3.1–4.3.12. 25

[17] L. Lopes and H. Sun, "Performance Assessment of Active Frequency Drifting Islanding Detection Methods," *IEEE Transactions on Energy Conversion*, vol. 21, no. 1, pp. 171–180, 2006. 25, 27

[18] M. E. Ropp, M. Begovic, and A. Rohatgi, "Analysis and performance assessment of the active frequency drift method of islanding prevention," *IEEE Transactions on Energy Conversion*, vol. 14, no. 3, pp. 810–816, 1999. 25, 80

[19] W. Bower and M. Ropp, "Evaluation of islanding detection methods for utility-interactive inverters in photovoltaic systems," Tech. Rep. November, 2002. 25, 26, 80

[20] V. John, Z. Ye, and A. Kolwalkar, "Investigation of Anti-Islanding Protection of Power Converter Based Distributed Generators," *IEEE Transactions on Power Electronics*, vol. 19, no. 5, pp. 1177–1183, 2004. 25, 26

[21] G. Smith, P. Onions, and D. Infield, "Predicting islanding operation of grid connected PV inverters," in *IEE Proc - Electr. Power Appl.*, vol. 147, no. 1, 2000, pp. 1–6. 25, 27

[22] G. K. Hung, C. C. Chang, and C. L. Chen, "Automatic phase-shift method for islanding detection of grid-connected photovoltaic inverters," *IEEE Transactions on Energy Conversion*, vol. 18, no. 1, pp. 169–173, 2003. 25, 27

[23] Z. Ye, "Study and development of anti-islanding control for synchronous machine-based distributed generators, National Renewable Energy Laboratory, U.S., November 2001 - March 2004," Tech. Rep. March, 2006. 25, 27, 28

[24] H. H. Zeineldin and S. Kennedy, "Instability criterion to eliminate the nondetection zone of the sandia frequency shift method," in *2009 IEEE/PES Power Systems Conference and Exposition, PSCE 2009*, 2009, pp. 1–5. 28, 81, 82

[25] W. Freitas, Z. Huang, and W. Xu, "A practical method for assessing the effectiveness of vector surge relays for distributed generation applications," *IEEE Transactions on Power Delivery*, vol. 20, no. 1, pp. 57–63, 2005. 28, 29

[26] S. Salman, D. King, and G. Weller, "New Loss of Mains Detection Algorithm for Embedded Generation Using Rate of Change of Voltage and Changes in Power Factors," in *Proc. IEE*, no. 479, 2001, pp. 82–85. 28, 29

[27] A. Samui and S. R. Samantaray, "Assessment of ROCPAD relay for islanding detection in distributed generation," *IEEE Transactions on Smart Grid*, vol. 2, no. 2, pp. 391–398, 2011. 28, 29

[28] K.-H. Kim and S.-I. Jang, "An Islanding Detection Method for Distributed Generations Using Voltage Unbalance and Total Harmonic Distortion of Current," *IEEE Transactions on Power Delivery*, vol. 19, no. 2, pp. 745–752, 2004. 28, 29

[29] F. Katiraei, A. Foss, C. Abbey, and B. Strehler, "Dynamic analysis and field verification of an innovative anti-islanding protection scheme based on directional reactive power detection," in *2007 IEEE Canada Electrical Power Conference, EPC 2007*, 2007, pp. 183–187. 28, 31

[30] K. El-arroudi, G. Joós, and I. Kamwa, "Intelligent-Based Approach to Islanding Detection in Distributed Generation," *IEEE Transactions onPower Delivery*, vol. 22, no. 2, pp. 828–835, 2007. 30

[31] R. Azim, Y. Zhu, H. A. Saleem, K. Sun, F. Li, D. Shi, and R. Sharma, "A decision tree based approach for microgrid islanding detection," in *Proc. 2015 IEEE Power and Energy Society Innovative Smart Grid Technologies Conference (ISGT)*, 2015, pp. 1–5. 30

[32] K. El-Arroudi and G. Joós, "Data mining approach to threshold settings of islanding relays in distributed generation," *IEEE Transactions on Power Systems*, vol. 22, no. 3, pp. 1112–1119, 2007. 30

[33] N. W. A. Lidula and A. D. Rajapakse, "A Pattern Recognition Approach for Detecting Power Islands Using Transient Signals Part I : Design and Implementation," *October*, vol. 25, no. 4, pp. 3070–3077, 2010. 30

[34] ——, "A pattern-recognition approach for detecting power islands using transient signals-part II: Performance evaluation," *IEEE Transactions on Power Delivery*, vol. 27, no. 3, pp. 1071–1080, 2012. 30

[35] O. N. Faqhruldin, S. Member, E. F. El-saadany, S. Member, and H. H. Zeineldin, "A Universal Islanding Detection Technique for Distributed Generation Using Pattern Recognition," *IEEE Transactions on Smart Grid*, vol. 5, no. 4, pp. 1985–1992, 2014. 30

[36] Y. Zhu, R. Azim, H. A. Saleem, K. Sun, D. Shi, and R. Sharma, "Microgrid security assessment and islanding control by Support Vector Machine," in *Proc. IEEE Power and Energy Society General Meeting*, vol. 2015-Septe, 2015. 31

[37] R. Azim, K. Sun, F. Li, Y. Zhu, H. A. Saleem, D. Shi, and R. Sharma, "A comparative analysis of intelligent classifiers for passive islanding detection in microgrids," in *Proc. IEEE Eindhoven PowerTech Conf.*, June 2015, pp. 1–6. 31

[38] H. G. Far, A. J. Rodolakis, and G. Joos, "Synchronous distributed generation islanding protection using intelligent relays," *IEEE Transactions on Smart Grid*, vol. 3, no. 4, pp. 1695–1703, 2012. 31

[39] D. P. Mishra, S. R. Samantaray, and G. Joos, "A combined wavelet and data-mining based intelligent protection scheme for microgrid," *IEEE Transactions on Smart Grid*, vol. 7, no. 5, pp. 2295–2304, 2016. 31

[40] V. Menon and M. H. Nehrir, "A hybrid islanding detection technique using voltage unbalance and frequency set point," *IEEE Transactions on Power Systems*, vol. 22, no. 1, pp. 442–448, 2007. 32

[41] P. Mahat, Z. Chen, and B. Bak-Jensen, "A hybrid islanding detection technique using average rate of voltage change and real power shift," *IEEE Transactions on Power Delivery*, vol. 24, no. 2, pp. 764–771, 2009. 32

[42] R. Azim, F. Li, and X. Zhao, "A Hybrid Islanding Detection Technique for Inverter Based Distributed Generations," in *Proc. 2015 IEEE Electric Power and Energy Conference (EPEC)*, London, ON, Canada, 2015, pp. 239–243. 32

[43] P. Piagi and R. Lasseter, "Autonomous control of microgrids," in *Proc. 2006 IEEE Power Engineering Society General Meeting*, June 2006. 32

[44] I. J. Balaguer, Q. Lei, S. Yang, U. Supatti, F. Z. Peng, S. Member, Q. Lei, S. Yang, U. Supatti, and S. Member, "Control for Grid-Connected and Intentional Islanding Operations of Distributed Power Generation," *IEEE Transactions on Industrial Electronics*, vol. 58, no. 1, pp. 147–157, 2011. 32, 33

[45] I. J. Balaguer, U. Supatti, Q. Lei, N. S. Choi, and F. Z. Peng, "Intelligent control for intentional islanding operation of microgrids," in *2008 IEEE International Conference on Sustainable Energy Technologies, ICSET*, 2008, pp. 898–903. 32, 33

[46] R. H. Lasseter, J. H. Eto, B. Schenkman, J. Stevens, H. Vollkommer, D. Klapp, E. Linton, H. Hurtado, and J. Roy, "CERTS microgrid laboratory test bed," *IEEE Transactions on Power Delivery*, vol. 26, no. 1, pp. 325–332, 2011. 32, 33

[47] H. Zeineldin, E. El-Saadany, and M. Salama, "Intentional islanding of distributed generation," in *Proc. IEEE Power Engineering Society General Meeting*, June 2005, pp. 1496–1502. 33

[48] S. H. Lee, G. Son, and J. W. Park, "Power management and control for grid-connected dgs with intentional islanding operation of inverter," *IEEE Transactions on Power Systems*, vol. 28, no. 2, pp. 1235–1244, 2013. 33

[49] Q. Fu, a. Nasiri, V. Bhavaraju, a. Solanki, T. Abdallah, and D. Yu, "Transition Management of Microgrids With High Penetration of Renewable Energy," *IEEE Transactions on Smart Grid*, vol. 5, no. 2, pp. 539–549, 2014. 33

[50] F. Pilo, G. Celli, and S. Mocci, "Improvement of Reliability in Active Networks with Intentional Islanding," in *Proc. 2004 IEEE International Conference on Electric Utility Deregulation, Restructuring and Power Technologies*, vol. 2, April 2004, pp. 474–479. 34

[51] I. Grau, L. Cipcigan, N. Jenkins, and P. Papadopoulos, "Microgrid intentional islanding for network emergencies," in *Proc. of the 44th InternationalUniversities Power Engineering Conference (UPEC)*, 2009, pp. 1–5. 34

[52] M. Brenna, F. Foiadelli, P. Petroni, G. Sapienza, and D. Zaninelli, "Distributed generation regulation for intentional islanding in Smart Grids," in *Proc. 2012 IEEE PES Innovative Smart Grid Technologies (ISGT)*, 2012, pp. 1–6. 34

[53] H. Zeineldin, K. Bhattacharya, E. El-Saadany, and M. Salama, "Impact of intentional islanding of distributed generation on electricity market prices," *IEE Proc. Generation Transmission Distribution*, vol. 153, no. 2, pp. 147–154, 2006. 34

[54] R. Azim and F. Li, "A Decision Tree Based Approach for Controlled Islanding of Microgrids," in *Proc. 2016 IEEE PES Transmission and Distribution Conference and Exposition*, Dallas, TX, USA, 2016, pp. 1–5. 34

[55] K. Sun, S. Likhate, V. Vittal, V. S. Kolluri, and S. Mandal, "An online dynamic security assessment scheme using phasor measurements and decision trees,"

IEEE Transactions on Power Systems, vol. 22, no. 4, pp. 1935–1943, 2007. 35, 43

[56] Y. Sheng and S. M. Rovnyak, "Decision tree-based methodology for high impedance fault detection," *IEEE Transactions on Power Delivery*, vol. 19, no. 2, pp. 533–536, 2004. 35

[57] C. Liu, K. Sun, S. Member, Z. H. Rather, Z. Chen, C. L. Bak, and P. Thøgersen, "A Systematic Approach for Dynamic Security Assessment and the Corresponding Preventive Control Scheme Based on Decision Trees," *IEEE Transactions on Power Systems*, vol. 29, no. 2, pp. 717–730, 2014. 35

[58] N. Senroy, G. Heydt, and V. Vittal, "Decision Tree Assisted Controlled Islanding," *IEEE Transactions on Power Systems*, vol. 21, no. 4, pp. 1790–1797, 2006. 35

[59] R. Diao, K. Sun, V. Vittal, R. J. O'Keefe, M. R. Richardson, N. Bhatt, D. Stradford, and S. K. Sarawgi, "Decision tree-based online voltage security assessment using PMU measurements," *IEEE Transactions on Power Systems*, vol. 24, no. 2, pp. 832–839, 2009. 35

[60] S. Rovnyak, C. Taylor, and Y. Sheng, "Decision trees using apparent resistance to detect impending loss of synchronism," *IEEE Transactions on Power Delivery*, vol. 15, no. 4, pp. 1157–1162, 2000. 35

[61] Q. Jiang, M. Xue, and G. Geng, "Energy management of microgrid in grid-connected and stand-alone modes," *IEEE Transactions on Power Systems*, vol. 28, no. 3, pp. 3380–3389, 2013. 35, 36

[62] R. Azim, H. Cui, and F. Li, "Power Management Strategy Combining Energy Storage and Demand Response for Microgrid Emergency Autonomous Operation," in *Proc. 2016 IEEE PES Asia-Pacific Power and Energy Conference*, Xi'an, China, 2016, pp. 2620–2625. 35

[63] C. Gouveia, J. Moreira, C. L. Moreira, and J. a. Pecas Lopes, "Coordinating storage and demand response for microgrid emergency operation," *IEEE Transactions on Smart Grid*, vol. 4, no. 4, pp. 1898–1908, 2013. 35, 36

[64] S. P. Kani, M. H. Nehrir, and R. K. Sharma, "Multi-Timescale Power Management for Islanded Microgrids Including Storage and Demand Response," *IEEE Transactions on Smart Grid*, vol. 6, no. 3, pp. 1–1, 2015. 35, 36

[65] J. Y. Kim, J. H. Jeon, S. K. Kim, C. Cho, J. H. Park, H. M. Kim, and K. Y. Nam, "Cooperative control strategy of energy storage system and microsources for stabilizing the microgrid during islanded operation," *IEEE Transactions on Power Electronics*, vol. 25, no. 12, pp. 3037–3048, 2010. 35, 36

[66] F. Katiraei, M. R. Iravani, and P. W. Lehn, "Micro-grid autonomous operation during and subsequent to islanding process," *IEEE Transactions on Power Delivery*, vol. 20, no. 1, pp. 248–257, 2005. 35, 37

[67] S. A. Pourmousavi and M. H. Nehrir, "Real-Time Central Demand Response for Primary Frequency Regulation in Microgrids," *IEEE Transactions on Smart Grid*, vol. 3, no. 4, pp. 1988–1996, 2012. 35, 37

[68] P. Palensky, S. Member, D. Dietrich, and S. Member, "Demand Side Management : Demand Response , Intelligent Energy Systems , and Smart Loads," *IEEE Transactions on Industrial Informatics*, vol. 7, no. 3, pp. 381–388, 2011. 35, 37

[69] C. M. Colson and M. H. Nehrir, "Comprehensive real-time microgrid power management and control with distributed agents," *IEEE Transactions on Smart Grid*, vol. 4, no. 1, pp. 617–627, 2013. 35, 37

[70] T. Logenthiran, D. Srinivasan, A. M. Khambadkone, and H. N. Aung, "Multiagent system for real-time operation of a microgrid in real-time digital

simulator," *IEEE Transactions on Smart Grid*, vol. 3, no. 2, pp. 925–933, 2012. 35, 38

[71] T. Logenthiran, D. Srinivasan, and A. M. Khambadkone, "Multi-agent system for energy resource scheduling of integrated microgrids in a distributed system," *Electric Power Systems Research*, vol. 81, no. 1, pp. 138–148, 2011. 36, 38

[72] H. S. V. S. Kumar Nunna and S. Doolla, "Energy management in microgrids using demand response and distributed storage - A multiagent approach," *IEEE Transactions on Power Delivery*, vol. 28, no. 2, pp. 939–947, 2013. 36, 38

[73] X. Fang, F. Li, Y. Wei, R. Azim, and Y. Xu, "Reactive power planning under high penetration of wind energy using Benders decomposition," *IET Generation, Transmission and Distribution*, vol. 9, no. 14, pp. 1835–1844, 2015. 39

[74] X. Fang, Q. Hu, F. Li, B. Wang, and Y. Li, "Coupon-Based Demand Response Considering Wind Power Uncertainty: A Strategic Bidding Model for Load Serving Entities," *IEEE Transactions on Power Systems*, vol. 31, no. 2, pp. 1025–1037, 2016. 39

[75] X. Fang, F. Li, Y. Wei, and H. Cui, "Strategic scheduling of energy storage for load serving entities in locational marginal pricing market," *IET Generation, Transmission and Distribution*, vol. 10, no. 5, pp. 1258–1267, 2016. 39

[76] X. Fang, Y. Wei, and F. Li, "Evaluation of LMP Intervals Considering Wind Uncertainty," *IEEE Transactions on Power Systems*, vol. 31, no. 3, pp. 2495–2496, 2016. 39

[77] X. Fang, F. Li, Q. Hu, and Y. Wei, "Strategic CBDR bidding considering FTR and wind power," *IET Generation, Transmission and Distribution*, vol. 10, no. 10, pp. 2464–2474, 2016. 39

[78] T. Hill and P. Lewicki, *STATISTICS: Methods and Applications*. Tulsa, OK: StatSoft, 2007. 41, 42

[79] L. Breiman, J. Friedman, R. Olshen, and C. J. Stone, *Classification and Regression Trees*. New York: CRC Press, 1999. 41, 42

[80] Y. Sheng, V. V. Phoha, and S. M. Rovnyak, "A parallel decision tree-based method for user authentication based on keystroke patterns," *IEEE Transactions on Systems, Man, and Cybernetics, Part B: Cybernetics*, vol. 35, no. 4, pp. 826–833, 2005. 46, 48

[81] W. H. Kerting, "Radial distribution test feeders IEEE distribution planning working group report," *IEEE Transactions on Power Systems*, vol. 6, no. 3, pp. 975–985, 1991. 50, 84

[82] P. Kundur, *Power System Stability and Control*. New York: McGraw-Hill Professional, 1994. 51, 84, 109

[83] I. H. Witten, E. Frank, and M. a. Hall, *Data Mining: Practical Machine Learning Tools and Techniques*, 2011. 55, 87, 95, 112

[84] Z. W. Geem, J. H. Kim, and G. V. Loganathan, "A new heuristic optimization algorithm: Harmony Search," *Simulation*, vol. 76, no. 2, pp. 60–68, 2001. 74, 82, 88

[85] IEEE, "IEEE Recommended Practice for Utility Interface of Photovoltaic (PV) Systems," 2000. 74, 88, 89, 91

[86] Underwriters Laboratories Standard 1741, "The standard for inverters, converters, and controllers for use in independent power systems," 2001. 74, 89, 92

[87] L. A. C. Lopes and Y. Zhang, "Islanding detection assessment of multi-inverter systems with active frequency drifting methods," *IEEE Transactions on Power Delivery*, vol. 23, no. 1, pp. 480–486, 2008. 95

[88] M. C. Falvo, D. Sbordone, I. S. Bayram, and M. Devetsikiotis, "EV charging stations and modes: International standards," in *2014 International Symposium on Power Electronics, Electrical Drives, Automation and Motion*, 2014, pp. 1134–1139. 125

[89] S. Shao, M. Pipattanasomporn, and S. Rahman, "Grid integration of electric vehicles and demand response with customer choice," *IEEE Transactions on Smart Grid*, vol. 3, no. 1, pp. 543–550, 2012. 127

[90] ——, "Demand response as a load shaping tool in an intelligent grid with electric vehicles," *IEEE Transactions on Smart Grid*, vol. 2, no. 4, pp. 624–631, 2011. 127

Vita

Riyasat Azim joined Professor Fangxing 'Fran' Li's research group at The University of Tennessee Knoxville in August 2012 to pursue Ph.D. degree in Electrical Engineering. He received his B.S. degree from Islamic University of Technology, Gazipur, Bangladesh in November 2008, and M.S. degree from Islamic University of Technology, Gazipur, Dhaka, in July, 2012. His research interests include grid integration of renewable energy resources, microgrid control and management, smart grid technology, development of analytical tools for power system applications etc.